Investigation of the roles of WT1+KTS and VVT1-KTS in murine genito-urinary development

Lahiri, Diya

Award date:
2003

Awarding institution:
University of Bath

INVESTIGATION OF THE ROLES OF WT1+KTS AND WT1-KTS IN MURINE GENITO-URINARY DEVELOPMENT

Submitted by

Diya Lahiri

for the degree of PhD of the
University of Bath

2003

ProQuest LLC
789 East Eisenhower Parkway
P.O. Box 1346
Ann Arbor, MI 48106-1346

For my grandparents

It was I who forged this chain very carefully, I thought my invincible power would hold the world captive leaving me in a freedom undisturbed.
Thus night and day I worked at the chain with huge fires and cruel hard strokes.
When at last the work was done and the links complete and unbreakable,
I found that it held me in its grip.

Rabindranath Tagore

Abstract

INVESTIGATION OF THE ROLES OF WT1+KTS AND WT1-KTS IN MURINE GENITO-URINARY DEVELOPMENT

Diya Lahiri

The Wilms' tumour suppressor gene, WT1, encodes a zinc finger transcription factor essential for the development of the urogenital system. Alternative splicing within the gene causes an insertion or deletion of three amino acids creating two classes of isoform, WT1+KTS and WT1-KTS. Mutation of the isoforms, and disruption of their ratios are linked to human disorders of the urogenital system. These isoforms are thought to have distinct roles within the nucleus. The aim of the work were to investigate the role of these isoforms in murine genito-urinary development. Transgenic lines of mice expressing a WT1-KTS transgene were generated, and bred to *Wt1* knockout animals to study the effects of the WT1- KTS isoform on genito-urinary development in isolation from the other isoforms. Analysis of these animals showed there may be an effect in animals expressing the WT1-KTS transgene and heterozygous for *Wt1*. Using green fluorescent protein fusion constructs in cell culture, it has been demonstrated that the dynamic subnuclear localization of the two isoforms result, in part, from the presence of a nucleolar localization signal within the zinc finger regions. Combining transgenic techniques with cell culture work, these findings help elucidate the mechanisms by which the *Wt1* isoforms are distributed in the nucleus, and suggest a model explaining how their separate functions are maintained.

TABLE OF CONTENTS

ACKNOWLEDGMENTS

The completion of this thesis seemed dubious to me on occasion over the last four years. That I am submitting it, owes a great deal to my colleagues, friends and family. In particular I wish to acknowledge the following people without whom this thesis would have been impossible. Firstly, I wish to thank Andrew for his guidance on every aspect of my PhD and the calm manner in which it was executed. I am particularly grateful to James for his co-supervision and his knowledge on all things cellular and molecular while Treve, Sharon, Tia, Marika, Tracey and Bill have provided inexhaustible assistance on all things murine. Furthermore, I would like to acknowledge the wealth of expertise in developmental biology and the generous manner in which it was offered by all members of the Ward, Kelsh, Slack and Tosh laboratories in the University of Bath. I would also like to acknowledge Cesare, Tom and Arsen for providing me with an outlet to express my "views" during the writing of this thesis.

Finally, to Baba and Ma, I thank them for all that I am, and to my sister Nayana, for showing me the meaning of courage.

ABBREVIATIONS

Word.

bp	base pairs
cM	Centimorgans
Chr	chromosome
DAB	diaminobenzidine
DDS	Denys Drash syndrome
DEPC	diethylpyroocarbonate
EDTA	ethylene diamine tetra-acetic acid, sodium salt
ES	embryonic stem cell
FITC	fluorescein isothiocyanate
FS	Frasier syndrome
GDNF	Glial derived neurotrophic factor
GFP	green fluorescent protein
H&E	haematoxylin and eosin
IGF-2	Insulin-like growth factor-II
Kb	kilobase
LIF	Leukaemia inhibitory factor

Mb	megabase
PAS	periodic acid-Schiff reagent
PBS	phosphate buffered saline
PCNA	proliferating cell nuclear antigen
SDS	sodium dodecyl sulphate
WT1	Wilms tumour suppressor
YAC	yeast artifical chromosome

Chapter 1

INTRODUCTION

1.1 Genito-urinary Development

The kidney and gonads are both organised within the genito-urinary system. WT1 is essential for the correct development of this system as illustrated by human disease studies and transgenic animal data. The function of the gene in gonad and renal development can be understood by firstly examining the development of both sub-systems, then looking at the roles of various interacting molecules and finally by analysing the mechanisms by which the WT1 gene acts.

1.1.1 Kidney Development

In birds and mammals three kidney like structures, metanephros, mesonephros and pronephros appear during development. The pronephros and mesonephros are transitionary and the functional kidney develops from the metanephros. The mesonephros plays a key role in gonadal development, giving rise to the gonadal somatic cells. In lower vertebrates such as fish and amphibians, the pronephros acts as the functional kidney in the immature stages whereas the mesonephros is the functional adult kidney (Slack, 2001).

The metanephric kidney of mammals is composed of a set of nephrons. These are the basic structural units of the kidney consisting of the glomerulus and its associated tubule and collecting duct. Blood vessels invade the kidney and are closely associated with the collecting duct system at the Bowman's capsule (BC) in the glomerulus. It is here that waste fluid is filtered out of the blood and is then

passed into the tubule where it undergoes ion exchange and corresponding movements of water before passing into the collecting duct, ureter, bladder and out of the body as urine. The nephrons of the kidney, working together allow the kidney to remove waste from the system, and failure for this system to develop can have severe implications for the viability of the organism as illustrated by many diseases of the kidney. In the mouse, development of the kidney (nephrogenesis), starts at around embryonic day 10.5 and continues until after birth (Saxen, 1987). Nephrogenesis involves a series of inductive interactions between mesenchymal and epithelial tissues, resulting in a complex functional kidney (Figure 1) (Davies and Bard, 1998 Review). Grobstein originally described evidence for the existence of inductive interactions using cultured kidney explants (Grobstein, 1955), since then many molecules playing a role in nephrogenesis have been uncovered and a variety of interactions can be mimicked in culture. The first event marking the beginning of kidney development is the induction by the metanephric blastema of a ureteric bud (UB) from the Wolffian duct. At the same time, the mesonephros, axial and paraxial structures running along the length of the embryo either side of the midline, gives rise to the Mullerian duct (MD), which will then form the gonads. The metanephric mesenchyme (MM) continues to induce the UB to grow and bifurcate whilst reciprocal inductive signals from the epithelial UB cause the mesenchyme to condense and differentiate. These signals from the UB block apoptosis of the MM, causes it to aggregate, condense, epithelialise and undergo a series of morphological changes (progressively including stereotypical comma-shaped and s-shaped bodies), before elongating to form the tubules of the nephron. The glomerulus forms at the proximal end of the tubule and consists of a cup shaped BC lined with a single layer of podocyte cells at the membrane, aptly named for their unusual foot processes, and the collection of capillary blood vessels where they come into contact with the kidney (Figure 2).

Figure 1. Nephrogenesis

Nephrogenesis begins around E10.5 in mice and involves a series of inductive interactions between mesenchymal and epithelial tissues, resulting in a complex kidney. The epithelial ureteric bud (UB) induces the surrounding metanephric mesenchyme to condense and epithelialise resulting in the formation of the glomeruli and renal tubules. In parallel, the MM induces the UB to grow and bifurcate to form the collecting duct system. The fully developed metanephric kidney of mammals is comprised of a set of nephrons consisting of the glomerulus and its associated tubule and collecting duct. Capillaries invade the kidney and waste is filtered out of the blood before being passed into the tubules and undergoing ion exchange and corresponding movements of water. Waste is finally removed through the ureter, and out of the body as urine.

Figure 2. Nephron formation

Following inductive interactions, the UB causes the MM to aggregate, condense and epithelialise. During these processes, the MM undergoes a number of morphological changes. The MM progresses through structures such as the comma shaped and s shaped bodies before elongating to form the tubules of the nephron with the glomerulus at the proximal end. The tubules convolute and differentiate and the distal end fuses to the collecing duct which originates from the UB which has elongated.

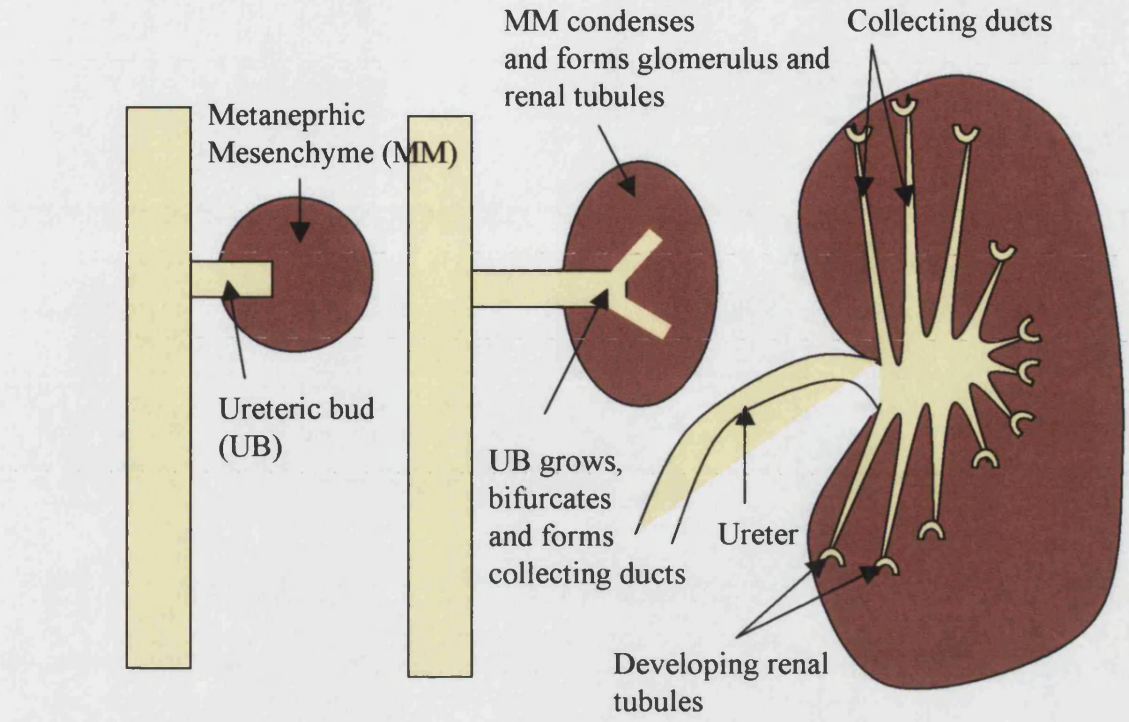
MM condenses
and forms glomerulus and
renal tubules
Collecting ducts
Metaneprhic
Mesenchyme (MM)
Ureteric bud
(UB)
UB grows,
bifurcates
and forms
collecting ducts
Ureter
Developing renal
tubules

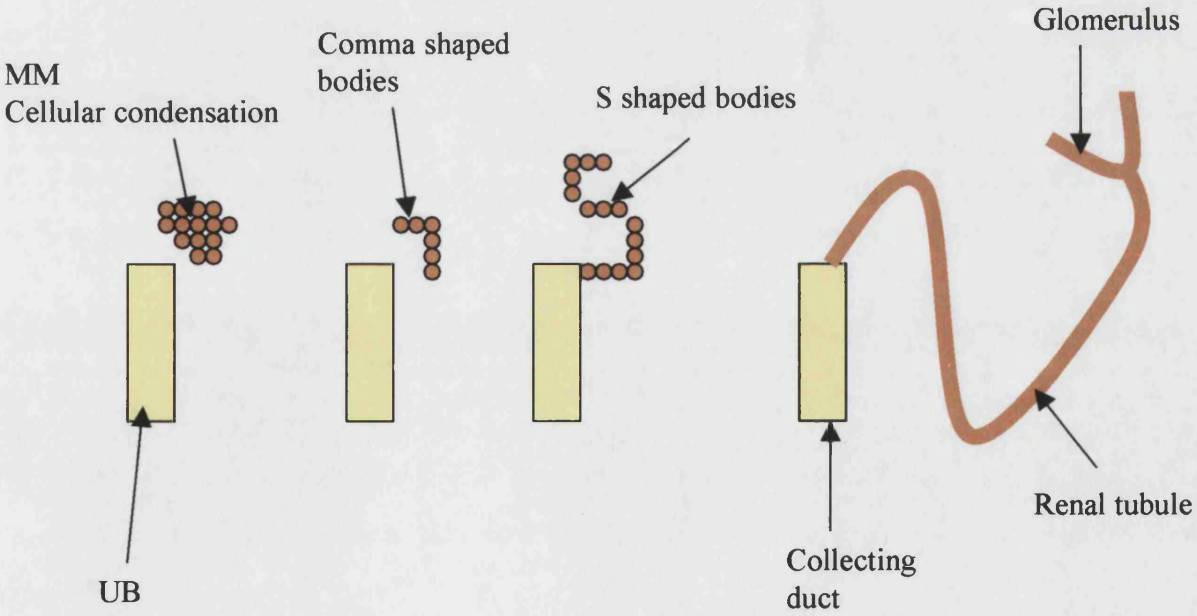
MM
Cellular condensation
Comma shaped
bodies
S shaped bodies
Glomerulus
UB
Collecting
duct
Renal tubule

The tubules convolute and differentiate to become the site for selective reabsorption of the fluid whilst the distal part fuses to the collecting duct (Davies and Davey, 1999 Review). The epithelial structures derived from the bud form the collecting duct system of the kidney whilst the mesenchyme gives rise to the glomeruli and tubules (Wolpert et al., 1998). This process of nephrogenesis continues throughout development, until about 6 weeks before birth in humans, and hours postnatally in the mouse, with the newer nephrons located peripherally to the older, existing nephrons. Development of the definitive kidney can be viewed as having three phases. The first is the initial induction of the UB into the metanephric blastema, the blocking of apoptosis of the MM and differentiation into stem cells at the periphery. This phase occurs from around E10.5-13.5 in the mouse and is followed by the second phase, when arborisation of the UB continues whilst nephrons form and begin to function (E13.5 till birth). Nephrogenesis slows down in the final phase, the blast cells are lost and the kidney begins to function normally. A fine balance of growth and apoptosis underlies kidney development with interactions between multitudes of molecules giving rise to the mature kidney (Bard, 2002 Review).

1.1.2 Molecules involved in Kidney Development

Over the last decade, research into the embryonic regulation of kidney development has uncovered a plethora of genes implicated in renal development. Whilst this report studies the function of the Wilms' Tumour suppressor 1 gene, it is crucial to note the role of other molecules of importance in the development of a mature kidney. These include a variety of families ranging from transcription factors to extracellular matrix proteins which reflect the variety of processes involved in nephrogenesis such as inductive signals, morphogenetic interactions between mesenchyme and epithelium, interactions

between the epithelium, neurons and blood vessels, and the regulated pattern of differentiation and pattern formation. A list of over 300 molecules involved in kidney function can be found in the kidney database (http://golgi.ana.ed.ac.uk/kidhome.html), a number have associated transgenic animal data supporting their roles in kidney development and function (Davies, et al. 2003). Many of the molecules that regulate these processes have important roles elsewhere in the embryo but for the purposes of this report, the discussion will be limited to the control of nephrogenesis. Some of the key molecules are described below to illustrate the pathways involved in nephrogenesis. Amongst them are transcription factors, for example Pod-1 (Quaggin et al., 1999) and Lim-1 and also homeobox containing genes such as Emx-2 and hoxb7. Adhesion molecules such as Cadherin-6 (Mah et al., 2000), signalling molecules including those involved in angiogenesis and vascularisation like vascular endothelial growth factor (VEGF) (Miquerol et al., 1999), and its receptor flk-1 (Kappel et al., 1999), have also been shown to have a role in kidney development.

1.1.2.1 Glial derived neurotrophic factor and its receptor RET

GDNF and RET form a signalling complex that regulates ureteric bud growth (Lechner and Dressler, 1997). RET, a member of the receptor tyrosine kinase family was found to be expressed fairly early in embryonic development in the Wolfian Duct and the UB. Later, RET expression was seen to be restricted to the tips of the UB (Schuchardt et al., 1994). Targeted inactivation of *RET* in mice resulted in renal agenesis (Schuchardt et al., 1994; Schuchardt et al., 1996) and it is an important marker of the UB (Srinivas et al., 1999a). GDNF was originally found as a factor promoting survival of midbrain dopiminergic neurons (Lin et al., 1993) and was later identified as the RET ligand. GDNF expression can be first observed at about embryonic day 11.5 (E11.5) in the MM and later restricted to

the peripheral mesenchyme, complementing RET expression (Hellmich et al., 1996). Kidneys fail to form in both *gdnf* and *ret* knockout mice and these mice die shortly before birth (Sanchez et al., 1996; Schuchardt et al., 1994). Investigation of the heterozygous knockout phenotype highlighted the abnormalities. The tubules in *gdnf* heterozygous knockout mice form but these mice lack UBs (Moore et al., 1996; Pichel et al., 1996; Sanchez et al., 1996) similar to the phenotype described in *ret* heterozygous knockout mice (Schuchardt et al., 1994). Mesenchymal GDNF signal is transmitted via the RET receptor, to epithelial cells and may result in inducing proliferation of epithelial cells.

1.1.2.2 LIF, WNT-4 and EMX-2

Once induced, the UB invades the MM and grows, branches and induces nephron formation. Leukaemia inhibitory factor (LIF) has been found to be essential in the induction of nephrogenesis in cultured explant experiments, however, there may be a certain degree of redundancy in its function as *lif-1* knockout mice do not show kidney abnormalities. It has been postulated that additional factors such as fibroblast growth factor-2 is probably the inducing signal for the mesenchyme and both WNT-4 and BMP-7 may also be required *in vivo* for this process (Stark et al., 1994). The homeobox-containing transcription factor EMX-2 may be a regulator of blastemal condensation as its expression is restricted to the UB and in *Emx-2* knockouts, the UB invades the MM normally but after that the kidneys fail to develop (Miyamoto et al., 1997). It may be that *EMX-2* regulates the function of *WNT-4* and *LIF-1* (Schedl et. al., 2000).

1.1.2.3 PAX-2

Pax-2 is a transcription factor expressed within the developing kidney (Dressler et al., 1990). It has been seen to be expressed in the earliest condensates of MM and in the comma-shaped bodies. Expression declines in s-shaped bodies and is absent in mature kidneys (Dressler and Douglass, 1992). *Pax-2* knockout (null) mutant mice lacked tubules or genito-urinary tracts and the heterozygous animals had much smaller kidneys than normal as a result of increased apoptosis and a reduction of ureter branching. Thus, Pax-2 has been thought to be one of the factors essential for kidney growth (Ryan et al., 1995) and seems to be required for the mesenchyme to epithelium transition as illustrated by the transgenic animals and in patients with *Pax-2* heterozygous mutations associated with the development of dysplastic kidneys. Pax-2 levels have been shown to be increased in Wilms' tumours (Dressler and Douglass, 1992) and the relationship between Pax-2 and Wilms' tumour will be further discussed later.

1.1.2.4 BMP-7

BMP-7 is a member of the TGFβ superfamily of secreted signalling molecules which have many roles in morphogenic events (Kingsley, 1995). BMP-7 transcripts were found in mesonephric ducts, tubules and later in metanephric condensates, comma-shaped and s-shaped bodies (Dudley et al., 1995). Knockout mice died soon after birth with dysplastic kidneys (Dudley et al., 1995; Godin et al., 1998). BMP-7 is a potential target for both WT1 and PAX-2 as it may be controlled by signals from the ureter. It is thought to be secreted by the metanephric blastema and controls the rate of nephrogenesis by suppressing tubulogenesis.

1.1.3 Transgenic models of kidney development

Bearing in mind the limitations of transgenic models, for example, phenotypes of null animals may not provide a correct representation of human disorders, transgenic data still provides some of the best indication of gene function and there have been a number of transgenic mice generated for some of the molecules involved in kidney development. A detailed list can be found in the kidney database (Davies et. al., 2003) but the discussion in this report will again be limited to the transgenic models of genes interacting with WT1 or involved in similar processes. *Gdnf* knockout mice had no kidneys as the ureteric bud failed to grow (Sanchez et al., 1996). *Bmp-7* knockout mice had smaller kidneys and died soon after birth with severe hypoplasia, fewer nephrons and collecting ducts and polycystic tubules (Godin et al., 1998). *Pax-2* mice heterozygous knockouts had much smaller kidneys while homozygous knockouts lacked genito-urinary tracts altogether (Ryan et al., 1995). *Wt1* homozygous null mice exhibited kidney agenesis (Kreidberg et al., 1993) and the WT1 transgenic data will be discussed further later in Section 1.2.

1.1.4 Gonadal Development

Gonadal development also falls within the genito-urinary system and therefore exhibits many of the same features as kidney development. Although they have much in common, the development of the gonads is a fascinating and unique process in mammals resulting in either male or female gonads which are quite distinct from each other and therefore definitive features of sex determination. A brief discussion of some of the key aspects of gonad development in mammals will be presented in this section.

Gonadal development can be divided into two phases. Early gonad development when the gonads are deemed to be indifferent, that is, the same in both sexes. Early gonad development commences at about embryonic day 10 in mice. Late gonad development is when sex determination comes into play and the male and female gonads develop differently, the sex determination switch occurs at around embryonic day 12.5. The gonads are derived from the intermediate mesoderm. The gonads develop in mammals in close association to the mesonephros (mentioned earlier is the introduction as an embryonic kidney). The Wolffian duct (WD) originates within each mesonephros. Another pair of ducts, the Mullerian duct (MD) also run parallel to the WD. In early, indifferent gonads, both set of ducts are present. The gonads arise from a thickening of the ventrolateral surface of each mesonephros. Ceolomic epithelia (CE) within each mesonephros invaginate to form the WDs which turn towards the midline and fuse. Around E11-13, while the gonads are developing, the germ cells migrate from the base of the allantois across the gut and into the gonads. Meanwhile, the epithelial cells from the coelum form sex cords which undergo differentiation into the mesenchyme that will eventually surround the germ cells on the genital ridge (Ginsburg et al., 1990 Review). Up to this point, there is no difference between the male and female gonads. The germ cells will eventually be surrounded by three cell types which all have bipotential fates, these are the supporting cells (sertoli or follicular), the hormone secreting cells (Leydig or Thecal) and connective tissue. The supporting cells are derived from the coelomic epithelia, the steroidogenic cells produce the sex hormones for the development of secondary sexual characteristics, and the interstitial cells of the connective tissue line the structures of the gonads (Slack, 2001 Review).

After the sex determination switch, in the male, the cords of cells growing into the germinal ridge go through a transition from sex cords to testis cords, then form a

complex system of semi-niferous tubules composed of epithelium containing a number of cell types including the Sertoli cells which will surround the germ cells and provide them a growth environment. The Leydig cells differentiated from the mesenchyme between the tubules are the supporting cells, responsible for secretion of testosterone. The tubules become connected to the WD, which will give rise to the vas deferens, they shorten and become encapsulated to form the testis and the MD regresses and degenerates. The tubules remain solid until after birth when they hollow out and the germ cell derived spermatogonia appear.

In the female, the cords of cells remain near the surface as granulosa (follicle) cells which will surround the germ cells and provide the growth environment for the oogonia. The mesenchyme differentiates into Thecal cells which have a similar function to the Leydig cells in the male, to provide the sex hormone oestrogen. The gonad becomes encapsulated to form an ovary and the posterior end of the MDs fuse to form the proximal vagina and uterus, while the anterior end forms the oviducts (Fallopian tubes) while the WD degenerates (Swain and Lovell-Badge, 1999 Review).

1.1.5 Molecules involved in gonad development

Mutation studies have helped identify some of the genes involved in sex development. The pathways are not always clear as the consequences of mutation are often too severe. The molecules can be divided into those essential for early development, necessary in both male and female gonad development before E12, and those necessary for sex determination, hence late development after E12, which are more sex specific.

1.1.5.1 Molecules involved in early gonad development

In early development, one of the earliest molecules to be expressed in the presumptive gonad is steroidogenic factor 1 (SF1) which belongs to the orphan receptor family of nuclear receptors, and has no known specific activating ligand. *SF1* encodes a two zinc finger transcription factor and was found to be involved in steroid biosynthesis in areas associated with endocrine function such as the gonads, pituitary, hypothalamus and adrenals (Ingraham et al., 1994). SF1 is necessary for differentiation and maintenance of development. As mentioned in the section on kidney development, LIM-1 and PAX-2 were found in the mesenchyme and were needed for the differentiation of intermediate mesoderm, they were

also required for the same function in gonad development. Another molecule discussed earlier was the transcription factor EMX-2. EMX-2 was also found to be required for normal gonad development, and was seen to be expressed in the genital ridge, WD and Coelomic epithelia (Miyamoto et. al., 1997).

1.1.5.2 SRY, SOX9 and the sex determining switch

The sex determining switch marks the end of early gonad development. Until E12 male and female gonads are morphologically identical. Sex determination is a cell fate decision. The Y-linked *Sry* gene has been thought to trigger the switch for sertoli cell fate in a cell that would otherwise become a follicle cell. SRY is a HMG box, transcription factor and expression is seen just before sexual dimorphism and appears in a wave so that each cell expresses SRY for only a few hours from E10.5-11. We can presume that SRY is therefore not involved in the maintenance of cell identity or function but must act on downstream genes. With the discovery of *SRY*, it was thought that the mechanism for sex determination had been solved. XY mice with a null mutation for *Sry* were female and XX mice with an *Sry* transgene were phenotypically male (Koopman

et al., 1991). Sox-9 however, has also been found to be vital for the sex determination process. The protein has been detected in low levels in both male and females but by E11.5, before sexual dimorphism appeared and after Sry expression, the levels in males increased and it was switched off in females. By E12.5 one can see Sox-9 expression in Sertoli cells and this expression persists in Sertoli cells but not in ovaries. This suggests that while *Sry* may be the determination switch (Swain and Lovell-Badge, 1999), the signal is maintained by *Sox-9*. The precise details of the mechanisms by which *Sry* and *Sox-9* function are still unknown.

1.1.5.3 DAX-1 and female development

Dax-1 encodes a nuclear hormone receptor protein, and could be thought of as the "antitestis" gene (Swain et al., 1997). It acts antagonistically to *Sry* and is expressed in the genital ridge at the same time as Sry but as differentiation proceeds, Dax-1 levels decreased in the testis but persisted in the ovaries. *Dax-1* had an inhibitory effect on *Wt1* and *Sf-1*, which are both activators of the anti Mullerian hormone (AMH), a member of the TGFβ family (Parker et al., 1999). AMH was seen to cause the regression of the MDs in males, and is suppressed in females to allow the MD to form the uterus and oviducts (Hoyle et al., 2002; Jeffs et al., 2001). It can be said that sertoli cell fate is the key sex determination event. After this switch, very little is known about later development. The sex hormones, of course, are thought to play a large role in maintenance of sexual characteristics, testosterone in males, progesterone and oestrogen in females, however not much is known about the molecules involved in the direct differentiation of the testis, cord formation and other late events.

1.1.5.4 Late sexual development

WNT-4 is a molecule involved in controlling steroid production. Leydig cells start producing testosterone after testicular cord formation and this is thought to be regulated by *Wnt-4* (Swain and Lovell-Badge, 1999). The default sex for germ cells is female and the differentiation is thought to be controlled by factors produced by Sertoli cells. In early differentiated testis the germ cells undergo mitotic arrest and in early ovaries, they undergo meiotic arrest. The Sertoli cells sustain germ cells during development and spermatogenesis by cell-cell interactions and Desert hedgehog (*Dhh*) is a gene involved in this process. *Sox-9* activation of *Dhh* may be the mitotic signal for germ cells in males as this is absent in ovaries (Bitgood et al., 1996).

1.1.6 Transgenic models of gonad development

As in kidney development, transgenic animal data provides some of the most incisive data regarding gene function in gonad development. This method is especially problematic in sex development as there may be severe phenotypes resulting in non-viable animals or animals that are unable to reproduce. Out of the genes involved in early gonad development, *Sf1* homozygous knockout animals had no gonads even though the genital ridge still forms, no ventro-lateral hypothalamus and impaired gonadotrope function (Ingraham et al., 1994). This correlates with its role in differentiation and maintenance of early development. *Lim-1* knockout mice had no gonads (Shawlot and Behringer, 1995,Tsang, 2000 #112) and although *Pax-2* knockout mice had no kidneys, the gonads still formed so there seems to be a redundancy in *Pax-2*. *Emx-2* knockouts did have gonads but they were poorly developed, the mesonephric tubules degenerate. *Emx-2* may respond to a signal downstream of WT1, as WT1 expression was not affected in Emx-2 mutants (Guo et al., 2002a; Miyamoto et al., 1997).

In later development, XY knockout mice for *Sry* were phenotypically female and XX mice carrying *Sry* transgenes were phenotypically male. Mutations in *Sox*-9 in XY mice resulted in male to female sex reversal, whilst ectopic Sox-9 in XX gonads, was sufficient to induce testis formation, therefore substituting for Sry (Koopman et al., 1991; Vidal et al., 2001).

1.1.7 Human developmental disorders of the genito-urinary system

In humans, developmental disorders of the kidney and sex organs illustrate defects in the genes reported earlier in this discussion. There are numerous diseases with defects in genito-urinary system characterised by loss of function or gain of function mutations. In sexual development, many of the syndromes can be characterised by sex reversal, dysplasia or neoplasia, and with the exception of sex reversal, the same characteristics as found in many kidney diseases.

Human mutations in the *SRY* gene resulted in gonadal dysgenesis and XY sex reversal. *SOX*-9 mutations caused the human skeletal disorder campomelic dysplasia and its associated XY gonadal dysgenesis (Guo et al., 2002a; Parker et al., 1999; Vidal et al., 2001). *WNT-4* mapped to a chromosomal region associated with duplications that cause ambiguous gonads and internal feminisation of XY patients (Staal et al., 2001). The *SF1* gene functioned in both the adrenal and gonads and as expected, mutations in the gene, caused adrenal failure and XY dysgenesis. XY dysgenesis was also a symptom of a multigene deletion affecting the *DMRT1* gene (Hoyle et al., 2002). A duplication of the "antitestis" gene Dax-1 resulted in adrenal hypoplasia (the adrenals and gonads developed from the same primordia) and hypogonadism (Hoyle et al., 2002; Jeffs

et al., 2001; Swain et al., 1997), whilst human mutations in the *AMH* gene resulted in persistence of MD derivatives in XY but no sex reversal (Beau et al., 2001; Munsterberg and Lovell-Badge, 1991). *WT1* mutations resulted in syndromes with sex reversal and XY pseudohermaphrotidism (to be discussed in Section 1.2).

Human kidney disease resulting from developmental abnormalities often manifests itself with a variety of other symptoms as many of the genes have multiple roles in development. For example, somatic rearrangements of *RET* resulting in its constitutive overexpression, have been associated with some papillary thyroid carcinomas. Deletions or mutations with decreased activity of *RET* and *GDNF* were associated with autosomal dominant forms of Hirschprung's disease whilst germline mutations caused multiple endocrine neoplasia. Only recently have *RET* and *GDNF* been implicated in unilateral aplasia of the kidney in association with Hirschprung's disease (Lin et al., 1993; Pichel et al., 1996; Schuchardt et al., 1994; Srinivas et al., 1999b). *PAX*-2 has also been implicated in many non-renal disorders but it is also strongly associated with human kidney diseases. *PAX-2* haploinsufficiency leads to renal-coloboma syndrome, an autosomal dominant disease characterised by kidney, optic nerve and retinal defects. The other renal abnormalities associated with *PAX-2* include bilateral hypoplasia, unilateral aplasia, and glomerular and interstitial fibrosis. Persistent PAX-2 expression has also been associated with human renal disorders. Human fetal and infantile multicystic dysplastic kidneys displayed persistent PAX-2 expression as did other proliferative kidney diseases, such as autosomal dominant polycystic kidney disease, renal cell carcinoma and Wilms' tumour (Schedl and Hastie, 2000). Fetal kidney abnormalities, renal dysplasia and anuria have been found to be associated with mutations in the angiotensin receptor gene (Schedl and Hastie, 2000). Finally, *WT1* has been

implicated in numerous kidney disease and neoplasias and the following section will concentrate on WT1 structure, roles and characteristics of WT1, as well as its involvement in human disease and mouse models of these disorders.

1.2 Wilms' tumours suppressor 1 (WT1)

1.2.1 WT1, Wilms' tumour, and human developmental disorders

One of the main reasons for investigating the function of WT1 is its association with a wide range of disorders many involving abnormalities of the genito-urinary system but also leukaemia, and other neoplasias. WT1 was first identified from cases of Wilms' tumour over a decade ago and since then, the number of syndromes associated with the gene have steadily increased. Wilms' tumour (nephroblastoma) is the most common pediatric intra-abdominal solid tumour. It affects 1 in 10,000 children, most within the first five years of life (Hastie, 1993). The tumours are derived from undifferentiated kidney mesenchymal cell Rests (Knudson and Strong, 1972) and it is often associated with other syndromes, such as WAGR, Denys-Drash, Frasier and Beckwith-Weidman syndromes. WAGR syndrome has a particularly high incidence of Wilms' tumour, hence the name WAGR (**W**ilms' tumour, **A**niridia, **G**enitourinary abnormalities and mental **R**etardation) (Franke et al., 1979), and chromosome 11p13 is deleted in many WAGR cases (Rose et. al, 1990; Miles et. al., 1998). This provided strong evidence that the 11p13 locus was important in WAGR and therefore in Wilms' tumour. The Wilms' tumour suppressor 1 gene (WT1) was eventually mapped to this region (Pritchard-Jones et al., 1990). WT1 disruption is linked to 10% of sporadic Wilms' tumour cases, while there is a loss of heterozygosity at the 11p15 locus (containing the WT2 gene) in a further 40% of cases, it is also associated with many of the characteristics of WAGR syndrome such as the genito-urinary abnormalities WAGR patients display (Hastie, 1993). Mutations in

WT1 are also associated with Denys Drash syndrome (DDS), a sporadic syndrome resulting in pseudohermaphroditism, kidney defects and Wilms' tumour. Frasier syndrome (FS) is similar to Denys Drash, and manifests itself in renal disease, XY gonadal dysgenesis and gonadal tumours (Frasier et al., 1964). Patients with either of these syndromes often develop abnormalities in their glomerular epithelium leading to diffuse mesangial sclerosis, and either focal or segmental sclerosis respectively (Koziell et al., 2000). On occasion, WT1 mutations have been associated with cases of the three different types of renal sclerosis in the absence of DDS or FS (Schedl and Hastie, 2000).

There are a number of neoplasias including leukaemia, also associated with disruptions in the *WT1* gene. WT1 overexpression has often been seen in many types of leukemia in humans, especially acute myeloid leukemia and the protein has been shown to be expressed in heamopoietic precursor cells. Mesothelioma is a rare tumour derived from the peritoneal lining and often associated with a history of asbestosis. Missense mutations in *WT1* have been found in cases of mesotheliomas where asbestosis does not factor (Hastie, 1993). Other solid tumours in which *WT1* mutations have been implicated are desmoplastic small-round cell tumours, gonadoblastomas (in children with WAGR syndrome with *WT1* deletions), and some DDS associated granulosa cell tumours of the ovary (Mrowka and Schedl, 2000). The wide range of WT1 associated diseases of the genito-urinary system and neoplasias demands questions about its gene structure and function that cause it to be essential in maintaining normal development and cell cycle regulation. The role of the gene in genito-urinary development and cell cycle regulation can be investigated by looking more closely at the structure of the gene and protein.

1.2.2 WT1 gene and protein

The Wilms' tumour suppressor 1 gene was mapped to chromosomal locus 11p13 in humans and the corresponding homologous region in the mouse is proximal to chromosome 2 at 0.58 centimorgans (Pritchard-Jones et al., 1990) (https://www.ensembl.org). It was discovered that the gene contains 10 exons encoding a possible 24 different protein isoforms as a result of RNA editing and alternative splicing with four main isoforms resulting from 2 possible alternative splicing events (Scharnhorst et al., 1999). The *WT1* gene encodes a 56-65 KDa protein (size depending on the isoform) with a zinc finger domain at the C-terminal (4 zinc fingers encoded by a different exon each), and a proline/glutamine rich N-terminal (Haber et al., 1990). It is a zinc-finger transcription factor containing a transregulatory region, DNA binding region, self-association domain, nuclear localisation signal, activation and repression domains (Figure 3) (Haber et al., 1990). Computer modeling has demonstrated the presence of a potential N-terminal RNA recognition motif similar to that in constitutive splicing factors (Kennedy et al., 1996). Truncated WT1 protein that contained either the N-terminal domain or the zinc-finger domains was enough to confer nuclear localisation. Furthermore, yeast two hybrid experiments demonstrated the first 182 residues of the protein contain a dimerisation and oligormerisation domain that it has been suggested as an explanation of dominant-negative mutation, particularly those prevalent in DDS. However, the reasons for WT1 self-association are as yet, unclear (Davies et al., 2000).

Transient transfections and promoter-reporter assays have helped identify the proteins which WT1 may transcriptionally activate. Many molecules containing WT1 binding sites have been described, for example, WT1 repressed promoters of the genes encoding insulin-like growth factor II (*IGF-2*) (Caricasole et al., 1996; Duarte, 1997; Ward et al., 1995), *PAX-2* (Ryan et al., 1995; Yang et al.,

Figure 3. WTI gene and protein

The *Wilms' tumour suppressor 1* gene (WT1) contains 10 exons encoding 25 possible isoforms of a 56-65Kda protein. The gene consists of 4 kruppel-like zinc fingers located at the C-terminal and a proline/glutamine rich N terminal. The protein is a transcription factor containing a transregulatory region, DNA binding region, self-association domain, a nuclear localisation signal, and activation and repression domains. Four of the isoforms arise through alternative splice events. The first alternative splice event results in the presence or absence of 17amino acids in exon 5 while the second results in the insertion or deletion of 3 amino acids, lycine, lhreonine or serine (KTS) between the third and fourth zinc finger.

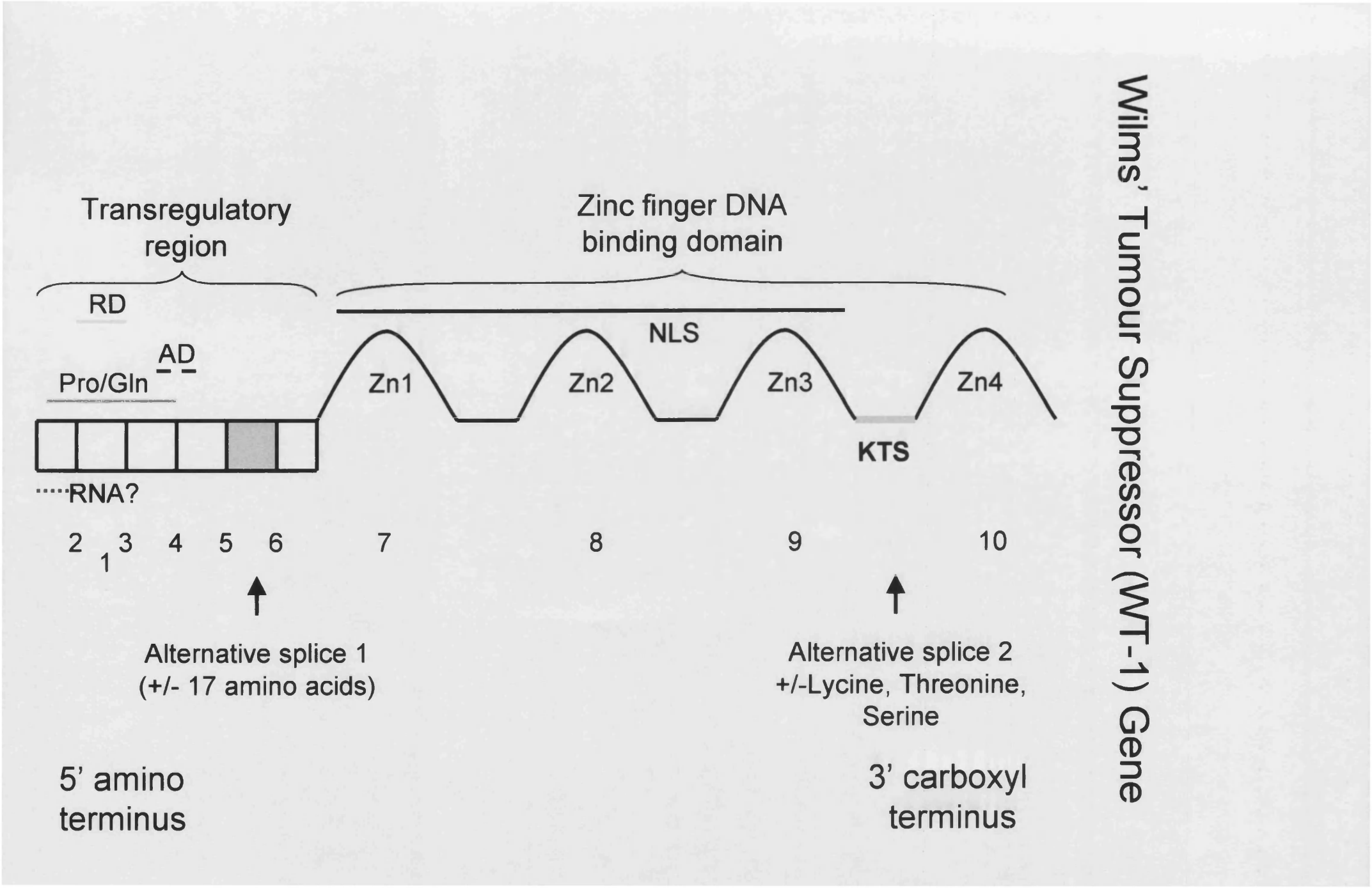
Wilms' Tumour Suppressor (WT-1) Gene
Transregulatory region
Zinc finger DNA binding domain
RD
AD
Pro/Gln
NLS
Zn1
Zn2
Zn3
Zn4
KTS
RNA?
1
2
3
4
5
6
7
8
9
10
Alternative splice 1
(+/- 17 amino acids)
Alternative splice 2
+/-Lycine, Threonine, Serine
5' amino terminus
3' carboxyl terminus

1999), and *TGFβ* (Jin et. al., 1999), whilst it was essential for the transcriptional activation of *DAX-1, SRY-1* and *P21* to name but a few (Parker et al., 1999). Other molecules such as platelet-derived growth factor (*PDGF*) and *BCL-2* have been shown to either be activated or repressed (Jin et. al., 1999 #51; Little et. al., 1995; Jin et. al., 1999) and WT1 was shown able to repress its own activity by self-association (Hastie, 1993). These transcriptional properties are essential for the tumour suppression role of WT1 in cell cycle regulation. The transactivational properties of WT1 are mainly attributed to the DNA binding properties of one isoform (WT1-KTS) (Bickmore et al., 1992; Hamilton et al., 1998; Little et al., 1995). DNA binding is mediated by the four, Kruppel-like C_2H_2 zinc fingers of WTI, three of which show a high homology to the three zinc fingers of the early growth response 1 gene (*EGR-1*) and can therefore also bind to the EGR-1 binding site. Two other potential binding sites within the protein allowed interaction with molecules such as *PDGF-1* and *BCL-2* respectively (Jin et al., 1999; Little et al., 1995).

It is likely that WT1 functions not only as a transcription factor but also has posttranscriptional roles. The proposed nontranscriptional roles are mostly carried out by the WT1+KTS isoform. Localisation of the protein to potential nuclear assembly sites suggested an interaction with elements of the cell splicing machinery (Larsson et. al., 1995; Hastie et. al., 2001; Charlieu et. al., 1995; Bickmore et. al., 1992; Kohsaka et. al., 1999). More recent studies have demonstrated a protein-protein interaction between WT1 and splicing factors including U2AF65 and small nuclear ribonucleoproteins (snRNPs) (Davies et al., 1998). Mechanisms by which WT1 may mediate aspects of mRNA processing are as yet unclear.

1.2.3 WT1 isoforms

Two alternative pre-mRNA splicing events have given rise to distinct gene products. The first alternative splice event resulted in the insertion of three amino acids, lysine, threonine and serine (KTS) between the third and fourth zinc finger. The isoforms are known as WT1+KTS (insertion of the three amino acids), and WT1-KTS (ommision of the three amino acids) (Figure 4) (Davies et al., 1998; Haber et al., 1990; Larsson et al., 1995; Renshaw et al., 1997). These two isoforms result from the use of alternative splice donor sites, separated by 9 nucleotides, at the 3' end of exon 9. WT1 zinc fingers 2, 3 and 4 are similar in structure to the zinc fingers of EGR-1 and the WT1-KTS isoform is able to bind DNA sequences resembling the EGR-1 consensus target site. Insertion of KTS was thought to disrupt the critical spacing between zinc fingers and alters the DNA binding capacity of the protein. It is for this reason that WT1-KTS is involved in transcriptional activation whilst WT1+KTS seems to play a role in RNA processing. For example WT1-KTS is linked to the induction of cell cycle arrest via the induction of the cyclin dependent kinase inhibitor P21 (Englert et al., 1997). Ectopic expression of WT1-KTS in some cell types leads to a G_1 cell cycle arrest. Following the stable transfection of WT1-KTS in rhaboid tumour cell lines, there was a marked increase in levels of BCL-2 (Del Rio-Tsonis et al., 1996). *DAX-1* and *MIS* activation by WT1-KTS are essential for gonadal development (Parker et al., 1999). Less is known about the roles of WT1+KTS in RNA processing but as mentioned earlier, it is associated with different molecules of the splicing machinery and mRNA processing.

The KTS isoforms are conserved throughout evolution in most species. The pufferfish *Fugu ripens* is one known exception where the KTS has been changed to KPS but the homologous isoforms still exists as WT1+KPS or WT1– KPS (Miles et al., 1998). Mutation studies showed that insertion of residues other

Figure 4. WT1+KTS and WT1-KTS isoforms

One of the two alternative splice events resulted in the insertion or deletion of three amino acids, lycine, threonine and serine (KTS) between the third and fourth zinc finger of the WT1 protein. Insertion of the KTS has been thought to disrupt the structure and hence the DNA binding of the isoform resulting in two isoforms with distinct properties. It is for this reason that WT1-KTS is thought to have higher DNA binding affinity and transactivational activity whilst WT1+KTS seems to play a role in RNA processing which may explain its association with splicing factors.

WT1 +KTS	WT1 -KTS	
+	+++	DNA binding affintity
No	Yes	Transcriptional Activation
Yes	No	Co-localisation with splicing speckles
+++	+++	RNA binding affintity

than KTS can influence the binding properties of WT1 in a yeast two-hybrid system (Davies et al., 2000). Following site directed mutagenesis, the C-terminal portion of WT1 including a KPS motif was introduced into a yeast two-hybrid system. The C:WT1+KPS displayed as strong an affinity as the C:WT1+KTS constructs in binding the splicing factor U2AF65. In fact, mutagenesis of any or all of the amino acids failed to affect the binding with U2AF65. The addition or deletion of amino acids also did not seem to alter protein function *in vitro*. Mutants with insertions containing additional amino acid (KTTS and KTATS) behaved similarly to the WT1+KTS protein, as did proteins with smaller insertions (AA and A). Only when the whole region was deleted, ΔKTS, was U2AF65 binding completely diminished. These results suggested that although the two isoforms have different properties, these differences do not rely on the precise amino acid content, or size of the insertion, rather important factor was the disruption of the zinc finger spacing resulting from the addition of extra amino acids (Davies et al., 2000).

The second alternative splice event occurs at exon 5. By inclusion or exclusion of the entire exon, isoforms are expressed that either have or do not have the 17 amino acids encoded by exon 5 located between the transactivation and DNA-binding domains. This alternative splice is evolutionarily conserved but only within mammals (Natoli et al., 2002b). The precise function of the 17 amino acid insertion remains unclear although some transcriptional activation is seen when the 17 amino acids were fused to a DNA binding domain in reporter assays, however, no phenotype was seen in mice when exon 5 was knocked out (Natoli et al., 2002a). Expression of the various WT1 isoforms is evolutionary conserved in terms of temporal and spatial patterns, and also the WT1-KTS;WT1+KTS splice isoform ratio. Transcripts encoding the KTS insertion appear to account for about 80% of the cellular mRNA, while those encoding

exon 5 account for about 60%. The ratio between WT1+KTS and WT1-KTS is approximately 2:1, this is highly conserved and essential for development, a fact illustrated by Frasier syndrome when these ratios were altered (Larsson et al., 1995; Little et al., 1995; Natoli et al., 2002b).

Additional isoforms of WT1 have been reported, resulting from RNA editing and the use of an upstream CUG initiation codon. An alternative initiation codon at an internal AUG results in yet another WT1 isoform, a truncated 36-38kDa protein. The physiological significance of these isoforms is still unclear (Scharnhorst et al., 1999) although recently it was shown that animals lacking a mammalian specific alternative N terminal extension isoform developed normally and were viable (Miles et al., 2003).

1.2.4 WT1, Denys Drash and Frasier syndromes

Denys Drash and Frasier syndromes were mentioned earlier in the introduction. They are key to understanding the role of WT1 in normal development as both are diseases of the genito-urinary system arising from mutations in the zinc finger region of the WT1 gene. DDS mutations of the WT1 gene are point mutations always affecting single amino acids in the zinc fingers. Mutations of WT1 involving the KTS alternative splice events were found in patients with Frasier syndrome and are therefore particularly relevant to this report as they underline the significance of the WT1 KTS isoforms. The abnormalities in kidney and sexual differentiation that are evident from patients with DDS and FS highlight the critical role of WT1 in normal gonadal as well as renal development.

Denys Drash is a rare, congenital childhood syndrome primarily affecting males. The genito-urinary defects are often variable but include ureteral abnormalities,

horseshoe kidneys, and urethral malformations (Coppes et al., 1993). Mesangial sclerosis, pseudohermaphrotidism and predisposition to Wilms' tumour are more developmental abnormalities that have been seen to arise from specific mutations of the WT1 gene (Bardeesy et al., 1994). Podocytes exhibited decreased or absent WT1 expression but persistent Pax-2 expression (Yang et al., 1999). Over 60 germline mutations have been described which leave much of the WT1 protein intact but affect the DNA-binding zinc finger domain. Most of the mutations were missense mutations within exons 8 and 9, and the others, deletions, insertions and premature terminations which resulted in truncated proteins. All of the mutations had one thing in common, they altered the structure of the DNA-binding domain, and changed the ability of the protein to bind DNA and RNA (Pelletier et al., 1991). It was suggested that the mutant protein acted in a dominant-negative manner, as DDS patients present more severe defects in comparison to patients with heterozygous deletions of WT1. In gene targeted experiments using a truncated form of the WT1 in the zinc finger region, mice demonstrated a phenotype with some of the characteristics of DDS, even though the mutant allele accounted for only 5% of the total amount of WT1 protein (Patek et al., 1999). The mutant protein may be altered in its ability to dimerise with the wild type protein and might perhaps associate with other gene products.

Frasier syndrome (FS) presents in a pattern similar to DDS with some key clinical differences (Frasier et al., 1964). The nephropathy tends to occur later in life and progression to renal failure is more gradual, suggesting that WT1 is necessary for normal kidney function even after development is completed. There is no predisposition to Wilms' tumour but gonadoblastoma has been seen to be far more common than in DDS and complete male to female gender reversal occur more frequently in patients with Frasier syndrome. Gonadal

development is normal in XX female patients. FS was found to arise from point mutations downstream of the second splice donor site in intron 9 (Barbaux et al., 1997). The intronic mutations interfere with recognition of the splice donor site and result in the loss of WT1+KTS from the mutated allele (with a presumptive concomitant rise in WT1–KTS production from the allele), while the wild type allele still produces both WT1+KTS and WT1–KTS isoforms. Therefore, changing the ratio of the two isoforms could be sufficient to cause the severe defects seen in FS. Although the two syndromes are different, due to their overlapping features and the involvement of WT1, there were cases when DDS or FS patients were misdiagnosed and vice versa, resulting in confusion of the clinical data (McTaggart et al., 2001). Classification should therefore be performed at the molecular level with DDS giving rise to a dominant negative function due to the presence of a mutant protein, and FS arising from a change in the isoform ratio but no production of abnormal WT1 proteins (Koziell and Grundy, 1999).

1.2.5 WT1 Transgenic animal data

The animal data on WT1 mutation has provided some of the best evidence for gene function. Bearing in mind that animal models have their limitations in studying the human form of a disease, and the fact that, to date, no mice have been seen to develop Wilms' tumour (one chimeric animal for the DDS truncation mutation was seen to develop a renal tumour (Patek et al., 1999)), they still supply a powerful tool in the research into WT1. Null mutations were introduced into the murine WT1 gene, by gene targeting in embryonic stem cells (ES cells) (Kreidberg et al., 1993). The mutation resulted in embryonic lethality in homozygotes (on certain strain backgrounds null mutants can survive till birth but then die shortly after) and mutant embryos demonstrated a failure to develop

kidneys and gonads. Specifically, at E11, the cells of the metanephric blastema underwent apoptosis, the UB failed to grown out from the WD, and the inductive events that lead to the formation of the metanephric kidney did not occur. In addition, the mutation caused abnormal development of the mesothelium, spleen, heart and lungs. This illustrates the crucial role that WT1 plays in early urogenital development. Previously, it was thought that heterozygous WT knockout mice had no phenotypic defects but recent data shows there is a degree of abnormal kidney function, illustrated by increased levels of albumin and protein in the urine, in comparison to negative levels in the Wild type (Wagner, 2003). Rescue of the null phenotype has been attempted to examine whether the human *WT1* gene is able to complement the knockout mutation in mice. This was done using a 280kb yeast artificial chromosome (YAC) in an attempt to introduce the entire genomic locus, to ensure proper expression of all the isoforms and correct transcriptional regulation of the *WT1* gene (Moore et al., 1999; Moore et al., 1998). The transgene only partially rescued the knockout phenotype when crossed onto the knockout background. These mice were viable for 48h after birth and although complete rescue of the epicardial and diaphragmatic abnormalities was achieved, these mice died. Further analysis of the kidneys of these mice showed renal abnormalities ranging from, failure of ureteric budding, branching, or normal nephrogenic development until formation of comma-shaped bodies. Mature glomeruli never formed however and this may result from the absence of crucial modifier genes or essential regulatory sequences, absent from the YAC. Interestingly, the YAC has been shown to rescue ocular defects that have been recently reported in $WT^{-/-}$ mutants, illustrating a role for WT1 in the normal development of the retina (Wagner et al., 2002).

Creation of a mouse model of DDS has also been attempted. Expression of a truncated form of WT1 from a DDS-like mutation, targeted to one of the endogenous *Wt1* alleles, did show features which are characteristic of patients with analogous mutations, such as diffuse mesangial sclerosis and gonad dysgenesis, however a mouse line carrying this mutation could not be established due to infertility associated with the mutation although it was reported that one mouse developed a renal tumour (Patek et al., 1999).

More recently, mouse strains have been generated in which a specific isoform of WT1 has been removed to identify functions of WT1+KTS and WT1-KTS (Hammes et al., 2001). Heterozygous mice with a reduction of WT1+KTS develop glomerulosclerosis and represent a model for Frasier syndrome, and show complete XY sex reversal (due to the reduction of Sry expression). Homozygous mutants of both strains die after birth from kidney defects. This data again demonstrates different functions for both splice variants. Lack of expression of WT1 in podocytes is a key factor in DDS patients, and it has been suggested that primary lesions in the podocytes causes glomerular disease which is one of the most common causes of renal failure. The mechanisms by which these glomerulopathies occur are poorly understood. It has been recently demonstrated, by combining *Wt1* null mice and inducible YAC transgenes, that reduced expression levels of WT1 result in some of these glomerular abnormalities depending on gene dosage (Moore et al., 1999). At the same time, the podocyte specific genes, *nphs1* and *podocalyxin* are dramatically downregulated in mice with decreased levels of Wt1 (Palmer et al., 2001), suggesting that these genes act downstream of *Wt1*.

Gene targeting of exon 5 of WT1, encoding the other splice event resulting in the presence or absence of 17 amino acids, has resulted in viable, fertile adult mice.

This data suggests that the mammal specific exon of WT1 is not essential for development or fertility (Natoli et al., 2002b). Similarly, the knockout of a mammal specific alternative leader also resulted in normal development and fertility in mice (Miles et al., 2003).

1.2.6 Role of WT1 during genito-urinary development

The expression pattern of WT1 during embryogenesis is highly complex. The gene has been shown to be only weakly expressed in uncondensed metanephric mesenchyme therefore it is likely that the initial differentiation is independent of WT1. During mesenchyme to epithelium transition when the comma-shaped and s-shaped bodies are formed there was a significant increase in levels of WT1. Expression reached its highest levels at the proximal part of the s shaped bodies where the glomerular podocytes are formed. Levels then decreased until expression was limited only to the podocytes of the BC by the time the kidney reached full development. The expression pattern of WT1 during kidney development allows us to infer WT1 activity is necessary for the transition of cells between mesenchyme to epithelium. As well as the kidney, high levels of WTI are found in the spleen, gonads, and the mesothelium layer surrounding the body cavity and thoracic organs (Armstrong et al., 1993; Little et al., 1992). The complex pattern of WT1 expression and the resulting phenotypes from mutations of the gene lead us to believe that *WT1* is required at multiple stages during kidney development. In the knockout (null) mice (Kreidberg et al., 1993), the metanephric blastema underwent apoptosis. Apoptosis even occured when this knockout blastema was recombined with ureteric buds from wild type animals in organ culture, suggesting it was necessary for both the inductive signal, inducing outgrowth of the ureter, and for receiving the survival signal from the ureteric bud (Kreidberg et al., 1993). A multitude of positive and negative feedback

mechanisms operate during the formation of the kidney. The mechanism that establishes the metanephric blastema remains unknown but the next key event is the expression of WT1. In its absence, the blastema undergoes spontaneous apoptosis, in its presence, the MM synthesises GDNF, which signals to the duct system via RET, which in turn signals back to the MM. WT1 is responsible for the subsequent development of the MM, and clearly has a role in growth. In its absence, cells undergo apoptosis and mutations can lead to uncontrolled proliferation as illustrated by Wilms' tumour.

PAX-2 interaction with WT1 is essential for the following phases of nephrogenesis in the blast cells that cap the duct tips and are the site of future nephrons (Ryan et al., 1995). PAX-2 was seen to be down regulated in the prepodocytes at the same time as WT1 is at it highest levels, and the inhibition of blast cell proliferation marking the cessation of nephrogenesis is likely to be regulated by WT1 (Mrowka and Schedl, 2000). Binding studies have shown that WT1 can repress *PAX-2* promoter activity but regulation of WT1 activity by PAX-2 has also been described. Insulin-like growth factor II (IGF-2) is thought to be another growth response gene in the proliferation of blast cells and has shown to be repressed by WT1 (Drummond et al., 1992). This could explain the increased levels of IGF-2 in Wilms' tumours where WT1 function has been perturbed. The late occurrence of FS and the expression of WT1 in podocytes (Guo et al., 2002b), which persists throughout adult life, and the glomerular abnormalities seen in the podocytes of DDS patients, allow us to argue that WT1 is also needed well beyond nephrogenesis.

The importance of WT1 in the gonads has also been illustrated by the phenotypes of mutant mice and human disease. WT1 is expressed diffusely in the undifferentiated gonads. Its expression becomes more restricted following

sexual differentiation, in the pre-Sertoli and Sertoli cells of the testis, and the follicle and epithelial cells of the ovary (Pritchard-Jones et al., 1990). This suggests that WT1 is required at the earliest stage of the undifferentiated gonad, before sex determination occurs and that it also has a later role within the supportive cells of the mature gonad. *WT1* mutations have been reported in undifferentiated gonadoblastomas arising in patients with DDS but not in more mature ovarian and testicular tumours (Pelletier et al., 1991). There is coexpression of WT1 and the orphan receptor SF1 in Sertoli cells and both transcription factors display similar knockout phenotypes. It is thought that there is an interaction between the two factors and the regulation of early gonad development by activation of SF1, through the direct binding of WT1-KTS, has been described (interestingly WT1+KTS does not interact with SF1). The interaction of the two proteins has a direct effect on the activation of the AMH promoter which is consistent with male to female sex reversal associated with DDS, resulting from the inactivation of WT1–KTS and hence, reduced expression of AMH.

DAX-1 is another nuclear orphan receptor whose function is linked to the role of WT1 in gonad development. DAX-1 protein also has been shown to have WT1 binding sites and may modulate the regulation of AMH by WT1 and SF1. This modulation of WT1 and SF1 is thought to repress AMH, preventing the regression of the Mullerian duct, thus promoting progression to female characteristics. Finally, the interaction between WT1 and SRY still remains unclear but SRY associated induction of WT1 transcripts has been described (Lee and Haber, 2001). WT1 function with relevance to gonadal differentiation is likely to involve interactions with these well-characterised regulators of gonadal development and others, which as yet, remain to be identified.

1.2.7 WT1 interacting proteins – Brain acidic soluble protein (BASP1)

Mechanisms by which WT1 function is regulated by interacting proteins have to some extent been covered in previous sections. To date, the protein has not been shown to associate with transcriptional co-repressors. As described previously proteins such as SF1 and Sry are thought to be co-activating proteins as well as proteins such as PAR-4 and WTAP (Little et al., 2000). The WT1 transcriptional suppression domain of WT1 is thought to be located within its N-terminus and is proposed to function by recruiting a cosuppressor protein to WT1 that blocks the function of the transcriptional activation domain. Using a functional assay, a group led by Dr Stefan Roberts, have provided evidence that the WT1 suppression domain contains a co-suppressor. Brain acidic soluble protein (BASP-1) has been identified as a component of the WT1 co-suppressor to regulate its transcription function during development (Carpenter et al., 2002). Despite no phenotypically difference in knockout mice of the 17amino acid alternative splice insert, the WT1 17AA isoform can be overexpressed in Wilms' tumours and other malignancies and has been shown to have effects both on cell division and cell survival. Protein truncations of WT1 were tested in an in vitro transcription assay. Analysis of Gal-4 fusion proteins described that just 10 amino acids of WT1 at the N-terminal were sufficient to confer inhibition of an SP1 transcriptional activation domain. The isolated WT1 suppression domain was able to titrate a cosuppressor, later identified to be BASP-1. The implications for the identification of a cosuppressor to WT1 are great, as they may give us an insight into mechanisms by which the protein functions.

1.3 Subcellular localisation of WT1

1.3.1 Sub nuclear compartmentalization

As described earlier, the WT1+KTS and WT1–KTS isoforms of WT1 have distinct roles dependent on their structure and their localisation within the nucleus. It can be assumed that protein structure may be the pivotal element, with alternative conformations resulting from differences in isoform structure or mutation that allow the binding of diverse groups of protein families (Section 1.2.7 describes the differential binding of some of the isoforms or mutants). These alterations in protein structure, including binding domains (DNA binding and RNA binding) and localisation signals, restrict the protein to specific regions of the nucleus and may allow it to interact with different factors. It is therefore necessary to understand the role and structure of the nucleus before we can understand how WT1 may function.

The nucleus was originally described in 1802 and was the first intracellular structure discovered. It has only been the development of powerful microscopy and molecular techniques since then, that have allowed in depth study of the nucleus. Findings from recent research have shown that the nucleus is a highly dynamic organelle containing distinct sub-compartments (Dundr and Misteli, 2001). These structures are characterised by the absence of delineating membranes but are still considered compartments for several reasons. Firstly, they contain specific resident proteins and can be morphologically identified by light and electron microscopy. More recently, most of them have been visualised in living cells by the use of green fluorescent protein (GFP) technology. Finally, some of these compartments can be isolated biochemically (Lamond and Earnshaw, 1998). The mechanism by which these subcellular compartments are isolated and processed has been the subject of much research and as yet,

remains unclear (Misteli, 2001a). The main function of the interphase nucleus includes transcription, pre-mRNA splicing and ribosome assembly.

1.3.2 The Nucleolus

The best studied nuclear component of the nucleus is the nucleolus. It is the most prominent nuclear structure originally discovered due to its high refractive index and density. It is assembled around clusters of tandemly repeated ribosomal genes which are transcribed by RNA pol I. The regions containing the tandem arrays of rDNA genes constitute the nucleolar-organising region (NOR) and are the basis of the structural organisation of the nucleolus responsible for the targeting of all processing and assembly components required for ribosome biosynthesis (Lyon and Lamond, 2000). The nucleolus itself can be separated into three distinct regions depending on their morphology. Fibrillar centres (FCs), are surrounded by dense fibrillar centres (DFCs), and granular components radiate out from the DFCs. Nascent rRNA transcripts move away from the DNA template and are detected first in the dense fibrillar component and later in the granular component (Carmo-Fonseca et al., 1991). Biogenesis of rRNA involves a complex set of post-transcriptional processing reactions and it is well established that the initial pre-RNA resides in the DFCs, whereas late processing events take place in the granular component. Finally pre-ribosomal particles are translocated to the cytoplasm through the nuclear pores. *In situ* hybridisation experiments have shown that active rDNA genes are located to the periphery of FCs and are excluded from the FC (Scheer and Hock, 1999). The DFCs are thought to be the site of transient accumulation of elongating and primary transcripts as indicated by the absence of rDNA from the DFC. Pre-rRNA cleavage is initiated in the DFC and is finished in the granular component. Nascent pre-RNA transcripts enter the DFC where they undergo a series of

processing steps. Later, processing and assembly steps occur in the granular component before they are fully processed and with the association of ribosomal proteins, are assembled into large and small preribosomal subunits before being exported to the cytoplasm (Dundr and Misteli, 2001). The nucleolus is also a site for the functional pathways of methylation and of the conversion of uridine to pseudouridine of pre-RNA, which also occur in DFCs. These processing and modification events are assisted by small nuclear ribonucleoproteins (snRNPs). Two major classes of small nucleolar RNAs have been identified, some of which (U3, U8, U14, and U22) are required for pre-rRNA cleavage (Scheer and Hock, 1999). Fibrillarin is a protein located at the DFCs and necessary for pre-rRNA methylation. There is evidence suggesting that the nucleolus not only carries out ribosome biogenesis, but it is also the site of assembly and interaction between multiple ribonucleoprotein machines, as well as processing and transcriptional modification of splieceosomal small nuclear RNA (U6)(Dundr and Misteli, 2002).

In addition to being a site dedicated to ribosome biogenesis, and maturation of transcripts, the nucleolus acts as a sequestering compartment for cell cycle regulatory complexes. For example, the nucleolus is implicated in the regulation of the tumour-suppressor protein p53, retention of the p53 interacting protein, MDM2 within the nucleolus by p19ARF, prevents the degradation of p53 and results in the activation of p53 nuclear import and accumulation. Primary fibroblasts isolated from p19ARF deficient animals are able to proliferate indefinitely, suggesting the presence of p19ARF in the nucleolus is a key regulator of proliferation and the cell cycle (Lohrum et al., 2000).

In animal and plant cells, nucleoli are very dynamic structures. Fully active nucleoli are large, with no clear boundaries visible between the three components. In contast, cells following induced transcriptional arrest

(Actinomycin D or RNAse inhibition treatment), have small and compact nucleoli where the three components tend to segregate into adjacent blocks (Olson et al., 2000). The nucleolus of multicellular organisms disassembles during mitosis and various nucleolar proteins leave the structure. The granular centre of the nucleolus disappears first followed by the DFC as the NORs simultaneously become visible on chromosomes. At the end of mitosis, small round structures called pre-nucleolar bodies (PNBs) appear in the newly formed nuclei, before the onset of transcription initiation by RNA pol I triggering the recruitment of PNBs to the NORs to form a complete nucleolus (Dundr and Misteli, 2001).

1.3.3 Cajal bodies and Coilin

Initially described as "nuclear accessory bodies" by Cajal over a century ago, also called coiled bodies, due to their characteristic appearance as coiled fibrillar strands in using electron microscopy, Cajal bodies (CBs) are small spherical structures present as 1-5 copies per nucleus and are of varying size. CBs are generally found within the nucleus and are highly mobile structures, mostly found within the nucleoplasm but known to associate with, and maybe even pass through the nucleolus (Matera, 1998). The nucleopcytoplasmic-shuttling protein p80-coilin has been identified as a marker of CBs and has lead to evidence suggesting the functional associated of the CBs and the nucleolus (Hebert et al., 2001). Firstly, the formation of CBs inside the nucleolus can be induced by a single point mutation of p80-coilin as well as the Nopp140 protein, which is known to associate with coilin *in vitro*. Furthermore, treatment of cells with the protein phosphatase inhibitor Okadaic acid causes the redistribution of Coilin to the nucleolus.

Recent research suggests that CBs might be involved in transport and maturation of snRNPs. GFP-tagged proteins firstly localise to CBs before they pass through the nucleolus and reach their final destination in the FC (Matera, 1999; Tucker et al., 2001). An alternative model for CB function suggests that CBs are the assembly sites for the transcription machinery of the nucleus (Hebert et al., 2001). This is supported by the observation that factors involved in transcription and capping were initially targeted to CBs. The observed localisation of some pol I and pol II components to CBs has indicated that CBs also function as a platform for assembly of pol I and pol II transcriptiosomes. Although much is to be discovered about the precise role of CBs, there is a definite link between CBs and the nucleolus. CBs may be involved in trafficking and storage of proteins between the nucleoplasm and nucleolus and like the other components of the nucleus, have a dynamic structure.

1.3.4 Speckles and paraspeckle domains

Splicing of pre-mRNA takes place in the nucleus by a two-step transesterification mechanism characterised by the "spliceosome" or splicing machinery. The major subunits of the splicing machinery are the U1, U2, U5 and U4/U6 snRNAs, which assemble with additional protein splicing factors to form the active complex. Each snRNP comprises one or two small nuclear RNAs (snRNAs). The spliceosome is another dynamic structure that goes through cycles of assembly and disassembly during the splicing of each intron. Splicing factors are located in clusters of interchromatic granule-associated zones, ("speckles"), gem bodies (see below) and coiled bodies. Immunofluorescence, microscopy and GFP data has shown that most active genes are either excluded from, or lie at the very periphery of these speckles and that many of the splicing factors such as U2AF 35, are located to these areas of interchromatin granules. It is for this

reason that a speckled staining pattern colocalises with many splicing factors. Often associated with the Cajal bodies are the gem bodies, these nuclear bodies are found in the nucleus and cytoplasm. The survival of motor neurons protein (SMN) was first identified as mutated in the disease spinal muscular atrophy. It has since been found that SMN is tightly associated with gem bodies in the nucleous and interacts with Sm proteins, another component of spliceosomal SnRNPs and splicing machinery. Hence the gem bodies are also involved in the mechanisms of splicing.

Recently a proteomic study of purified human nucleoli has identified novel proteins, including the Paraspeckle Protein-1 (PSP1) (Andersen et al., 2002). This study showed that PSP1 accumulated in a new nucleoplasmic compartment, named paraspeckles. 10 to 20 paraspeckles were detected in the nuclei of a number of human cell types. The paraspeckles corresponded to discreet bodies within the nucleoplasm, often located adjacent to splicing factors which relocalised at the nuclear periphery when transcription is inhibited (Fox et al., 2002). The function of these bodies is unclear but they could provide yet another clue to the functional complexity of the nucleus.

1.3.5 Nuclear proteins and localisation signals

Proteins in common pathways often concentrate into specific areas of the nucleus. This was one of the ways in which the different compartments of the nucleus were identified. For example, even though proteins involved in pre-mRNA splicing moved rapidly around the nucleus, they appeared to concentrate into speckles, in the same way as the proteins involved in rDNA processing and ribosome biogenesis located within the nucleolus. A combination of mass spectrometry, in combination with database analysis and the possibility of

purifying and fractionating the nucleus, have allowed the identification of the nuclear protein content. Proteomics, has allowed the characterization of subnuclear components including the spliceosome, nucleolus and nuclear pore complex to allow investigators to identify families of proteins and hence elucidate some of the characteristics of the proteins and the functions of the organelles in which they reside. Proteomics has added to our knowledge of some novel amino acid sequence motifs, such as nucleolar localisation signals (NLS) and novel subcompartments of the nucleus (the paraspeckle domain) (Bickmore and Sutherland, 2002).

The ability of a protein to localise to a particular subcompartment of the nucleus could be due to its amino acid content, and isoelectric point (pI). For example, the speckles and Cajal bodies contain the most basic proteins whereas proteins located to the periphery of the nucleus tend to be more acidic. A variation of the pI of different proteins, reflects differences in the amino acid content. Nuclear proteins often have higher occurrences of lysine and arginine residues, perhaps due to the presence of nuclear localisation signals in these proteins. These proteins are often found located to the interior of the nucleus while proteins without an NLS may be found at the nuclear periphery suggesting they use diffusion as a mechanism to enter the nucleus.

Proteomic analysis of the motifs showed that 80-86% of nuclear proteins contained an NLS, the others were thought to enter the nucleus by diffusion or by their association with other proteins. Apart from an NLS, proteins localizing to the nucleolus tended to have both nucleic acid binding domains and protein-protein interaction domains. Speckle-localizing proteins had more complex structures with over half of their proteins containing RNA recognition motifs. Although the nucleolus is also involved in RNA processing, the RNA recognition

domains were not so abundant in the nucleolus. Despite the functional relationship between speckles and Cajal bodies, the Sm proteins were the one type of common protein between the two components. There were of course many proteins that fell outside of the characterisation but proteomics remains a potentially powerful tool in understanding nuclear organisation (Bickmore and Sutherland, 2002; Lamond and Earnshaw, 1998; Lamond and Gasser, 2002).

The presence of NLSs have been well characterised in proteins. However, the existence of nucleolar localisation signals (NoLS) is much less clear. A prerequisite for nucleolar accumulation is translocation of a protein from the cytoplasm to the nucleoplasm. In the nucleoplasm, proteins may bind by their functional domains. Nucleolar accumulation could then proceed by two possible mechanisms: one in which the process is an active mechanism, either mediated by a signal in the protein that directs it to the nucleolus, or mediated by its association with other molecules or complexes that are actively transported to the nucleolus. The second process would involve a passive mechanism of nucleolar entry, mediated by diffusion and accumulation would result from retention by binding to nucleolar components. Research into this area has provided evidence for both mechanisms.

It is known that NoLS signals are often basic regions and many proteins which accumulate in the nucleolus contain basic elements which, when knocked out, destroy nucleolar localisation in the protein. The basic region of p80-coilin when uncovered by the deletion of an acidic region, results in the accumulation of coilin in the nucleolus (Tucker et al., 2000). Herpesvirus protein MEQ and PRRSV nucleocaspid protein, and two cellular proteins, rat spermatidal protein TP2 and human HICp40 have all been reported to contain NoLSs consisting of stretches of basic residues. Other data describes characterisation of specific amino acid

sequences, point mutations of which, results in the abolishment of nucleolar localisation. For example the nucleolar retention of U3 snRNA is mediated by a C'D box motif (Speckmann et al., 1999). The NoLS of human angiogenin (amino acids IMRRRGL) is sufficient to import GFP into the nucleolus (Lixin et al., 2001). The ING1 candidate tumour suppressor uses the RRQR amino acid sequence to direct GFP to the nucleolus. This sequence was also conserved in other nucleolar proteins including HIV-Tat and HIV-Ret (Scott et al., 2001). One group has described proline-rich nucleolar retention motifs that require phosphorylation to regulate them (Catez et al., 2002). Another group described the presence of two NoLSs within one protein, both of which were required for nucleolar retention and the deletion of either was sufficient to impede localisation (Scott et al., 2001). Many of the sequences involved in nucleolar localisation seemed to involve Arginine repeats. Arginine is a basic amino acid, and the requirement for a simple basic repeat structure is consistent with data favoring the passive method of nucleolar localisation, however, point mutation of these specific sequences is enough to change nucleolar localisation which suggests a more active method is involved.

As the data suggest, there are definite factors involved in nucleolar retention, and this may involve a mixture of passive and active mechanisms. Research has uncovered a number of sequences involved in nucleolar localisation and many of the proteins involved can be grouped together by their shared characteristics.

1.3.6 WT1 subcellular localisation

Colocalisation and Immunoprecipitation studies have shown that the subnuclear localisation pattern of WT1 was very similar to the speckled pattern described for splicing factors. They colocalise in the two major nuclear domains known to

contain snRNPs, the speckles and coiled bodies. The subnuclear localisation of WT1 has been shown to be dynamic, with actinomycin D treatment, known to inhibit cellular transcription and causing some splicing factors to relocate to large foci or surround the remnants of the nucleolus, leading WT1 to locate to areas surrounding the nucleoli (Englert, 1998; Larsson et al., 1995).

WT1 was coimmunoprecipitated by monoclonal antibodies against a number of well-defined splicing factors and transcription factors such as U3, a component of the splicing machinery. When the individual splice isoforms were investigated, the subnuclear localisation depended on the presence or absence of the KTS insert. WT1-KTS GFP constructs localised in a diffuse pattern with some domains of localisation but no nucleolar staining in Cos7 cells. WT1–KTS isoforms failed to relocate to the nucleolus upon actinomycin D treatment whereas WT1+KTS GFP constructs localised to speckled areas in a similar pattern to that of many speckling factors. Actinomycin D treatment of WT1+KTS transfected cells, caused the WT1+KTS to relocate to the periphery of the nucleus. Staining the cells with antibodies specific for splicing and transcription factors identified WT1-KTS to be colocalised in a transcription factor-like pattern (colocalisation with the transcription factor Sp1), and WT1+KTS to be colocalising with splicing speckles (Larsson et al., 1995), though location of WT1+KTS was different from the essential splicing factor SC35 (Englert et al., 1995). This correlates with the idea of WT1-KTS being involved in transcriptional activation and WT1+KTSs involvement with the splicing machinery.

Interestingly, expression of WTAR, a naturally occurring Wilms' tumour associated mutation with an in-frame deletion of Zinc finger 3, and WT1 delZ, a construct lacking the entire zinc finger domain (analogous to a Denys Drash mutation), result in enhanced speckling (Englert et al., 1995). It is suggested

from this data that the N-terminal region of the WT1 protein is required for its association with speckles, a hypothesis backed up by the study of deletion constructs showing that amino acids 76-120 of the WT1 protein were enough to confer the speckling characteristics (Englert, 1998). Involvement of the KTS in binding to the splicing factor U2AF65 has been mentioned previously. Davies et al. (2000) used KTS mutations (replacement of the KTS region with various insertions, discussed further in Section XX (Chapter 4) to investigate the effects on nuclear distribution. The mutant proteins were transiently transfected into Cos7 cells and the nuclear localisation examined. All the mutants displayed good colocalisation with splice factors and showed similar speckled patterns to WT1+KTS within the nucleus. Only ΔKTS (deletion of the entire KTS region) mutants adopted the WT1-KTS distribution patterns. This data corroborates the group's findings that differences in the function of the two KTS isoforms result from disruption of the zinc fingers. Interestingly, although WT1+KTS binds to U2AF65 and the speckling pattern results from the presence of WT1+KTS and not WT1 –KTS, the N terminus is required for the speckling (but not binding with U2AF65). Thus the localisation of WT1 with speckles and the association with U2AF65, a factor of the splicing machinery, are separable features of WT1.

1.4 Aims of the thesis

The underlying reason for studying the KTS isoforms of WT1 is their implication in disease phenotypes. Animal experiments and human diseases have highlighted that the balance of these isoforms is essential for normal genito-urinary development. Patients with DDS produce dominant mutant WT proteins impeding the function of normal protein. This can be reconstructed in animal models where a truncation of WT1 mimicking a mutation analogous to DDS results in similar phenotypes of the disease in mice. In Frasier syndrome, patients lose the production of WT1+KTS from the mutant allele, resulting in a reversal of the normal 2:1 ratio of WT1+KTS: WT1-KTS. Overall, the amount of protein appeared to be unchanged with elevated levels of –KTS being produced, at the expense of WT1+KTS which was reduced to half the normal amount. Mice with similar heterozygous mutations of WT1+KTS had a phenotype with features similar to FS patients. That this isoform ratio is crucial can be seen not only by human disease but by the fact that homozygous mice for either mutations of WT1+KTS or WT1–KTS, die from kidney defects. Furthermore, the isoforms appear to play different roles in transcription and RNA processing and this is reflected both by their interactions with other proteins, and their subcellular localisation.

There are however, many questions that still remain unclear and this project attempts to answer some of them by investigating the function of the isoforms both *in vivo* in the mouse (Chapter 3) and *in vitro*, with cell culture experiments (Chapter 4). The report can be divided into two areas: Firstly, the investigation of the differential localisation of the WT1+KTS and WT1–KTS isoforms in cell culture with regards to their function. The second area of experiments

investigates the overexpression of a single WT1 isoform with regards to genito-urinary development in the mouse.

1.4.1 Overexpression of WT1-KTS in transgenic animals

Transgenic experiments were used alongside cell culture experiments to give a comparison of *in vitro* versus *in vivo* analysis of the role of KTS isoforms in genito-urinary development. The mice reported to have heterozygous mutations within either isoform provide a good model for the effect of reduced levels of isoform in development. The effects of reduced levels of WT1+KTS resulted in animals presenting clinical characteristics analogous to Frasier Syndrome. Another method of looking at one isoform in isolation from another is to look at the overexpression of one particular isoform. Previously in our lab, transgenic lines were generated overexpressing WT1-KTS by the insertion of a transgene containing WT1-KTS under the regulation of the IGF2 P3 promoter and H19 enhancer sequences. The P3/H19 regulatory region allows the transgene to be expressed temporally and spatially in at least some sites of WT1 expression allowing the overexpression of WT1-KTS in wild type mice. To look at the effects of the transgene on a WT1 null background, mice carrying the transgene (P3:WT1-KTS) were crossed to mice heterozygous for the null allele ($WT1^{+/-}$). As WT1 homozygous knockouts ($WT1^{-/-}$) are embryonic lethal, the resulting $WT1^{-/-}$;P3:WT1-KTS mice were analysed at embryonic day 11.5 to allow examination for any evidence of rescue of the null phenotype by the expression of the single WT1–KTS isoform. Analysis of heterozygous WT1 knockout animals expressing the transgene ($WT1^{+/-}$;P3:WT1-KTS) was also carried out to identify possible dosage effects of changes in isoform ratios.

Analysis of the resulting animals was carried out with a variety of methods. Animals were genotyped and both histological and molecular analyses used to identify any phenotypical changes. Depending on phenotypic abnormalities, the organs of mutant animals, or mutant embryos underwent a series of tests. Detection of antibodies to proteins of interest identified changes in the normal expression of these proteins, abnormal proliferation or apoptosis events were also characterised in samples of interest. Finally, kidney function was assessed by urine analysis in adult mice with no other detectable phenotypes. These experiments answered questions about the function of WT1–KTS when isolated from WT1+KTS and provided one possible method of developing a mouse model for Frasier syndrome. Embryos with no WT1+KTS carrying the WT1–KTS transgene ($WT1^{-/-}$;P3:WT1-KTS), animals with normal endogenous WT1 isoform ratios carrying the WT1–KTS transgene ($WT1^{+/+}$;P3:WT1-KTS) (therefore increasing the amount of WT1–KTS while maintaining normal levels of WT1+KTS), animals with half the amount of WT1+KTS and WT1–KTS carrying the transgene ($WT1^{+/-}$;P3:WT1-KTS) (therefore these animals expressed half the amount of both endogenous isoforms but also expressed transgenic WT1–KTS) were studied with the aim of evaluating isoform dosage effects on genito-urinary development.

The expression pattern of WT1 protein, apoptosis and proliferation in the Ob mouse, a mutant previously described in the group with defective spermatogenesis, was used for comparison with WT1 transgenic mice with genito-urinary defects. This highlighted differences in abnormalities occurring from defects in the WT1 pathway as opposed to other mechanisms involved in renal and gonad development. The Ob mouse mutant provided us with positive controls for abnormalities of protein expression, histological tests and analysis of

kidney function and allowed us to compare different mechanisms resulting in the pathogenesis of developmental disorders.

1.4.2 Investigation of the differential subcellular localisation of the KTS isoforms

To investigate the differential subcellular localisation of WT1, a series of cell culture experiments were carried out. It has been shown that WT1+KTS and WT1-KTS localise to different structures within the nucleus. Firstly, the nature of this localisation was characterised in a number of cell lines either expressing or not expressing endogenous WT1, using GFP:WT1+KTS and GFP:WT1-KTS fusion proteins. Treatment with Actinomycin D inhibits the activity of RNA polymerase in cells so the localisation of the KTS isoforms in transcriptionally quiescent cells upon actinomycin D treatment was also investigated. This data allowed a visualisation of the subcellular locaslisation of KTS isoforms, to identify those regions of the cell to which wild type WT1 KTS isoforms locates, both under normal conditions, and in response to the inhibition of transcription.

After a general characterisation of WT1-KTS and WT1+KTS localisation had been made, the next step was to identify which organelles and sub-compartments the molecules localised to. This was done by colocalisation analysis with molecules known to be associated with different compartments of the cell through the use of antibodies and GFP fusion proteins. Upon complete analysis of the subcellular localisation of wild type KTS isoforms, the final objective was to identify mutations in the structure of the protein that affect its function or its localisation within the cell and hence identify regions of importance in the proteins. This was achieved by mutational analysis of the isoforms to create mutants by site directed mutagenesis. Analysis of these mutants gave us

insights into the protein structure with relation to its function. Finally, any regions which when mutated changed the localisation of the protein alerted us to sequences encoding a putative signal directing the protein to its correct location.

Chapter 2

MATERIALS AND METHODS

2.1 Molecular biology and Microbiology

2.1.1 Growth media, antibiotics, and bacterial host-strains

The growth media used for bacterial cultures, preparation and storage are as follows:

LB (Luria-Bertani) medium; 1% (w/v) bacto-tryptone, 0.5% (w/v) bacto-yeast extract, 1% (w/v) NaCl

LB agar; as above with the addition of 1% (w/v) agar

SOB medium; 2% (w/v) bacto-tryptone, 0.5% (w/v) bacto-yeast extract, 0.05% NaCl, 2.5mM, 2.5mM KCL, 10mM $MgCl_2$.

All media was autoclaved to sterilise for 20 minutes at 15lb/sq. in.

All bacteria were cultured in LB medium in a shaking incubator (G25 New Brunswick Scientific), or on Agar plates at 37°C overnight. Plasmid vectors containing antibiotic resistance genes were grown in media supplemented with the appropriate antibiotic:

Ampicillin or Carbenacillin (sigma) 50μg/μl. Bacteria transformed with vectors containing the lacZ gene such as pBluescript II (Stratagene), were grown on LB agar plates in the presence of IPTG (isopropyl-β-D-thiogalactopyranoside) and X-GAL (5-bromo-4-chloro-3-idoyl-β-D-thiogalactopyranoside) as detailed in Sambrook *et al.* 1989. For short-term storage of bacterial cultures, stock plates were prepared by streaking the desired culture onto solid medium. These stocks were stored at 4°C. Long-term stocks were prepared by the addition of sterile

glycerol (BDH) to overnight bacterial cultures to a final concentration of 20% (v/v). These stocks were kept indefinitely at -70°C.

2.1.2 Cloning vectors

The following cloning vectors and constructs were used for subsequent experiments.

Cloning Vector	Size	Vector Details	Source
pBluescript II KS+	2.96 kb	Phagemid cloning vector Ampicillin resistance	Stratagene
pcDNA3	5.4 kb	Cloning vector Ampicillin resistance	Invitrogen
pGFP	6.1 kb	PcDNA3 containing 714bp cDNA encoding GFP Ampicillin resistance	Dr James Dutton University of Bath
NucGFP	6.1 kb	PcDNA3 containing 714bp cDNA encoding GFP Ampicillin resistance	Dr David Tosh University of Bath
PGFP-WT1+KTS PGFP-WT1-KTS PGFP-WT1DDS	8.6 kb	PGFP containing WT1 coding cDNA, either with WT1+KTS, WT1-KTS or WT1DDS stop mutation R394	Dr James Dutton University of Bath

2.1.3 Preparation of electrocompetent DH10B bacteria

The bacteria were streaked out from a frozen glycerol stock onto an SOB-Mg agar plate (15g agar per litre of SOB Section 2.1.1, and 5ml sterile 2M $MgCl_2$

was added just before pouring) and grown up overnight in a 37°C incubator. A single colony was then grown up in 1ml of SOB-Mg media and then inoculated into a 500ml flask containing 50ml SOB. The culture was grown for 12 hours at 37°C in an orbital shaker. 4ml of the culture was used to seed 400ml of SOB, incubated at 37°C with shaking until OD_{550} = 0.75. The cells were collected in chilled 250ml beakers and pelleted by centrifugation at 4500rpm at 4°C for 12 minutes, the supernatant was decanted and cells kept on ice. In the cold room the pellets were resuspended in 200ml of chilled sterile 10% glycerol and then pelleted before another 200ml 10% glycerol was used to resuspend them. The cells were pelleted a final time and all the supernatant removed. The cells were resuspended and pooled and the OD measured and adjusted to a density of 250 OD units per ml. Finally the cells were stored in 40μl aliquots and snap frozen on dry ice/ethanol and stored at -80°C.

2.1.4.1 Transformation of DNA into DH10B cells by electroporation

40μl DH10B electrocompetent cells were thawed on ice 2μl of the DNA or ligation mix were added and the reaction held on ice for 45 seconds. The cells and DNA were placed in a chilled Pulser cuvette, O.1cm electrode (BIO RAD). The cuvettes were placed in the eloectroporator (Gene Pulsor set to 1.25kV) and the voltage applied. 1 ml of SOB was then immediately added and the sample transferred to a 10ml tube (Falcon) and incubated at 37°C for 1 hour. 10μl and 100μl of the transformations were then plated onto LB agar plates.

2.1.4.2 Transformation of DNA into DH5α chemically competent cells

40μl competent cells were thawed on ice, and 2μl of the DNA or ligation were added. This reaction was incubated on ice for 30 minutes and then heat

shocked at 90°C for 42 seconds. The reaction was then incubated on ice for a further 10 minutes before the addition of 1ml pre-warmed LB. The transformations were shaken for 1 hour at 37°C in a shaker incubator before being plated out (100μl of transformation) onto LB agar with appropriate antibody selection.

2.1.4.3 Transformation of DNA into XL-10 Ultra competent cells (Stratagene)
These cells were used when increased transformation efficiency was required. The manufacturers protocol was followed as a guide. An aliquot of the cells was thawed on ice. Each aliquot contained about 140μl cells, enough for 2 transformation reactions. 3μl 2-Mercaptoethanol (Stratagene) was added to 70μl of cells in a 15ml tube (Falcon). The tubes were incubated on ice for 10 minutes with regular swirling. 1.5μl DNA was added to the tubes and they were incubated on ice for a further 30 minutes. Following incubation, the tubes were heat shocked at 42°C for 30 seconds and placed on ice for 2 minutes. After the addition of pre-warmed LB, the tubes were placed in a shaker incubator for 1 hour before plating 200μl onto LB Agar plates with appropriate antibiotic selection.

2.1.5 Plasmid miniprep protocol
2 ml aliquots of LB broth supplemented with 50μg/ml ampicillin were inoculated with the required bacterial clone and incubated overnight at 37°C in an orbital incubator with vigorous agitation. 1.5ml of the overnight culture was placed into an eppendorf tube and pelleted by centrifugation at 12,000rpm for 2 minutes. The supernatant was removed and 400μl of resuspension buffer was added (50mM Tris.HCl pH 8.5, 5.0mM EDTA, 15% sucrose) and the cell pellet

resuspended by vortexing. 50µl (12mg/ml in sucrose resuspension buffer) was added and the sample incubated at room temperature for 5 minutes. 300µl lysis buffer was added (70mM Tris.HCl pH 8.0, 70mM EDTA, 50mM EGTA, 0.2% Triton X-100, and solution titrated to pH8.0 with NaOH), the sample mixed and incubated at 70°C for 10 minutes, followed by centrifugation for 10 minutes at 13,000rpm. The resulting lysed cell pellet was removed using a toothpick and 1µl Diethyl pyrocarbonate (DEPC) was added. The sample was incubated at 70°C for 10 minutes, incubated on ice for 10 minutes, centrifuged at 13,000rpm for 2 minutes and the supernatant poured into a fresh tube. 900µl 100% EtOH was used to precipitate the DNA at room temperature and centrifuged for 15 minutes to pellet the DNA. The pellet was washed with 200µl 70% EtOH which was removed after centrifugation, the pellet was air dried and resuspended in 55µl TE with 10µg/ml of RNase added.

2.1.6 Large Scale plasmid preparation

Large-scale preparations (Maxi preps) were carried out using the Concert prep kit (Gibco) according to the manufacturers protocol.

2.1.7 Restriction digests

All restriction digestions were carried out in the buffer conditions recommended by the manufacturer (Promega) as most suitable for a particular enzyme. All enzymes used were Promega enzymes. The reactions were carried out in 10-100µl final volume with 1-5 units of enzyme per µg of DNA. For genomic tail digests, 45µl DNA containing approximately 500µg of DNA from a genomic preparation was used in a 50µl reaction with 0.5µl enzyme and 5µl buffer. These

reactions were incubated at the temperature recommended by the manufacturers overnight. When digesting plasmid DNA from minipreps, 5μl of the preparation was used with 1μl of enzyme and 1μl 10x buffer in a 10μl reaction. These reactions were left for at least 1 hour at appropriate temperatures. The enzyme was often heat inactivated at 75°C for 10 minutes or reactions which were to undergo further digestion were extracted with phenol:chloroform:isoamyl alcohol (25:24:1), and ethanol precipitation then resuspended in water before subsequent use.

2.1.8 DNA modification

To fill-in DNA with 3' overhangs DNA polymerase 1 large fragment (Klenow fragment) was used (1 unit) in the presence of dGTP, dATP, dTTP and dCTP (each to a final concentration of 1mM), the Promega core buffer was used with the enzyme, and the reaction was allowed to proceed at room temperature for 10 minutes. To render blunt ends of DNA with 5' overhangs, T7 polymerase was used in the presence of dNTPs and these were added to the heat inactivated restriction digest then incubated, for 10 minutes at room temperature.

2.1.9 Ligation of DNA molecules

The correct fragment of DNA was excise and purified by Qiagen gel extraction and ligated as follows. To obtain the optimal ratio of vector to insert DNA two combinations, 1:1 and 1:3 molar ratio of vector to insert were tried. Up to 100ng of insert and vector DNA was used with 1 unit of T4 ligase (Promega) in 10 x ligation buffer (30mM Tris.HCl , pH 7.8, 10mM MgCl2, 10mM DDT, 1mM ATP) in a final volume of 10μl. The ligation reactions were incubated overnight at room

temperature. The ligations were transformed and analysed by electrophoresis and digestion.

2.1.10 Agarose gel electrophoresis

Agarose gel electrophoresis was used for both analysis and separation of plasmid DNA and restriction fragments (Sambrook *et al.* 1989). 1% (w/v) agarose gels (1g agarose (USB) dissolved in 100ml 1x TAE) were used for most plasmid or genomic DNA analysis or separation and 2% gels were used for analysis of PCR products. Gels were made and electrophoresed in 1x TAE buffer (40mM Tris-acetate, 1mM EDTA). The agarose was dissolved by heating in a microwave and allowed to cool to around 55°C before the addition of ethidium bromide to a final concentration of 0.5μg/μl. The gel was then poured into gel trays (Bio Rad) and run at 60-100V for 1-6 hours. The DNA was visualised under long wavelength UV illumination on a transilluminator and photographs were taken using a Nikon imaging system. DNA size and quantity were estimated by comparison with standards of known size such as 1kb or 100bp DNA ladders from Promega.

2.1.11 Purification of DNA by Gel Extraction (Qiagen gel extraction protocol)

The gel slice containing the DNA fragment of interest was cut out of the agarose gel and 3x volume solubilisation buffer (Qiagen UK gel extraction kit) was added. The sample was incubated at 60°C with regular vortexing until the agarose gel had completely dissolved. 1x the volume of propanol was added and the sample was poured into a Qiagen spin column placed in a collecting column. The column was centrifuged for 1 minute at 13,000rpm and the solution in the column was discarded. 500μl solubilisation buffer was added to the spin column and

centrifuged for 1 minute at 13,000rpm. The column was washed by addition of 750μl of wash buffer which was allowed to stand for 1 minute before centrifuging for 1 minute at 13,000rpm. Finally the DNA was eluted by the addition of 30μl TE which was left for one minute before centrifuging for 1 minute at 13,000rpm.

2.1.12 Site directed mutagenesis

Following the Stratagene Quikchange protocol. Two WT1 20-nucleotide primers (forward and reverse) were designed across the WT1 region of interest flanking the potential nucleolar localisation signal to be mutated with an approximately equal number of bases on either side of the site to be mutated. The primers include the mutated nucleotides instead of the wild type base (primers produced by Invitrogen). Mutagenesis PCR was carried out on 200ng of the relevant plasmid using a Techne thermo cycler. Reactions were as follows: 200ng DNA, 25μM dNTP mix, 40μM reverse and forward primers, 5μl 10x buffer, in a total volume 50μl. The reactions were placed in the thermo-cycler at 95°C for 5 minutes and then allowed to cool to room temperature before being incubated on ice. 1μl pfu turbo was added to each reaction and placed back in the thermo-cycler on the mutagenesis programme: 55°C for 25min then 18 cycles of 95°C 1 minute, 55°C 1 minute, 68°C 20 minutes. When the programme was complete, 10μl of each reaction was analysed by agarose electrophoresis, the remainder was digested with 1μl Dpn1 (NEB) for 1 hour. 1μl of this final reaction was transformed into electrocompetent cells then after DNA preparation, the mutants were sequenced with appropriate primers.

2.1.13 Sequencing

All sequencing was carried out in the University of Bath Sequencing facility using the ABI prism sequencer. Sequencing reactions were set up containing 5pmol DNA, sequencing primers in a total of 6μl.

2.2 Transgenic animal experiments

2.2.1 Mouse breeding plan

WT1 knockout (WT1KO) strains were maintained. WT1KO is a null mutation resulting from targeted mutation of exon 1 of *Wt1* (Kreidberg et al., 1993). In addition, 3 strains of mice expression a WT1-KTS overexpression construct (P3:WT1-KTS) (Duarte, 1997) were also maintained (Wani, Wefi and Wines). The WT1KO mice were crossed with the P3:WT1-KTS and the resulting litters were genotyped. Mice heterozygous for the WT1KO allele, carrying the transgene ($WT1^{+/-}$;P3:WT1-KTS) were bred and crossed to $WT1^{+/-}$ mice. The females were checked daily for the presence of a vaginal plug and then sacrificed 11 days after the appearance of a plug. The embryos were presumed to be 11.5 days into gestation at this point. Adult mice from the age of 4 months were also monitored and sacrificed for histological analysis.

2.2.2 Genomic DNA preparation

Approximately 0.5cm tail tip biopsies were taken from anaesthetised mice and 525μl tail buffer (50mM Tris. HCl pH 8.0, 100mM EDTA, 100mM NaCl, 1% SDS), and 35μl (10mg/ml) proteinase K (Boeringher Manheim) was added. This was digested overnight at 55°C and then treated with 0.7μg/ml Rnase A for 1 hour at 37°C. NaCl was added to 1.25M, and then an equal volume of chloroform/isoamyl alcohol 24:1 (vol/vol) was added and gently mixed for 2 hours at room temperature. The solution was centrifuged at 15000 rpm for 10 minute, and the upper, aqueous layer removed to a fresh microfuge tube. An equal volume of isopropanol was added and mixed gently to precipitate the DNA. This was then centriguged at 15000rpm for 10 minute, and the supernatant aspirated off. The pellet was washed for 1 hour at 4°C with 300μl ice-cold 70% ethanol,

centrifuged and the ethanol aspirated off. The genomic DNA pellet was then dissolved in 200μl TE (10mM Tris.HCL pH 8.0, 1mM EDTA) by mixing on a roller overnight.

2.2.3 Southern blotting

50μl of the genomic DNA was digested with 1μl Bgl II (Promega) and 5μl Buffer D (promega) overnight at 37°C. The samples were then run for 5 hours on a 1% agarose gel. The gel was denatured by submerging in denaturation solution (0.5M NaoH, 1.5M NaCl) with constant gentle agitation for 15 minutes at room temperature. The denaturation solution was then poured off and this was repeated for another 15 minutes. The gel was then submerged in neutralisation solution (0.5M Tris-HCl, pH 7.5, 3M NaCl) at room temperature for 15 minutes, and this was also repeated using fresh neutralisation solution for another 15 minutes. The gel was then placed on to a Whatman 3MM paper wick in a tray of 20x SSC. A piece of nylon membrane (Hybond-N+, Amersham) was placed in contact with the gel. On top of this, were placed 3 pieces of Whatman 3MM paper and a stack of paper towels. The whole apparatus was weighted down with a glass plate and sealed with saran wrap and capillary transfer of the DNA from the gel to the nylon membrane was allowed to proceed overnight. After transfer, immobilisation of the DNA was achieved by cross-linking in a UV crosslinker (UVP CL-1000) at 120,000μJ/cm^2.

2.2.4 Probe preparation

Two probes were used for genotyping mice, one recognising the IGF2 gene P3 promoter region and the other recognising exon 1 of the WT1 gene (Kreidberg et. al., 1993).

The P3 probe was isolated from the P3mm construct (Caricasole et al., 1996) by digesting 10μl of DNA with 3μl *EcoR1* and 3μl *EcoR1* buffer (promega) in a 30μl reaction at 37°C for 2 hours. The sample was run on a 1% Agarose gel with 3μl loading dye (Promega). The 1kb insert fragment was excised and purified (Qiagen gel extraction, Section 2.1.4).

The WT1 knockout probe was sent as DNA on paper. The probe was prepared by soaking in TE buffer at room temperature for 30 minutes and then transformed into electrocompetent DH5α cells (Section 2.2.1). The DNA was extracted from bacterial culture (Section 2.2.2) and digested for 2 hours at 37°C with 3μl *EcoR1* and 3μl Buffer D (promega). The DNA was run on a 1% Agarose gel and a 500bp fragment was excised and gel extracted.

2.2.5 Radiolabelling DNA probes

Random-primed DNA labelling was carried out using 4μl High Prime labelling (Boeringer Manheim), 4μl ^{32}P dCTP (Amersham) and 25ng of denatured (heated to 95°C for 5 minutes) probe DNA in a final reaction volume of 20μl. The reaction was incubated at 37°C for 1 hour after which the unincorporated label was separated by chromatography through a sephadex G-50 resin (Pharmacia) spin column. The probe was denatured by boiling for 5 minutes before use in Southern blot hybridisation (Section 2.2.6).

2.2.6 Southern blot hybridisation

Prehybridisation, hybridisation and washing were carried out in rotating hybridisation bottles in 30ml of solution, in a hybridisation oven (Techne) set at 65°C. The filter was prehybridised for 2 hours in 5x SSC (750mN NaCl, 75mM sodium citrate, pH 7.0), 5X Denhardt's reagent (50x Denhardt's contains 5g

Ficoll (type 400, Pharmacia), 5g polyvinylpyrrolidone, 5g BSA (fraction V; Sigma) and distilled water to a final volume of 500ml], 1mg/ml sonicated and denatured salmon testis (Sigma). Following prehybridisation the denatured probe was added and hybridisation was allowed to continue overnight. After hybridisation the filter was then washed twice in 2x SSC, 0.1% SDS for 15 minutes each, followed by two washes in 1x SSC, 0.1% SDS for 15 minutes each. The filter was then briefly air dried, wrapped in Saran wrap and autoradiographed with Kodak X-OMAT AR film at –70°C in an autoradiography cassette with intensifying screens (Kodak). Exposure varied from overnight to one week before the film was developed (X-OGRAPH Compact developer).

2.2.7 Embryo genotyping by PCR

The embryo yolk sac was used as the source of DNA for genotyping. Part of the yolk sac was placed in a 1.5ml microfuge tube, 200μl TE buffer was used and the sample was boiled. A dilution of 1 in 100 was made of this DNA solution and 1μl of this was used for each PCR reaction.

1μl genomic DNA solution was added to 24.9μl PCR reaction master mix to give final PCR reaction conditions (optimised for Mg^{2+} concentration) of: 75mM Tris.HCl pH 9.0, 20mM $(NH_4)_2SO_4$, 0.01% Tween-20, 3mM $MgCl_2$, 250μm dATP (promega), 250μM dCTP, 250μM dGTP, 250μM dTTP, 0.5units Taq polymerase (promega) and 0.2μM of the following primer pairs (but note that the 3 primers used for the knockout status and the three used for transgene status were used in two reactions).

For WT1 knockout status:

WT1+WT1ex1 detected the presence of an endogenous WT1 band

WT1+WT1ko detected the presence of the null allele

WT1 5' CAGCTCCCGTACGGCAGGATCG 3'
WT1ko 5' GCATCGCCCGGCAGGACGTCC 3'
WT1ex1 5' CATCGGCAGGGCCATAGCCGG 3'

For Transgene status:
WT12.5 and P3 detected the presence of endogenous P3
WT12.5 and WT1Tg detected the presence of the transgene
P3 5' CTGTGAGAACCTTCCAGCCTTTTC 3'
WT1.2 5' GCCCAGCGACCCGTAAGC 3'
WT1Tg 5' GAGCCATCCGGACCGGAGTCC 3'

PCR reactions were carried out in a Techne heated lid PCR machine. This was programmed to denature the samples for 5 minutes at 94°C, then cycle at 94°C for 1 minute, 60°C for 1 minute, 74°C for 1 minute for 40 cycles, followed by a 10-minute extension at 74°C. Loading dye was added to the samples and they were run on 1.8% agarose gels, stained with ethidium bromide, and then examined and photographed under UV.

2.2.8 Histology

Embryos were fixed in Zamboni's fixative overnight at 4°C, prepared by mixing 200ml 0.2M sodium phosphate buffer pH 7.3 with 200ml 2% paraformaldehyde and 70ml saturated picric acid. The fixed embryos were then dehydrated through 70%, 80%, 90%, 95%, 95% 100% and 100% EtOH (30minutes-1hour each depending on the embryo size), cleared in Histoclear (National Diagnostics) and embedded in paraffin wax. Tissue sections were cut at 5μM, floated on a water-bath and dried onto slides that had previously been subbed with TESPA (3-aminopropyltriethoxysilane) (Sigma).

2.2.9 Haematoxylin and Eosin (H&E) staining

Ehrlich's haematoxylin was purchased pre-prepared (Raymond Lamb). Slides were dewaxed in Histoclear 2 x 3 minutes, then rehydrated through 100%, 100%, 95%, 90%, 70% and 50% ethanol (2 minutes in each), followed by 1 minute in deionised water and 10 minutes in Ehrlich's haematoxylin. Slides were washed in running cold tap water for 1 minute until the stain turned blue, rinsed in deionised water, then dipped in acid alcohol (1% (w/v) HCl in ethanol) for 15 seconds followed by 30 seconds in 1% NH_3 in 70% ethanol. Slides were then left in 70% ethanol for 1 minute and stained for 1 minute in Eosin Yellow (BDH) (0.1% in 70% ethanol). Slides were then dehydrated though an ethanol series: 1 minute each in 70%, 90%, 95%, 100%, 100% ethanol, 2 x 2 minutes in Histoclear and mounted under coverslips in DPX (a mixture of distyrene, tricresyl phosphate and xylene) mountant (BDH).

2.2.10 Periodic acid-Schiff reaction (PAS) staining

Slides were dewaxed in Histoclear 2x 3 minutes and rehydrated through 2x 100%, 95%, 90%, 70% and 50% ethanol (2 minutes each), followed by 1 minute in deionised H_2O. They were then incubated for 6 minutes in 1% (w/v) periodic acid (BDH) in distilled H_2O, followed by 3 minutes wash in running tap water and 1 minute in distilled H_2O. The samples were then incubated for 15 minutes in Shiff's reagent (Sigma) that had been allowed to warm to room temperature. Slides were finally washed for 5 minutes in running H_2O before counterstaining in Haematoxylin, dehydration and mounting as described in H&E staining with the one modification of reducing the incubation in haematoxylin to 1 minute.

2.2.11 Immunohistochemistry

Antibody staining was carried out on embryo, and adult organ sections whose preparation was described earlier (Section 2.2.8). Slides were dewaxed in Histoclear 2 x 5 minutes and they rehydrated through 100%, 100%, 95%, 70% and 50% EtOH (1 minute in each), and placed in PBS. Slides were incubated in 10mM citric acid in a microwave oven for 3 x 5 minutes, then in 0.3% hydrogen peroxide for 30 minutes at room temperature followed by rinsing in PBS for 5 minutes. Each area to be stained was drawn around with an image pen and covered with DAB block (1% BSA (Sigma), 1% Tween 20(Sigma) in PBS). Slides were incubated for 1 hour at room temperature in a humidity chamber. The DAB block was flicked off and fresh DAB block was applied to half the slides whilst dilutions ranging from 1/100 to 1/2000 (Table 2.1) of the primary antibody were applied to the other half. The slides were incubated at 4°C overnight in a humidity chamber. After overnight incubation, the slides were washed in PBST (5l PBS + 50ml Tween 20 sigma) 3 x 5minutes at room temperature. All slides were then incubated at room temperature for one hour with the secondary antibody (1/200 in DAB block). After washing slides in PBST 3 x 5 minutes, the sections were covered with Vector Elite ABC reagent (Vector R.T.U Vectastain kit) and incubated at room temperature for 45 minutes. Slides were then washed in PBST 3 x 5 minutes before developing the stain with 14μl DAB and 7μl hydrogen peroxide (Vector vectastain kit) in 1 ml PBS. When the stain had developed (about 5 minutes) the slides were dehydrated through ethanol 70% and 95% for 15minutes, 100% x 2 for 1 min, then into histoclear mount 2 x 2minutes and finally mounted with DPX.

The following antibodies were used for immunohistochemistry of mouse histological sections.

Table 2.1 Antibodies used in immunohistochemistry

Antibody	Source	Dilution	Secondary Antibody
αWT1 C19	Santa Cruz Antibodies	1/1000	αRabbit biotinylated
αBASP1	Dr Stefan Roberts University of Manchester	1/500	αRabbit bioinylated
αPCNA3	Santa Cruz Antibodies	1/500	αUniversal biotinylated

2.2.12 In-situ hybridisation

2.2.12.1 Probe preparation

A concert preparation of pBS-BASP1 DNA (2μg/μl) was used for the probes. For the creation of a sense and antisense probe 20μg of DNA was digested either with 2μl Not1 (for the sense probe) or 2μl ECOR1 (for the antisense probe) with the equivalent buffers in a total volume of 50μl. Electrophoresis on an agarose gel showed linearisation of the plasmids and the digestions were purified by PCR purification. *In vitro* transcription reactions were carried out on 1μg linearised plasmid DNA o/n by adding transcription buffer 5x, 2μl NTP labelling mix, 2 μl DTT, Rnase inhibitor and T3 RNA polymerase for the sense probe and T7 RNA polymerase for the antisense stage. The reactions were incubated overnight at 37°C.

2.2.12.2 In-situ hybridisation

All the following solutions were made with DEPC treated water. Slides were dewaxed in Histoclear dewax for 2 x 10 minutes before rehydration in ethanol

100% 2 x 5 minutes, 95%, 90%, 80%, 70%, 50%, 30% each for 1 minute, then 5 minutes in PBS, 30 minutes in 4% PFA (in PBS) and finally 2x 5 minutes PBS. A proteolysis reaction was carried out on the slides by incubating them in Proteinase K for 2 minutes followed by a wash with PBS and then refixing in 4% PFA. The slides were washed with PBS 2 x 5 minutes then prehybridised with 2 x SSC for 2x 5 minutes then in Tris-glycine buffer for 30minutes. 1μl of the probe was added to 20ml hybridisation solution (40% formamide, 100x Denhardts, 20x SSC, tRNA, denatured herring sperm (Boehringer Manheim) 100μg/μl) and heated at 95°C for 5minutes. 6μl hybridisation buffer was added to each slide and placed in a humidity chamber and incubated for 24-48 hours at 65°C.

Following hybridisation, the slides were washed in varying concentrations of SSC and post-hybridisation buffer (20% formamide, 0.5x SSC). Washes of 5x SSC 3 x 15 minutes room temperature, post-hybridisation buffer at 60°C for 40minutes, 2xSSC 15 minutes room temperature were carried out followed by Rnase solution 37° 15 minutes. Final washes of 2x SSC room temperature washes for 15 minutes, post-hybridation buffer at 60°C 20minutes and 2x SSC 2 x 15 minutes room temperature were carried out. The αBASP 1 antibody was added (200μl per slide, 1/2000 dilution in blocking solution Roche), slides were covered with parafilm and incubated in a humidity chamber o/n at 4°C. After the addition of the primary antibody, slides were washed in PBS 3 x 10 minutes, 3 x 30 minutes and 2 x 1 hour. The stain was developed with incubation in NTMT staining buffer for 3 x 10 minutes (20ml 5M NaCl, 50ml 1M $MgCl_2$, 100ml 1M TrisHCL pH 9.5, 5ml 20% Triton), 0.5 ml staining solution was added to each slide (1 NBT/BCIP tablet in 10ml MQ H_2O) in the dark until a signal was seen and the reaction stopped by incubation in 1mM EDTA/PBS. Slides were counterstained in Fast Red (Vector), dehydrated through an ascending ethanol series and mounted in DPX.

2.2.13 Detection of Apoptosis in mouse tissue sections

The Apoptag Flourescein kit (Intergen Company) was used to detect apoptotic cells in paraffin tissue sections as per the manufacturers instructions and sections were analysed using fluorescent microscopy techniques (Section 2.3.4)

2.2.14 Collection and analysis of mouse urine

Urine samples were collected from mice directly into 1.5 ml microfuge tubes and proteinuria was determined by placing approximately 5μl of urine onto urine test strips (urinestix SG). Albuminuria was determined by running 5μl of the urine sample (with 5μl sample buffer and boiled for 10 min) on a Bio-Rad criterion ready gel for 1 hour at 200 V and subsequently stained for 30 minutes with Commassie Brilliant Blue before destaining in 40% MeOH, 10% HOAC for an hour.

2.3 Tissue culture and associated protocols

2.3.1 Standard tissue culture

Tissue culture was carried out following standard techniques (Paraskeva 1984). Cultures were grown in Tc 75cm^2 coated flasks (Gibco BRL) in a humidified incubator at 37°C with 5% CO_2 (v/v). The medium used was Dulbecco's modified eagle medium (DMEM) with sodium pyruvate, and glutamax-1 (Gibco), supplemented with 10% foetal bovine serum, 5% penicillin, and amphotericin (Gibco). Cells were frozen in freezing medium (10% DMSO in fetal bovine sereum (FBS)) into 1ml vials and stored in liquid nitrogen.

2.3.2 Cell Lines

The following cell lines were used in experiments all using standard tissue culture techniques.

Table 2.2 Cell lines used in cell culture experiments

Cell Line	Derived From	Source
Cos7	Monkey kidney	ECACC
HeLa	Human breast cancer	Dr Judith Sleeman University of Dundee
MCF7	Human breast cancer	Dr Judith Sleeman University of Dundee
M15	Mouse kidney	ECACC

2.3.2 Transient transfections

For transient transfections, cells were plated at approx. 150,000 cells per 35mm diameter Tc dish (Gibco) and transfected the following day with FuGene 6 Transfection Reagent (Roche) and 2μg DNA according to the manufacturers protocol. HeLa cells were transfected with Effectene (Qiagen) per the manufacturers instructions. Transfections were analysed the following day (after approx. 18 hours) under GFP fluorescence (FITC fluorescence) and DIC using a 60x objective on a fluorescence microscope (Nikon Eclipse E800 or E1000).

2.3.3 Protein Biochemistry

2.3.3.1 Sample preparation

Trypsinised cells were resuspended in PBS at a concentration of 1 x 10^6 cells/ml. 1 x 10^6 cells were pelleted in a 1.5ml microfuge tube by centrifugation at 13,000rpm for 3 minutes and the supernatant removed. The cell pellet was resuspended in 100μl of gel sample buffer (62.5 mM Tris-HCL, pH6.75, 10%(v/v) glycerol (AnalaR BDH), 5%(v/v) 2-mercaptoethanol (Sigma), 4%(w/v) SDS (AnalaR BDH), 0.01%(w/v) bromophenol blue). The cell lysate was boiled for 5 minutes and stored at -20°C until required.

2.3.3.2 Preparation of polyacrylamide gels

Gels were poured on Mini PROTEIN II slab cells (Bio-Rad) with 1.5mm spacers and a 7mm well former. A Resolving gel was poured (10% gel 9.67ml 30%(w/v) acrylamide/0.8%(w/v) bis-acrylamide (37.5:1) (National Diagnostics), 7.25ml 1.5M Tris-HCl, pH 8.8, 0.4% SDS, 12.08ml distilled water, 145μl 50%(w/v) ammonium persulphate (Sigma), and 4.7μl Tetramethylethylenediamine (TEMED) (Bio-Rad). The stacking gel was also made (4.5% gel 9.67ml 30%(w/v) acrylamide/0.8%(w/v) bis-acrylamide (37.5:1) (National Diagnostics),

2.6ml 0.5M Tris-HCl, pH 6.8, 0.4% SDS, 5.9ml distilled water, 75μl 50%(w/v) ammonium persulphate (Sigma), and 2.4μl TEMED (Bio Rad). Cell lysates were loaded onto gels as well as 10μl rainbow markers (14.3-200kDa Amersham). The gels were electrophoresed in running buffer (192mM glycine (Sigma), 25mM Tris (Sigma), 0.1%(w/v) SDS (AnalaR BDH)) at 200V until the bromophenol blue reached the bottom of the gel.

2.3.3.3 Western Blotting

Gels were soaked in transfer buffer (192mM glycine, 25mM Tris) for 15 minutes. A piece of Immobion-P polyvinylidine difluoride (PVDF) membrane was cut to the same size as the gel and washed in methanol for 5 minutes. The membrane was rinsed with distilled water and soaked in transfer buffer. Proteins were electroblotted onto the membrane in transfer buffer using the Mini Transblot Cell (Bio-Rad) at a constant current of 250mA for 2-4 hours. After the transfer, the membrane was washed in milk blocking buffer (10mM Tris-HCl, pH 7.4, 150mM NaCl (AnalaR BDH), 4% 9(w/v) Tween 20 (Sigma)) for 1 hour at room temperature. It was then incubated with primary antibody (αWT1 C-19 1:400) diluted in 10ml milk block buffer overnight, at 4°C, in a dark plastic box, on a rocking platform. After overnight incubation, the membrane was washed in milk blocking buffer 2 x 10minutes, Tween buffer (10mM Tris-HCl, pH7.4, 150mM NaCl, 0.2% Tween 20 (Sigma)) 2 x 10minutes, milk block 1 x 10minutes. After the washes, secondary antibody was applied (α goat biotinylated) in 10ml milk block at 4°C for 1 hour. The membrane was washed following incubation in secondary antibody in milk block 1 x 30minutes, Tween buffer 1 x 10minutes and rinsed in distilled water. Detection of protein bands was carried out by chemiluminescence using the CSPD ready to use system (Roche). 5 drops of the reagent were placed onto the membrane, which was then sealed into plastic

bags and placed in an autoradiograph cassette for 5 minutes before developing the autoradiograph (Kodak x-omat).

2.3.3.4 Protein assay

Soluble protein in cell lysates were measured spectophotometrically by using the Biorad protein assay system as prescribed by the manufacturers. This system exploits a dye-binding assay based on the Bradford protocol. 10μl aliquots of cell lysates were diluted with water to a final volume of 800μl, mixed with 200μl of protein assay reagent and allowed to stand for 10-20 minutes. 100μl aliquots were then dispensed into a flat-bottomed microtiter plates (Nunc). Protein-dependent colour development was measured spectrophotometrically at 620nm employing a Titertek Multiskan MCC/340 machine. By comparison with a series of protein standards of known concentration (bovine serum albumin), soluble protein content was estimated by extrapolation from a standard curve and expressed as mg soluble protein/ml of lysate using the Biosoft software programme.

2.3.4 Immunofluorescence

Cells transfected with WT1 GFP constructs were stained with a variety of antibodies (see below). The cells were grown in 35mm dishes and transiently transfected as described above. After approximately 18 hours, 2μl 4% parafomaldehyde was added and swirled around as an intial fixing step. The media was then pipetted off the dishes and 2ml 4% PFA added for 10 min at room temperature. The cells were washed with PBS and blocked for 30 minutes with DAB block. The appropriate dilution of the primary antibody in DAB block was added to the cells and the dishes left at 4° overnight. After the overnight incubation, the cells were washed 3x 10 min in PBST before addition of the

secondary antibody (Table belbelow). After a further 1 hour incubation at room temperature the cells were washed 3x 10 min before addition of streptavidin texas red 1/400 for 30 min. The cells were viewed under fluorescence on the fluorescence microscope (Nikon Eclipse E800 or E1000).

Table 2.3 Antibodies used in cell culture experiments

Antibody	Source	Antibody Dilution	Secondary antibody
αWT1 C19	Santa Cruz Antibodies	1/1000	αRabbit biotinylated
αBASP1	Dr Stefan Roberts University of Manchester	1/500	αRabbit biotinylated
αB23	Santa Cruz Antibodies	1/500	αGoat biotinylated
αPrP	Dr Angus Lammond University of Dundee	1/50	αMouse biotinylated

Chapter 3

INVESTIGATION OF THE ROLE OF WT1 ISOFORMS IN MURINE DEVELOPMENT

3.1 Summary

The role of WT1 in genito-urinary disease was discussed in Chapter 1. This chapter describes a series of experiments designed to further investigate the importance of the WT1+KTS and WT1–KTS isoforms in murine development. Breeding WT1-KTS transgenic mice (P3:WT1-KTS) with mice hetereozygous for the *Wt1* null allele ($WT1^{+/-}$), allowed the generation of mice heterozygous for the WT1 null allele and also carrying a WT1–KTS transgene ($WT1^{+/-}$; P3:WT1-KTS). Offspring resulting from such crosses allowed us to investigate the affects of expressing the WT1–KTS isoform in mice with different levels of endogenous WT1 and hence altering the ratios of WT1 isoforms. WT1 knockout embryos fail to survive and have severe genito-urinary abnormalities (Kreidberg et al., 1993). Analysis of embryos homozygous for the WT1 null mutation alongside $WT1^{-/-}$; P3:WT1-KTS embryos at similar time points showed the presence of the P3:WT1-KTS transgene is not sufficient to rescue the WT1 null phenotype in $WT1^{-/-}$; P3:WT1-KTS embryos. Analysis of adult mice revealed that $WT1^{+/-}$; P3:WT1-KTS animals over 6 months of age develop renal and genital abnormalities with 14/49 mice from two different P3:WT1-KTS transgenic lines presenting with a range of genito-urinary defects and other abnormalities in comparison with their age matched $WT1^{+/-}$ and Wild type littermates.

3.2 Introduction

3.2.1 WT1 null and transgenic mice

Transgenic mice were generated previously in our lab carrying a WT1-KTS expression construct consisting of cDNA sequences encoding WT1-KTS under the control of the *Igf2* P3 promoter and H19 enhancer sequences (the P3:WT1-KTS transgene) (Duarte 1997). The P3 promoter and *H19* enhancer of *Igf2* have been shown to be expressed strongly in the liver, kidney and gut (Brenton, 1999) and were intended to allow temporal and spatial expression of the transgene coincident with at least some aspects of endogenous WT1 expression. This experimental strategy was preferred to the use of regulatory elements for the WT1 gene since these remain ill-defined. Moore *et. al.* 1999 reported that the presence of a 280kb YAC spanning the *Wt1* gene and regulatory elements was able to rescue the midgestational lethality and cardiac defects of null mice. However this YAC failed to rescue the genito-urinary abnormalities, suggesting that further, essential WT1 regulatory regions lie outside of this 280kb region (Moore et al., 1999). Even more recently the production of transgenic mice carrying a 470kb YAC spanning the *Wt1* locus also failed to completely rescue the null phenotype (Guo et al., 2002). Given the disruption of the normal isoform ratio in the pathogenesis of Frasier syndrome, it was thought that the phenotypes of our P3:WT1-KTS transgenic mice might show similarities to this human disorder. Previous analysis of RNA in three transgenic lines named Wani, Wefi and Wines detected the presence of P3:WT1-KTS transgene-derived RNA by RT-PCR, although no obvious developmental abnormalities or embryonic lethality was observed in transgenic animals (Duarte 1997).

The second set of animals used in these experiments, were the WT1 null animals (Kreidberg et al., 1993) previously described in Chapter 1. A null allele

of *Wt1* results from a targeted mutation and animals homozygous for the null allele (WT1 knockout mice) die before birth. Heterozygotes have been previously seen to be phenotypically normal and viable but recent research has suggested that these animals do develop renal abnormalities such as proteinuria and glomerular sclerosis late in adult life (Wagner et al., 2003).

As previous analysis of the P3:WT1-KTS lines has shown no major renal or genital abnormalities and the $WT1^{+/-}$ animals showed a lesser degree of renal abnormality, a combination of the two was to be tested for evidence of enhanced phenotypic defects. Other transgenic experiments disrupting WT1–KTS or WT1+KTS isoform ratios have been described in Chapter 1, in which the resulting mice developed features similar to those of FS or DDS (Hammes et al., 2001; Patek et al., 1999). Hammes et al. 2001 described mouse strains in which specific isoforms were removed. Heterozygous mice with reduced levels of WT1+KTS develop glomerusclerosis and represent a model for FS. Homozygous animals die after birth from kidney defects (Hammes et al., 2001). This data suggests that there is a fine balance in the ratio of the two isoforms. It is known that there is a certain degree of redundancy between WT1+KTS and WT1-KTS but the exact function of the isoform ratio balance is as yet unknown. It is therefore possible that the expression of additional WT1–KTS on a wild type WT1 background as in our P3:WT1-KTS animals may not be sufficient to significantly alter the ratio of WT1–KTS:WT1+KTS. However, in animals heterozygous for the null allele and also carrying the P3:WT1–KTS construct ($WT1^{+/-}$; P3:WT1-KTS animals) the splice isoform ratio would be further perturbed and could provide further insight into the importance of the ratio balance between the two isoforms. It may be that decreasing the overall amount of WT1 whilst increasing the amount of a single isoform may be required for the pathogenesis of disease. It has been seen that the critical ratios are essential for

normal human development, with the shift of ratios towards the WT1-KTS form as a result of mutations affecting exon 9 splice donor choice, being proposed as the cause of Frasier syndrome (Barbaux et al., 1997). In support of this, removal of specific WT1 isoforms in mice resulted in the development of renal and genital abnormalities, that mimic FS and DDS (Hammes et al., 2001). The experimental strategy of Hammes et al 2001 was to lower the level of WT1+KTS or WT1-KTS by knocking out the respective alleles in order to alter the ratio balance of WT1+KTS and WT1-KTS (interestingly, levels of WT1-KTS went up in proportion to WT1+KTS reduction). Our $WT1^{+/-}$; P3:WT1-KTS mice has additional WT1-KTS (resulting from the P3:WT1-KTS transgene expression) whilst the levels of both endogenous WT1-KTS and WT1+KTS are reduced (heterozygous WT1 knockout phenotyope), hence potentially tipping the balance towards WT-KTS even more than in previous studies. Our experiments might therefore help further define the critical WT1 splice isoform ratios.

The experiments set out in this chapter result from mating animals from three of the P3:WT1–KTS transgenic lines Wani, Wefi and Wines, with animals heterozygous for the null allele ($WT1^{+/-}$). Resulting animals heterozygous for *Wt1*, and also carrying the transgene ($WT1^{+/-}$; P3:WT1-KTS) were studied as adults. $WT1^{+/-}$; P3:WT1-KTS mice were also intercrossed, or mated with $WT1^{+/-}$ animals, and offspring were analysed at embryonic day 11.5 (E11.5). Embryos and adults were genotyped by a combination of PCR and Southern analysis. Analysis of embryos and adult organs were analysed through histological, gross morphological and patho-physiological means.

3.2.2 Characterisation of the morphological abnormalities seen in in $WT1^{+/-}$;P3:WT1-KTS mice

3.2.2.1 OB mutant mice

A third set of animals was used as a comparison model for genital development. The OB transgenic mice were identified from a screen of transgene insertional mutants in our laboratory (Paisley, 2000). Breeding from male homozygous transgenic mice from this line proved impossible suggesting these mice were infertile. Analysis of Ob testes has shown that the testes are reduced in mass in comparison to fertile hemizygous or wild type littermates. Examination of the contents of the vas deferens of Ob mutants identified the presence of little or no mature sperm in comparison with control (wild type or Ob heterozygous littermates) animals. Testes of Ob animals also exhibited a significant difference in the relative abundance of various spermatogenic cell-types although it was not obvious that any one cell type was completely absent. This indicated that sterility was due to defects in spermatogenesis. These mice provided us with a mutant line with genital defects that differed in comparison with abnormalities in the testes of $WT1^{+/-}$; P3:WT1-KTS mice, highlighting that different mechanisms of spermatogenesis may be going awry in the two models. The gross morphology of the OB mice was investigated using immuno-histological methods.

3.2.2.2 Expression of WT1 and the putative co-suppressor protein Basp1

A further method of investigating processes resulting in the abnormal development of the genito-urinary system in the $WT1^{+/-}$; P3:WT1-KTS mice was to examine the expression pattern of WT1 in all the mutant lines described above. WT1 is highly expressed in the developing kidneys and testis but in adult animals expression is restricted to the podocytes of the kidneys and sertoli cells of the testis (Pritchard-Jones et al., 1990). This adult expression of WT1 in both kidneys and testes suggests that WT1 is functioning both at developmental

stages and in the adult although the role the protein maybe playing later in life remains unclear. Detecting expression of WT1 in $WT1^{+/-}$; P3:WT1-KTS, $WT1^{+/-}$ and OB animals allowed us ask whether the protein was still being produced and to detect any aberrant or ectopic expression. An antibody recognizing the Basp-1 protein was also used as a marker to address similar questions. Basp-1 was described in Chapter 1 as a possible co-suppressor of WT1 (Carpenter et al., 2002). It should therefore be expressed in similar locations to WT1 for co-suppressing activity to take place *in vivo.* The anti-Basp-1 antibody was therefore used to investigate abnormalities of the WT1 pathway in our mutants.

3.2.2.3 Cell cycle

The role of WT1 in cell cycle control is not clearly understood. WT1 has a role in growth regulation in the kidney as its loss was associated with widespread apoptosis of nephric mesenchyme (Kreidberg et al., 1993). WT1 mutations can lead to Wilms' tumour, characterised by the uncontrolled proliferation of blastemal, epithelial and stromal cells (Lee and Haber, 2001). There is an increased frequency of gonadoblastomas in children with WAGR syndrome and a small proportion of girls with DDS also develop granulosa cell tumours of the ovary, however WT1 mutations have not been seen in sporadic granulosa cell tumours or Sertoli cell tumours of the testis (Hastie, 1993). WT1 seems to act on the cell cycle either by repressing the expression of genes required to maintain cells in cycle or by activating genes required to take the cells out of cycle and into a state of terminal differentiation. The list of genes, whose promoters are activated or repressed (thereby modulating their activity) by ectopic expression of WT1 in transient transfection assays include platelet derived growth factor-A (*PDGF-A*) (Gashler, 1992), *IGF2* (Caricasole et al., 1996; Drummond et al., 1992; Hastie, 1993), *Pax2* (Ryan et al., 1995; Yang et al., 1999) colony stimulating factor 1 (*CSF1*) (Jin et al., 1999), *Bcl2* (Bard; 2001), and amphiregulin

(Lee, 1999) amongst others. The repression of a number of these genes, some of which encode embryonic growth factors, provides an attractive hypothesis to explain the tumour suppressor activity of WT1. The role of WT1 in Wilms' tumour and other neoplasias highlights the essential role of the protein in the cell cycle.

To investigate changes in the cell cycle of our mutant mice, apoptosis and proliferation patterns in adult kidneys and testes were analysed using immunohistochemical means. It was expected that the $WT1^{+/-}$; P3:WT1-KTS mutants with altered WT1 ratios might have altered proliferation and apoptosis, because of the existing evidence that WT1 functions in the cell cycle. In the OB mutant, in which the basis of the observed spermatogenesis defect was entirely unknown, it was thought that the analysis of apoptosis and proliferation might help to characterize the mutant phenotype.

3.3 Results

3.3.1 Breeding and genotyping of Wt1 null and P3:WT1-KTS transgenic animals

Mice were genotyped after weaning by either Southern blot analysis or PCR. Southern Blots were hybridized with the WT1KO probe (Kreidberg et al., 1993) or the Igf2 P3 probe (Chapter 2 Section 1) (Duarte 1997) (Figure 5).

3.3.2 Analysis of embryos

Animals identified as $WT1^{+/-}$; P3:WT1-KTS were either intercrossed or mated with those identified as $Wt1^{+/-}$ and animals from three transgenic lines were studied between embryonic day E11 and E13.5. Lethality of $Wt1^{-/-}$ animals was seen around E13.5 and for this reason embryos were routinely collected at E11.5. A total of 24 litters of embryos were analysed at this developmental stage (Table 1).

Figure 5. Examples of PCR and Southern blot analysis used to genotype mice.

Genotyping of *Wt1* and the P3:WT1–KTS transgene were carried out through Southern analysis or PCR. Panels A and B show genotyping by Southern analysis. (A) WT1 status of 6 mice. Mice 1, 2, 3 and 6 were heterozygous for the *Wt1* knockout allele (*Wt1*+/-) and mice 4 and 5 were wild type animals (*Wt1*+/+). The Southern blot was hybridized with probe A resulting in the production of a 5Kb wild type *Wt1* band and a 4Kb $Wt1^{-/-}$ band. (B) Transgene status of the same six animals. All animals had endogenous P3 and all six animals were transgenic for the P3:WT1–KTS transgene. Southern blots were probed with probe B which resulted in the production of 4.5Kb bands detecting endogenous P3 and a 4Kb band detecting the presence of the transgene. (C) The result of PCR amplifications used to genotype 7 different mice with primers specific for the wild type *Wt1* allele (upper panel) and also the *Wt1* knockout allele (lower panel). Sample 1 in was the negative (no DNA) control. Animals represented in lanes 3-6 were heterozygous for the *Wt1* null allele, while samples 2 and 7 had only the wild type allele. (D). The result of PCR analysis used to genotype 7 mice with primers specific for the endogenous P3 allele (upper panel) and the P3;WT1-KTS transgene (lower panel). Sample 1 was the negative control. Animals 5, 6 and 7 show endogenous P3 while the transgene is present in animals 4, 5 and 6. (E) Diagramatic representation of part of the *Wt1* allele and targeting vector regions showing location of southern probe A and PCR primers WT1 and WT1Ko. (F) A diagrammatic representation of the P3:WT1-KTS transgene showing the location of southern probe B and PCR primers P3 and WT1tg.

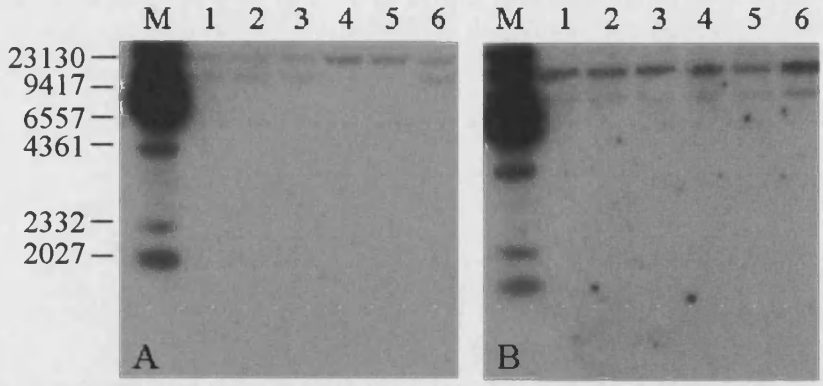
M 1 2 3 4 5 6
23130
9417
6557
4361
2332
2027
A
M 1 2 3 4 5 6
B

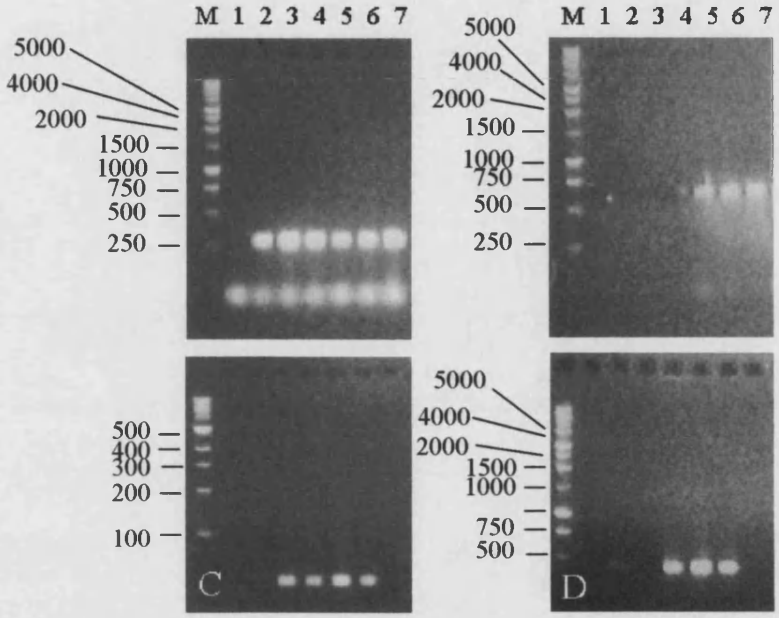
M 1 2 3 4 5 6 7
5000
4000
2000
1500
1000
750
500
250
M 1 2 3 4 5 6 7
5000
4000
2000
1500
1000
750
500
250
500
400
300
200
100
C
5000
4000
2000
1500
1000
750
500
D

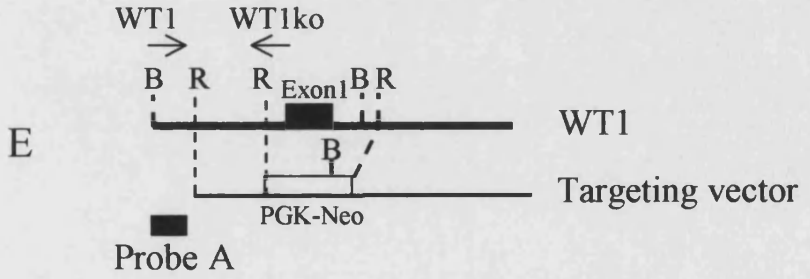
E
WT1
WT1ko
B R R Exon1 B R
WT1
B
Targeting vector
PGK-Neo
Probe A

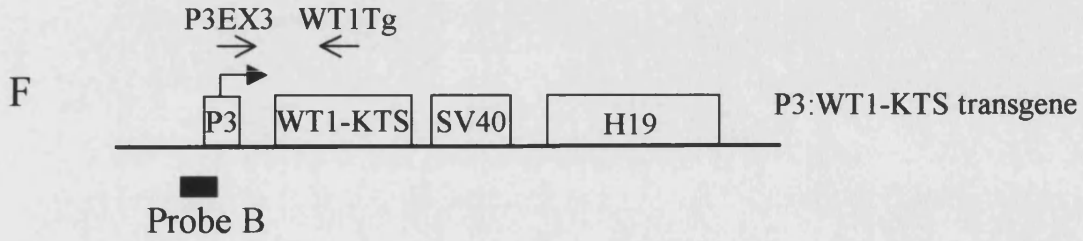
F
P3EX3
WT1Tg
P3
WT1-KTS
SV40
H19
P3:WT1-KTS transgene
Probe B

Table 1 Number of E11.5 embryos analysed from crosses of WT1+/- animals with P3:WT1-KTS animals

Transgenic line	Number of litters	Number of embryos analysed for each genotype					
		$WT1^{+/+}$	$WT1^{+/+}$;P3:WT1-KTS	$WT1^{+/-}$	$WT1^{+/-}$;P3:WT1-KTS	$WT1^{-/-}$	$WT1^{-/-}$;P3:WT1-KTS
Wani	10	8	5	12	14	4	4
Wefi	12	6	4	12	12	4	3
Wines	2	2	2	3	3	1	1

Chi square tests carried out for the three lines (Wani $p = 0.772$, Wefi $p = 0.832$, Wines $p = 0.985$) suggest that no embryos are being lost before birth and embryos were seen in the expected ratios.

The low number of Wines litters that were born from the breeding pairs over a number of months alerted us to a possible sterility phenotype associated with this line (discussed later). Histological analysis of $WT1^{+/+}$ wild type embryos (Figure 6 A, D), $WT1^{-/-}$ knockout embryos (Figure 6 B) and $WT1^{-/-}$;P3:WT1-KTS transgenic embryos (Figure 6 C) demonstrated that the knockout embryos were smaller in comparison to wild type littermates (Figure 6 A) and had severe developmental abnormalities including, cardiac defects and an absence of the kidney and gonads. Presence of the transgene (Figure 6 C) failed to rescue the knockout phenotype in the $WT1^{-/-}$;P3:WT1-KTS embryo. There were still cardiac defects and the gonads and kidneys again failed to develop correctly. At least 7 animals of each genotype were examined histologically allowing the conclusion that the smaller size of the $WT1^{-/-}$;P3:WT1-KTS as seen in the figure was atypical. The $WT1^{-/-}$;P3:WT1-KTS were of a similar size to $WT1^{-/-}$ littermates,

Figure 6. Histological analysis and WT1 expression patterns in wild type, Wt1-/- and WT1$^{-/-}$;P3:WT1-KTS embryos.

Analysis of embryos resulting from matings of WT1+/-; P3:WT1-KTS with WT1+/- animals. (A-C) Hematoxylin and Eosin (H & E) stained sections of e11.5 embryos show the presence of the kidney (k) in WT1+/+ animals (A), which is missing in WT1-/- (B) and WT1-/-; P3;WT1-KTS embryos (C). In both Wt1-/- embryos (with or without the P3;WT1-KTS transgene) there is severe disruption in development of the heart that has resulted in bleeding into the pericardium (B and C). Higher magnification view of the thoracic region of a wild type embryo (D and E), showing morphology with H & E staining (D) and anti-WT1 antibody staining (E). The kidney (k), genital ridge (gr), liver (l), heart (h) and mesothelium (m) are indicated. Scale bars A, B, C 10mm, D and E 5mm.

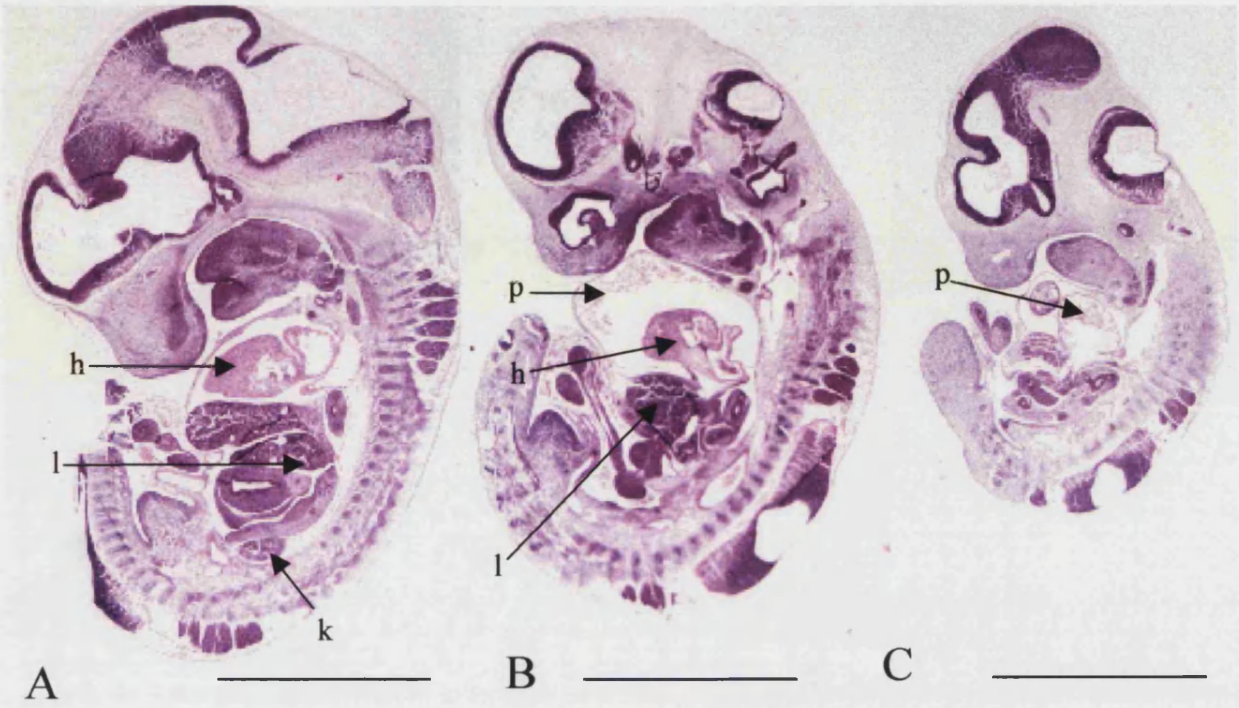
h
l
k
A
p
h
l
B
p
C

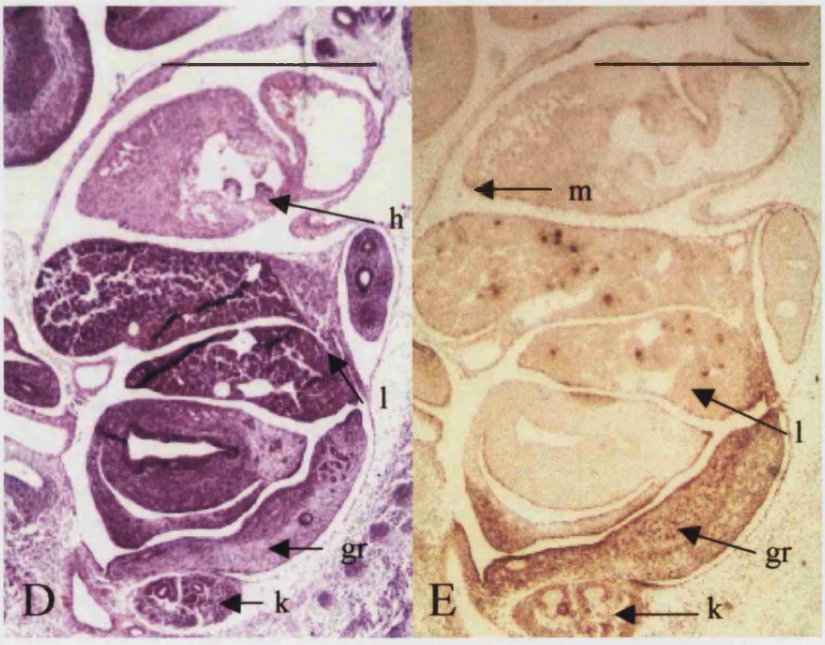
h
l
gr
k
D
m
l
gr
k
E

however, due to the general small size and the developmental abnormalities seen the embryos, it was not always possible to carry out histological analysis. The illustrated $WT1^{-/-}$;P3:WT1-KTS embryo provided a good example of the phenotypes seen in $WT1^{-/-}$;P3:WT1-KTS embryos. Immunostaining using an anti-WT1 antibody detected the presence of WT1 protein in the kidney and genital ridge and the mesothelium lining of all the organs in a wild type embryo (Figure 6 E). In comparison, WT1 was not detected in either knockout embryos or knockout embryos carrying the transgene.

3.3.3 Analysis of adult organs

Organs of animals over the age of 6 months were also analysed for two transgenic lines Wines and Wani (Table 2). Out of a total of 49 animals, 14 animals showed signs of gross abnormalities. The disorders ranged from liver tumours, kidney overgrowth and cysts, cystic or small testis and in one case a cystic eye none of these disorders were ever seen in wild type littermates. All of the disorders occurred in mice ranging from 6 to 9 months in age from 8 different litters. All mice were $WT1^{+/-}$;P3:WT1-KTS animals with the exception of one animal with the genotype $WT1^{+/+}$;P3:WT1-KTS. Out of all the animals, 13/49 were $WT^{+/-}$;P3:WT1-KTS mice and they all presented with morphological abnormalities. The data is mostly representative of the Wani transgenic line (47/49 mice), with only 2 mice from the Wines line. This was partly due to the fact that breeding of the Wines line was reduced due to the possible sterility of male animals. The cystic kidneys and testis seen in the Wines line were similar or less severe in pathology to the abnormalities seen in some of the Wani lines however given that the numbers of Wines animals analysed (2) were so small it is not possible to say whether the histopathology is consistent between the two lines.

Table 2 Number and genotype of adult mice developing pathologic disorders

Line	Genotype	Number examined	Pathology (number affected)
Wani	$WT1^{+/+}$	10	Normal (none)
	$WT1^{+/+}$;P3:WT1-KTS	12	Liver tumour (1)
	WT1+/-	12	Normal (none)
	$WT1^{+/-}$;P3:WT1-KTS	13	Cystic kidney (5)
			Cystic testis (2)
			Liver tumour (1)
			Cystic tesits, cystic kidney (1)
			Cystic kidney, liver tumour (1)
			Cystic kidney, cystic testis, liver tumour (1)
			Small testis (1)
			Cystic eye (1)
Wines	$WT1^{+/-}$;P3:WT1-KTS	2	Cystic kidney (2) Cystic testis (2)

3.3.3.1 Cystic Kidneys

Histological analysis of adult organs was carried out in a similar fashion to embryos. In wild type mice (Figure 7), PAS staining of the kidney allows distinction of the cortex (where the tubule system processes the waste fluid and finally passes it into the collecting system) and the medulla at the

Figure 7. Histological comparison of wild type and mutant adult mouse kidneys.

(A-C) Periodic Acid and Schiff's (PAS) staining of a longitudinal section through wild type (6 month old male) mouse kidneys showing the normal kidney morphology . (A)Two different regions of the kidney, the cortex (co) and the medulla (m) can be distinguished. The glomeruli (G) of the nephrons are contained within the cortex and the medulla contains the collecting tubules system. These regions are compact and regularly organised in the wild type kidney. (B) The glomeruli (G) are organised within the cortex region of the kidney and are associated with the renal vasculature and proximal collecting tubes (PCT). (C) The proximal collecting tubules (PCT) can be identified by prominent staining of the brush border (BB), that is absent from the distal convoluted tubules (DCT). There are more PCTs within the cortex and away from the periphery an increasing number of DCTs can be seen. (D-F) The morphology of PAS stained WT1+/-; P3:WT1-KTS cystic kidney sections differs distinctly from their wild type littermates. (D) A number of fluid filled cysts (c) can be clearly seen. There is widespread disorganization of the structure of the kidney, making it difficult to distinguish between the medulla and the cortex regions. The number of glomeruli (G) and the general size of the kidney was increased. (E) The glomeruli (G) were larger than glomeruli in wild type littermates and a number of glomeruli were seen to be encapsulated within cysts (c). (F) The tubule morphology appears disrupted, with the boundary between proximal collecting tubules (PCT) and distal convoluted tubules (DCT) less clear than in wild type sections. Tubule size is greatly increased with the brush border (BB) of proximal collecting tubules less clear than normal, with thickening of the distal convoluted tubules. Magnification x10 (A and D) or x60 (B, C, E and F). Scale bars 200μm

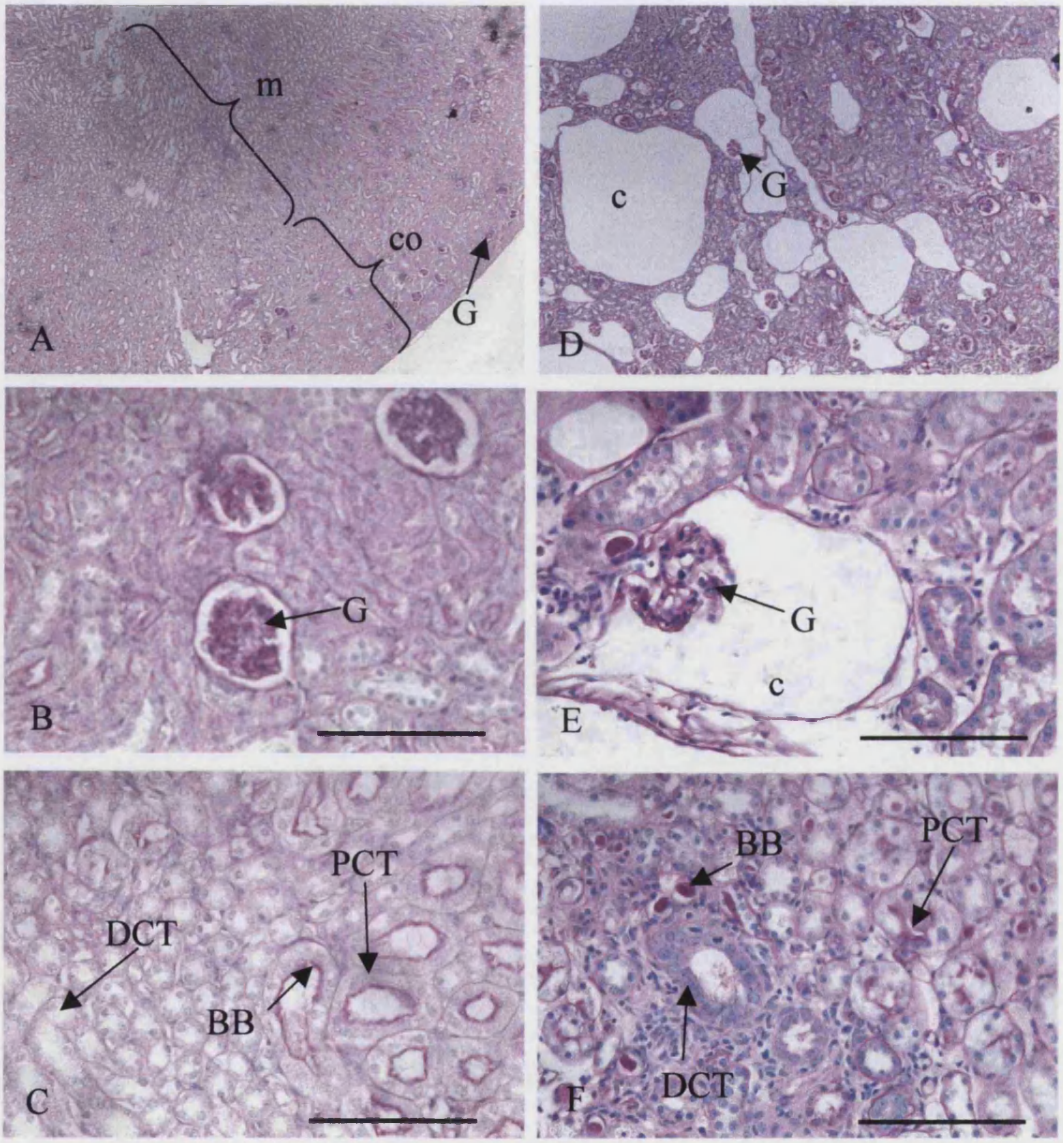
m
co
G
A
c
G
D
G
B
G
c
E
PCT
DCT
BB
C
BB
PCT
DCT
F

periphery (which contains the renal corpuscles where the glomerulus filters waste out of the capillary system). The wild type kidney is an ordered and compact structure with the medullary and cortical regions clearly defined (Figure 7 C). A number of $WT^{+/-}$;P3:WT1-KTS mutant kidneys (see Table 2) contained fluid filled cysts although the figure represents the histopathology of an affected Wines animal (Figures 7 D and E), there was also a general disorganization in kidney structure and it was difficult to distinguish the cortex and medullary regions (Figure 7 E). The cystic kidneys were on average three times the size of the wild type kidneys (cystic kidney section length 9mm compared to 27mm wild type kidney section), due to the accumulation of fluid and a number of cysts were seen to surround enlarged glomeruli (Figures 7 E). Whereas the glomeruli of wild type kidneys were seen exclusively toward the periphery of the kidney (Figure 7 A), there were glomeruli throughout the cystic kidneys and these glomeruli were enlarged (Figure 7 C and D). The tubule structures were also affected in mutant mice. In wild type kidneys the tubules are compact and well ordered. PAS differentiates between proximal collecting tubules by the prominent staining of their brush borders, compared with distal collecting tubules in which brush borders are absent (Figure 7 C). In the cystic kidneys, tubule structures were increased in size, tubules were engorged and brush borders appeared shriveled. The number of heamatoxylin-stained nuclei seemed to be greatly increased (Figure 7 F). The disorganization and increase in size was also apparent in the other cystic organs, and was associated with changes in cell proliferation and cell death (discussed later).

3.3.3.2 Abnormal Testes

In addition to the cystic kidneys, four Wani $WT^{+/-}$;P3:WT1-KTS animals also presented with abnormal testes (Table 2), 3/4 had enlarged testes while one animal had smaller testes than in wild type controls. Both of the Wines $WT^{+/-}$

;P3:WT1-KTS mice examined had enlarged, cystic testes. Upon histological analysis wild type testes were again, as with the kidney, found to be well ordered and compact structures. Tubules contained germ cells and spermatogonia in varying states of development. Spermatogonia are associated with sertoli cells that provide essential factors for germ cell development. Interstitial cells called Leydig cells provide hormones necessary for testis function (Figure 8 A and B). In the mutant testis (Figures 8 D), the testes contained large cysts. The section presented was from an affected Wines male however, the histopathology of the affected Wani animals was seen to be of a similar nature or less severe. The cysts seem to be derived from tubules and there was an apparent expansion of the interstitial cells associated with the abnormal tubules (Figure 8 C). Furthermore, it was not only organisation of the tubules within testes that was abnormal but also organisation within the tubules. Some tubules showed a complete lack of cells, and tubule conformation of others was visibly altered (Figure 8 C). This structural change was investigated further to see if there was an increase in proliferation resulting in the size increase seen, and at the same time any differences in apoptosis (see Section 3.3.5).

3.3.3.3 Liver tumours

Four animals were found to have liver tumours and the histological analysis of one of these can be seen in Figure 9. The liver is normally a compact structure tightly organised into small units, based on blood supply, called acini. These are characterised by an incoming blood supply in the portal tracts (branches of hepatic artery and portal vein), and a peripheral outgoing blood supply (central vein), associated with cords of hepatocytes. This hepatic triad can be clearly seen in the normal liver sections (Figure 9A) but is less apparent in the tumour section (Figure 9 B). There is an overall

Figure 8. Histological comparison of wild type and mutant adult mouse testes.

(A and B) PAS stained wild type adult (7 month) testis. (A) Organisation of a Wild type testis in histological section, with the seminiferous tubules (T) organised in a compact pattern, while the sertoli cells (S) are located at the periphery of the tubules and leydig cells (L) are found interstially between tubules. (B) H&E staining of the testes also identifies the same cell types and structures : Sertoli cells (S) of the testis located at the periphery of the tubules (T) while Leydig Cells (L) are found interstitially between tubules. (C and D) PAS stained WT1+/-; P3:WT1-KTS cystic testis (7 month) in histological section shows a greater disorganization than the testis of its wild type littermate. (C) There are greater gaps between the tubules (e) with an absence of cells within tubules, some tubules are totally devoid of cells (d) whilst others are surrounded by a larger mass of interstitial cells (f). (D) H&E staining of the cystic testis shows the presence of a large fluid filled cyst (c). Magnification x60 (A-D). Scale bars 200 μm

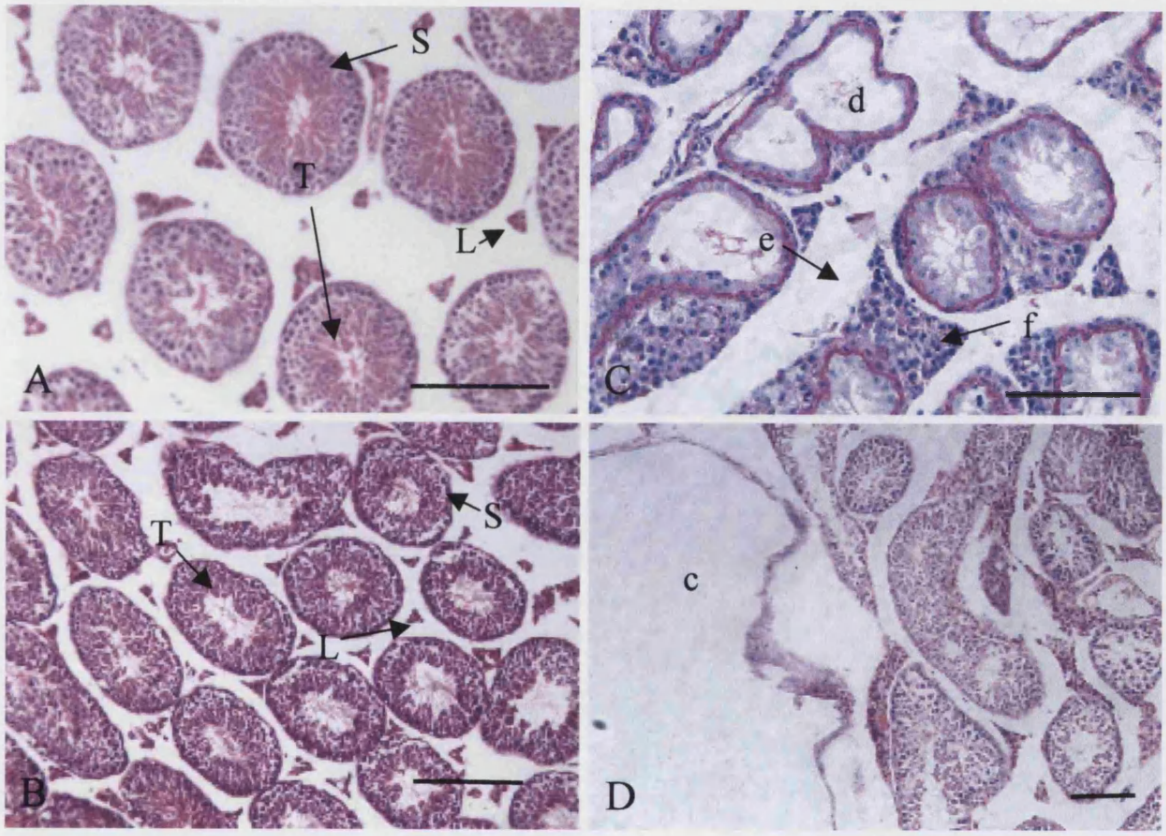
S
T
L
A
d
e
f
C
T
S
L
B
c
D

Figure 9. Histological comparisons of wild type and mutant adult mouse liver sections.

H & E stained liver sections from males at 7 months of age. Animals were wild type (A) and WT1+/-; P3:WT1-KTS (B), highlighting differences between wild type and tumour histology. The portal triad (pt) can clearly be seen in wild type sections whereas there was an overall disorganization in WT1+/-; P3:WT1-KTS liver tumours. Large blood filled cavities can be seen (n) as well as multiple vesicles (v). Although both sections were stained together the wild type section stained much more brightly with Eosin than the tumour section highlighting the differences in morphology between the two sections. Scale bars 200μm

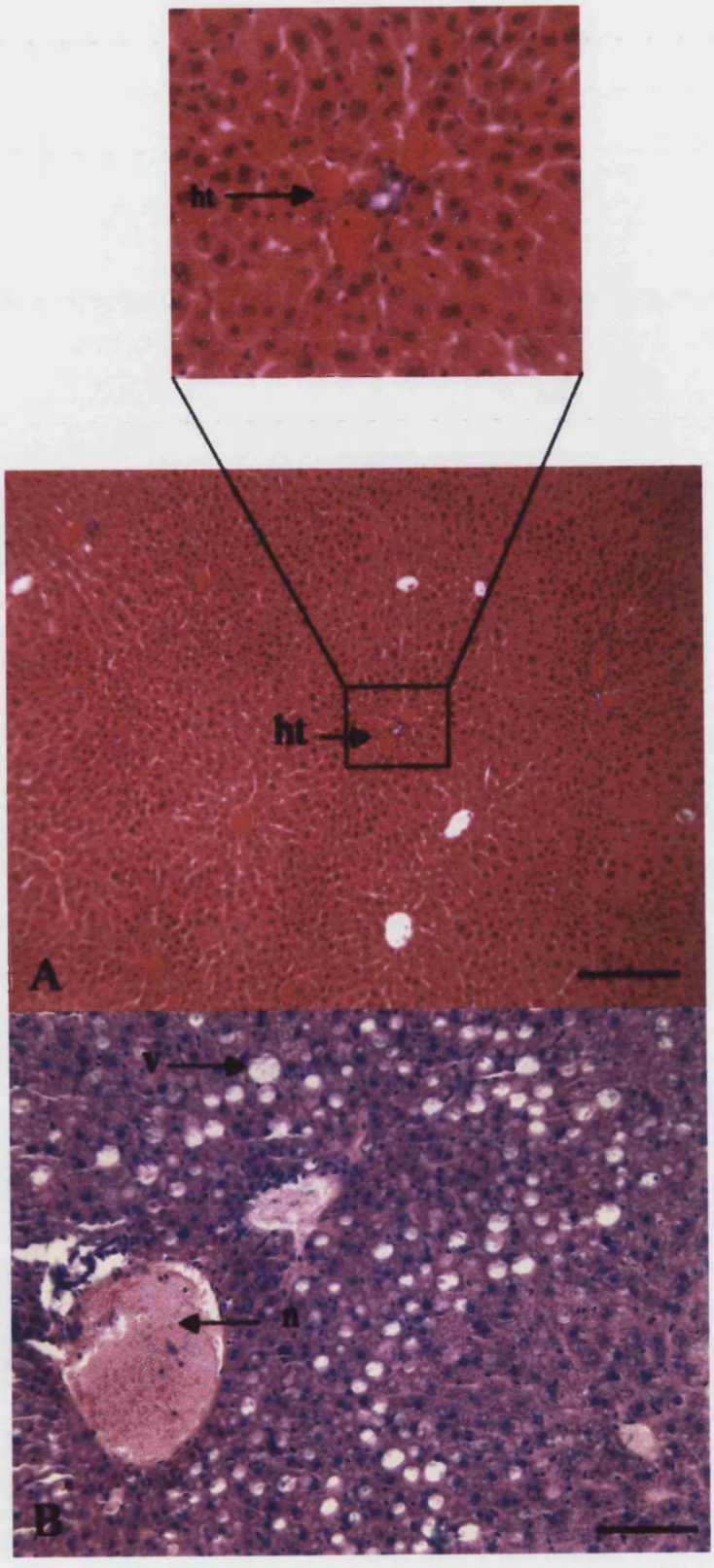
ht
ht
A
v
n
B

disorganisation within the tumour section associated with the presence of tumour cells. The liver was enlarged in each of the affected animals though the number of affected lobes varied in different animals (from one animal with only one affected lobe to another animal with only one seemingly normal lobe).

3.3.3.4 Enlarged eye

One of the Wani $WT1^{+/-}$;P3:WT1-KTS mice was found to have a grossly abnormal eye. Figure 10 shows histological analysis of a wild type eye (panels A and B) and the cystic eye (Panels C and D). The retina lines the back of the eye and is composed of three layers of nerve cell bodies and two layers of synapses. The outer nuclear layer contains the cell bodies of the rods and cones, the inner nuclear layer contains the cell bodies of the bipolar, horizontal and amacrine cells and the ganglion cell layer contains the cell bodies of ganglion cells. Light travels through the pigmented cells and the thickness of the retina before striking and activating the rods and cones. At a histological level, it was possible to see three layers of nucleated cells and the pigmented layer. Next to the pigmented layer, the first layer of nucleated cells is the outer nuclear layer, the second is the inner nuclear layer and the third is the nerve fibre layer. The mutant eye was greatly enlarged in comparison to the wild type and there seemed to be abnormalities in the different layers of the retina characterised by a disorganisation of heamatoylin stained cells and possibly changes in cell number, particularly of the retinal pigmented epithelium.

3.3.4 WT1 expression in adult organs

Using an anti-WT1 antibody WT1 expression was found to vary in different $Wt1^{+/-}$;P3:WT1-KTS animals with abnormal adult organs, and all differed from that of the wild type expression pattern. In wild type animals, WT1 was

Figure 10. Histological comparisons of wild type and mutant adult mouse eye sections.

Sections of eyes from wild type (A) and WT1+/-; P3:WT1-KTS (C) animals stained with H & E, illustrating the increased retinal size and disorganization within the mutant eye. There seem to be severe abnormalities in the retinal pigmentation (r). Anti-WT1 immuno-staining of the wild type eye (B) fails to detect any WT1 protein, however there is WT1 staining apparent in the mutant eye (D). Magnification x100. Scale bars 100μm

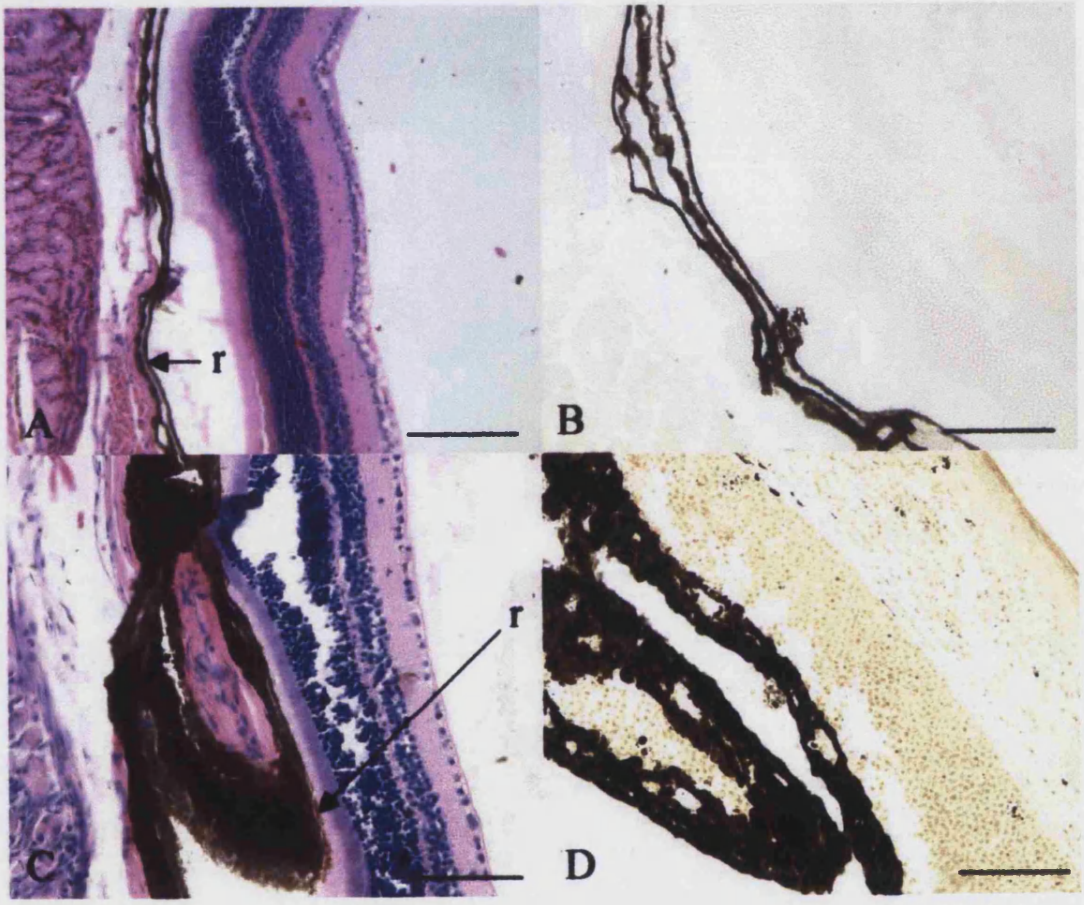
r
A
B
r
C
D

expressed in the podocyte cells of adult kidneys (Figure 11 B) and in the sertoli cells of the adult testes (Figure 11 D), but there was no WT1 expression detected in wild type adult liver (Figure 11 F) or retinal (Figure 10 B) sections. The abnormal organs of $WT1^{+/-}$;P3:WT1-KTS mice however, showed a variety of atypical expression patterns (Figure 10 D and Figures 12a, 12b, and 12c). Kidney sections from some mutant animals showed ectopic expression of WT1 in the tubules with a complete lack of expression in the glomeruli (Figure 12a A). Kidney sections from other mutant animals either showed WT1 expression in large foci associated with the glomeruli (Figure 12a C), or were found to be completely devoid of WT1 expression (Figure 12a B), or showed WT1 expression ectopically, in cells dispersed throughout the kidney (Figure 12a D).

Similarly, a variety of WT1 expression patterns were seen in the testes of different animals. Some testes sections showed a lack of WT1 expression (Figure 12b b), others an abnormal, disorganized expression pattern (Figure 12b C and 12b D) while some sections] showed tubules with patterns similar to those of wild type WT1 expression (Figure 12b B).

An ectopic pattern of WT1 expression in hepatocytes was seen in the livers of mice with enlarged, cystic and tumourogenic organs (Figure 12c A, B, C and D). WT1 expression was possibly in the nuclei of hepatocytes given that the protein is a nuclear factor although it was not clear from the images. The severity of the liver abnormalities was varied, ranging from enlarged livers and mice with one tumourous liver lobe, to a mouse with 3 lobes affected.

Finally, gross morphological and histological abnormalities were detected in one Wt1;P3:WT1-KTS mouse with a severely enlarged eye (Section 3.3.3.4) and this was associated with ectopic WT1 expression (Figure 10 D).

Figure 11. Morphology and WT1 expression in adult tissues from wild type mice.

Sections of kidneys (A and B), testis (C and D), and liver (E and F), were stained either with H & E (A, C and E) or an anti-Wt1 antibody (B, D and F). In the kidney, WT1 expression was seen in the podocyte cells (p) of glomeruli (g) but not in tubules (t). In the testis, WT1 expression was seen in Sertoli cells (st) within seminiferous tubules (tu) and WT1 expression was not seen in wild type adult mouse liver sections. Scale bars 200μm

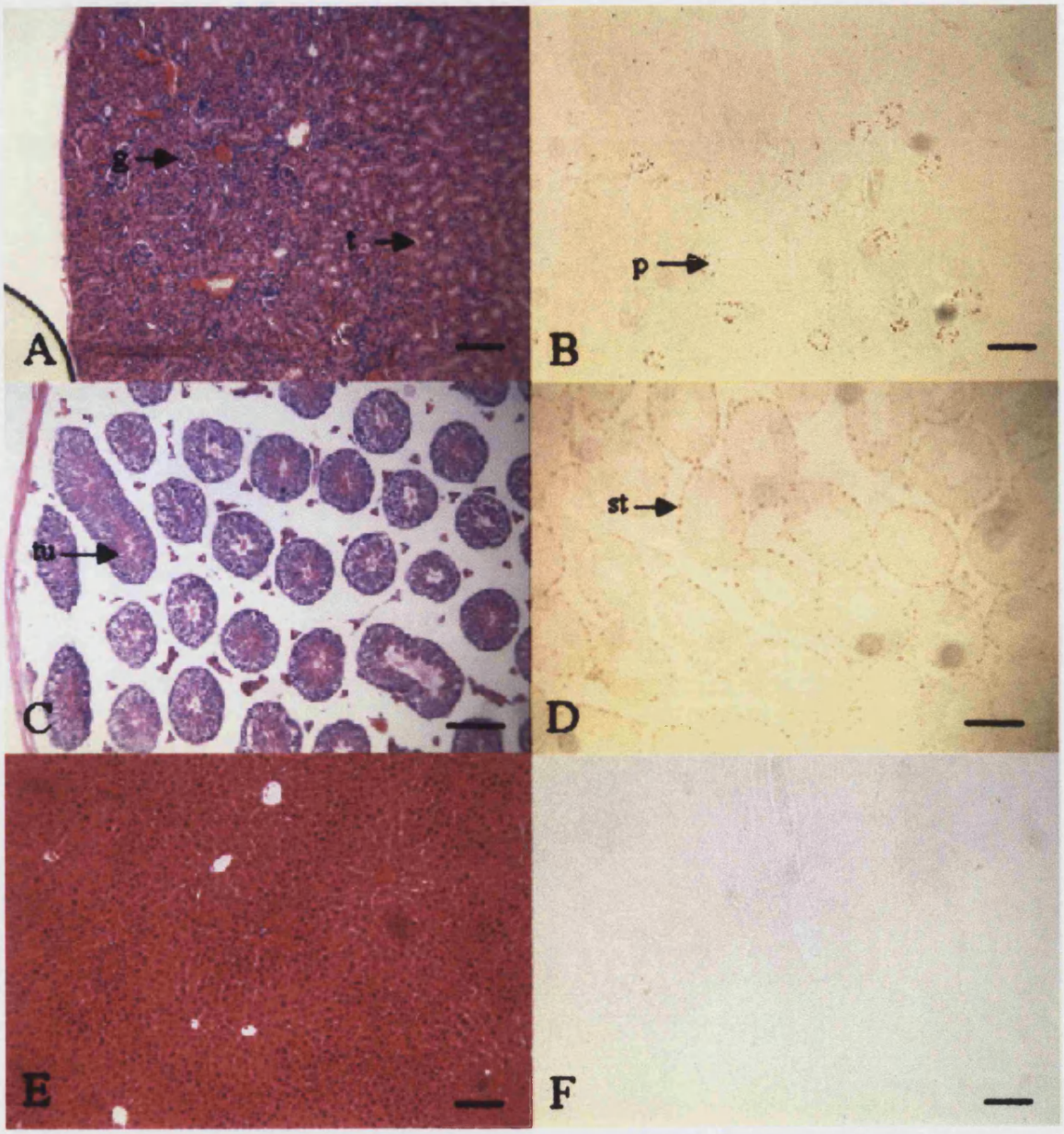
g
t
A
p
B
m
C
st
D
E
F

Figure 12a. WT1 expression pattern in adult mutant mouse kidneys. WT1 expression in four WT1+/-; P3:WT1-KTS mice kidneys (littermates of the animals in Figure 11) showed a range of patterns in kidneys (A, B, C, D). One animal had ectopic WT1 expression within the kidney tubules (t) while the glomeruli (g) were devoid of expession (Panel A). A second animal had kidneys which were devoid of WT1 expression (Panel B). Another animal retained podocyte expression of WT1 in the kidney (p) but larger foci were seen in regions associated with the glomeruli (g) and foci (f) that were independent of glomeruli were also seen to express WT1 (Panel C). The expression pattern of a fourth animal was similar to that of animal C with the kidneys showing ectopic WT1 expression in foci not associated with glomeruli (f) (Panel D). Panel E shows negative control mutant mouse kidney sections. Scale bars 200μm

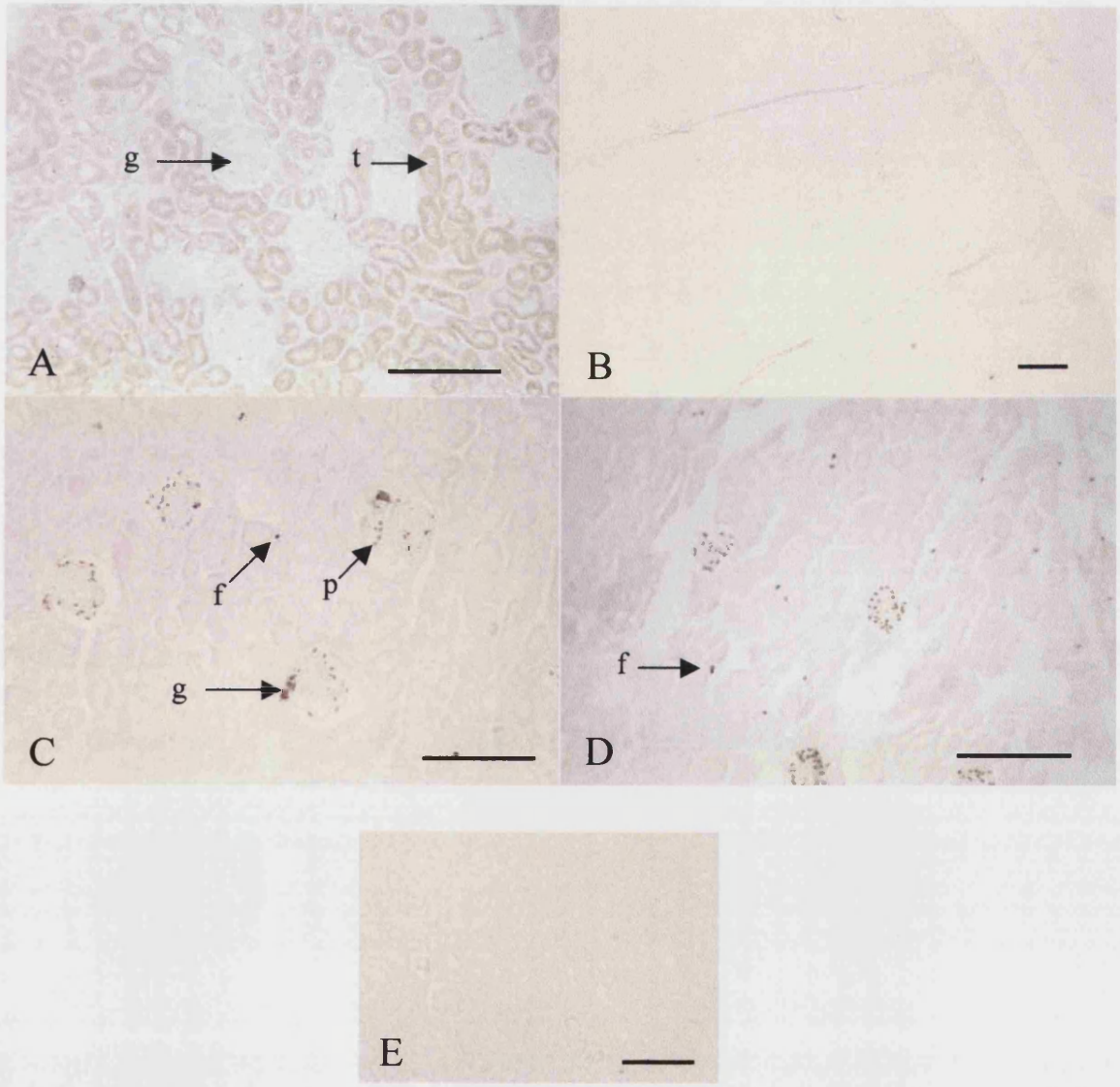
g
t
A
B
f
p
g
C
f
D
E

Figure 12b. WT1 expression pattern in adult mutant mouse testes. WT1 expression in four WT1+/-;P3:WT1-KTS mice testes (corresponding testes to figure 12a) showed a range of patterns in four different animals (A, B, C and D). One animal had testes devoid of WT1 expression (A) whilst a second had a more normal pattern of WT1 expression possibly in the sertoli cells (st). A final two animals had ectopic and increased expression of WT1 within a number of tubules (tu) (C and D). Panel E shows the negative control mutant mouse testes. Scale bars 200μm

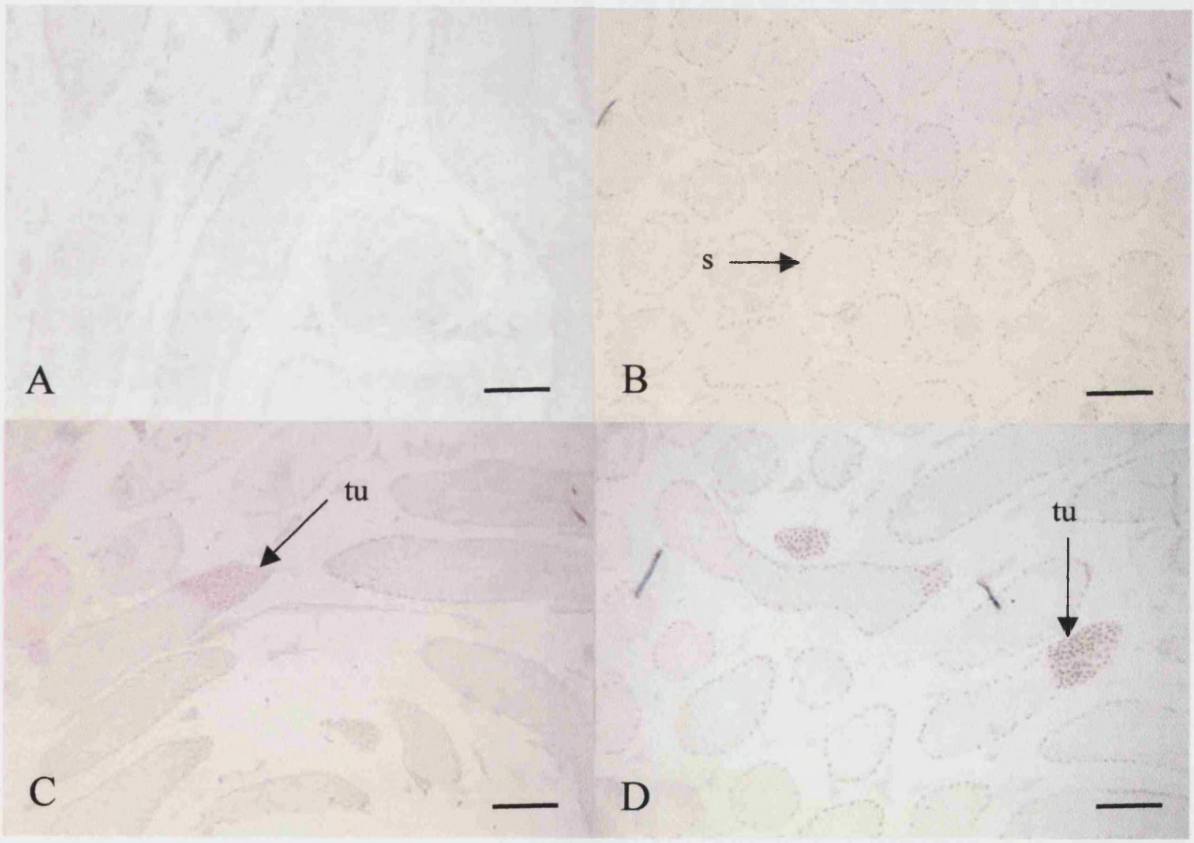
A
B
s
C
tu
D
tu
E

Figure 12c. WT1 expression pattern in adult mutant mouse livers. WT1 expression in four WT1+/-;P3:WT1-KTS mice livers (corresponding livers to figures 12a and 12b) showed the presence of multiple ectopic foci of WT1 expression seen throughout the liver. Wild type adult liver lacked any WT1 expression (figure 11). Panel E shows the negative control mutant mouse liver section. Scale bar 200μm

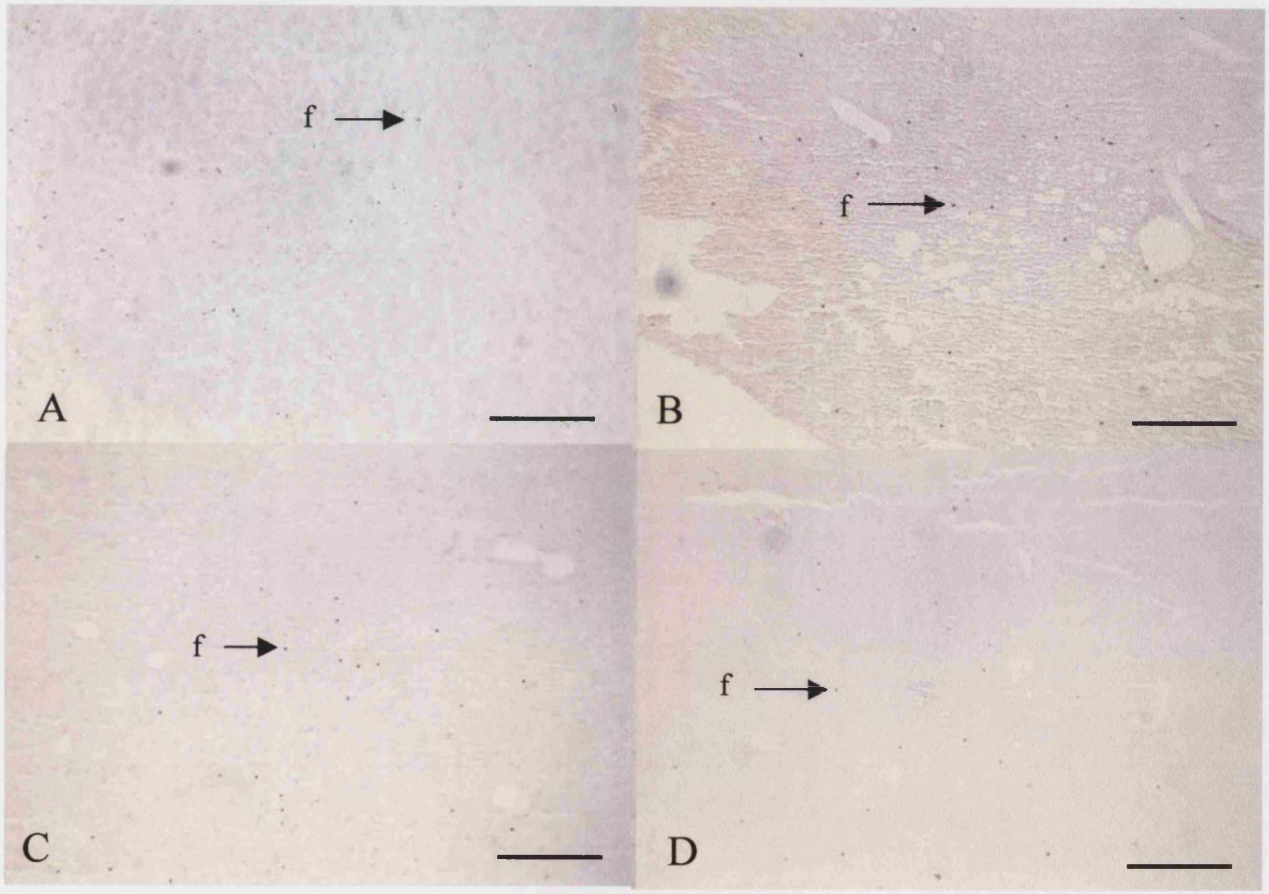
f
A
f
B
f
C
f
D

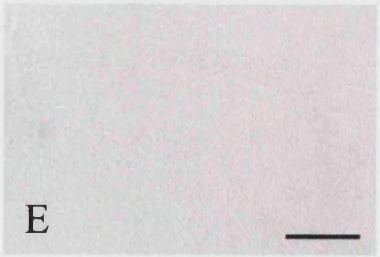
E

3.3.5 Apoptosis and Proliferation in adult organs

In order to investigate changes in cell turnover cell proliferation and apoptosis were assayed in kidney and testis from both wild type and mutant mice. Apoptotic cells were detected, using a DNA end-labelling method, within sections from wild type and mutant kidneys (Figure 13 A-D) and testes (Figure 13 E and F). Overall, there was a dramatic increase in apoptotic cells as illustrated by the cells stained red in mutant sections (Figure 13 B, D and F) in comparison to Wild type cells (Figure 13 A, C, E). The glomeruli of the wild type kidney were devoid of apoptotic cells with no red staining visible (Figure 13 A), while stained cells were present in glomeruli of mutant kidney sections (Figure 13 B). Similarly, apoptosis events were rarely detected in wild type kidney tubules (Figure 13 C), but numbers were greatly increased among cells of mutant kidney tubules, irrespective of the type of tubule (Figure 13 D). Apoptosis within the testis of mutant animals was again much increased in comparison with wild type animals (Figures 13 E and F). Apoptotic cells were located at the periphery of the affected tubules and seemed to surround the multi-nucleated DAPI stained cells (Figure 13 F). The position of the apoptotic cells suggests they may be either Sertoli cells or primary germ cells, or indeed may include both cell types, however this has not been clarified.

Proliferation events, evaluated using an antibody recognizing proliferating cell nuclear antigen (PCNA), were also changed in cystic kidneys and testis. The differences between wild type sections (Figures 14 A, C, E and G) and mutant sections (Figures 14 B, D, F and H) were clearly apparent with large foci of proliferation in the abnormal kidneys as opposed to single cells that

Figure 13. Comparison of apoptosis in wild type and mutant (WT1+/-;P3-KTS) adult mouse testes and kidneys.

Apoptosis within wild type kidneys (A and C), wild type testis (E), mutant cystic kidneys (B, D) and mutant cystic testis (F) at x60 magnification. DAPI stained cells (nucleated cells) stain blue under fluorescence whereas cells undergoing apoptosis fluoresce red. Wild type animals showed a negligible amount of apoptosis in the glomerulus (A) or kidney tubules (C) and in the seminiferous tubules of the testis (E). In WT1+/-;P3-KTS samples there was a marked increase in apoptosis at the periphery of glomeruli (B) and in all tubules (D) in the kidney, and at the periphery of seminiferous tubules in the testis (F). The mutant and wild type animals represented were littermates at 7 months of age. Scale bars 100μm

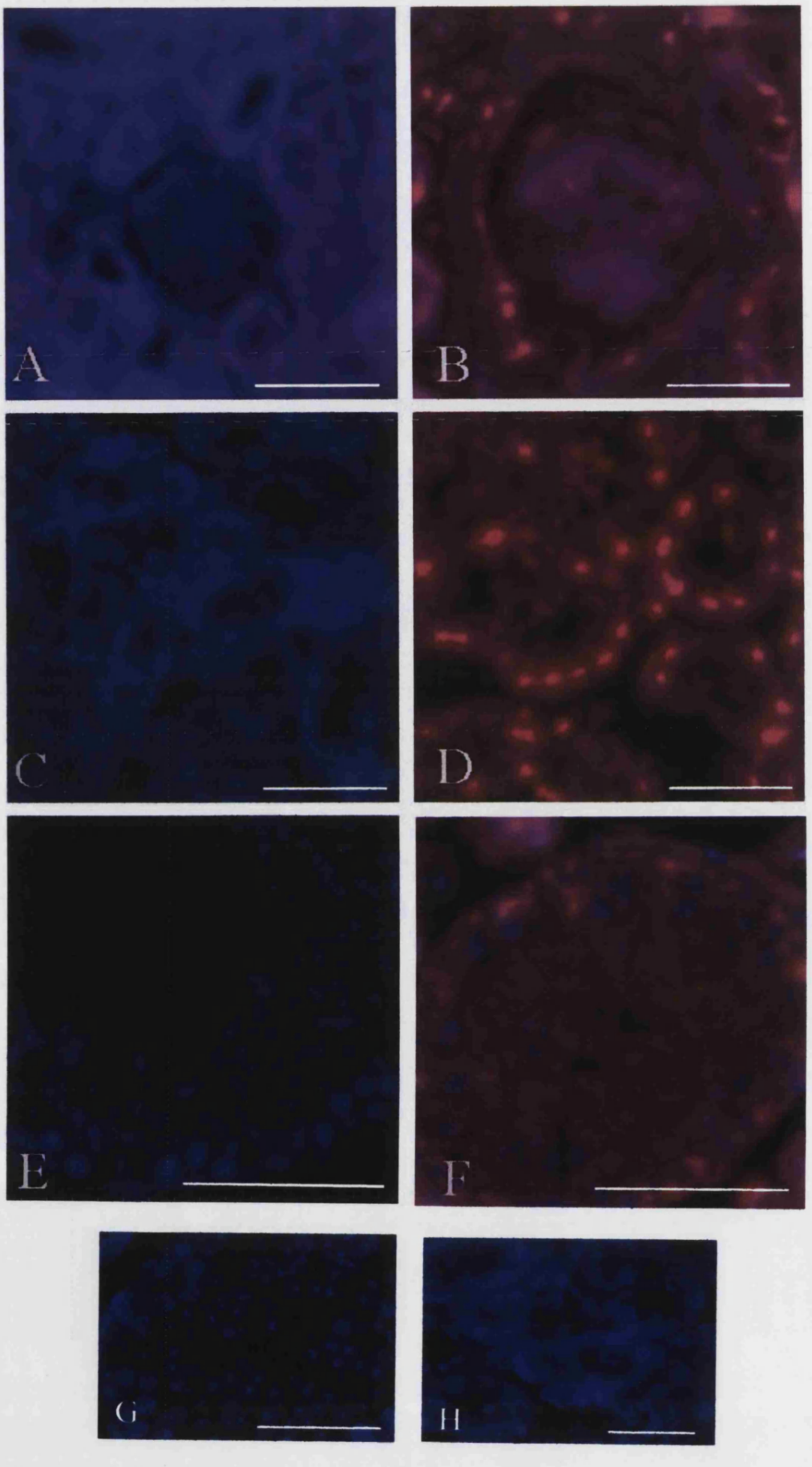
A
B
C
D
E
F
G
H

Figure 14. Comparison of proliferation within wild type and mutant (WT1+/-;P3-KTS) adult mouse kidneys and testes.

Anti-PCNA stained wild type and mutant kidney and testis sections counterstained with hematoxylin identify proliferating cells within these organs. PCNA staining was prominent within glomeruli of the wild type kidney (A) but was negligible within the tubules (C). In mutant animals, there was a marked increase of proliferation associated with cells around glomeruli (B) and within tubules (D). The pattern of proliferation in wild type adult testicular tubules was very specific and located to the periphery of seminiferous tubules (E and G). In mutant testes sections there was a dramatic change in proliferation with some tubules almost completely devoid of proliferating cells (i), others containing proliferating cells throughout the tubule (j), another subset of tubules seemed fairly normal (k) and a final group of tubules expressing proliferating cells in a disorganized pattern (l). All sections were photographed under x60 magnification except that in Panel E at x30 magnification. Scale bars 200μm

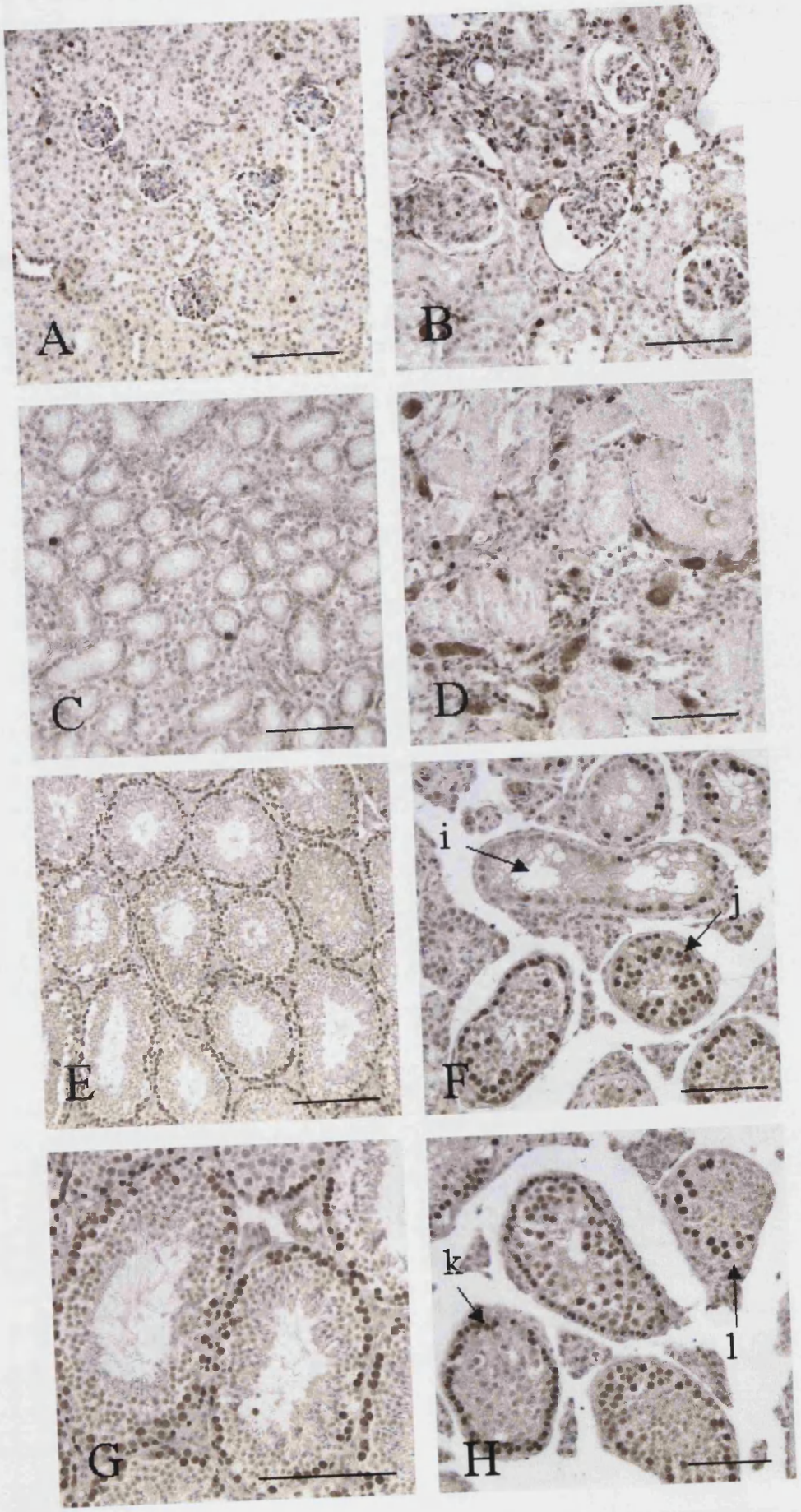
A
B
C
D
E
i
j
F
k
l
G
H

were more evenly dispersed in the wild type. In the glomerular regions of abnormal kidneys (Figures 14 B) there were clustered regions of proliferation whilst in the tubular regions a marked increase of proliferation was seen (Figure 14 D), however although the anti-PCNA foci of staining were also larger this may reflect the increase in size of the components of the kidney. The changes in proliferation in testes were easier to analyse as proliferation was entirely restricted to primary spermatogonia at the periphery of wild type tubules (Figure 14 E and G). In the mutant, although some seminiferous tubules showed seemingly normal patterns of proliferation, some tubules contained almost no proliferating cells and others contained proliferating cells located towards the lumen of the tubule, not just at the periphery (Figure 14 F and H).

3.3.6 Measurement of renal function in adult mice

After two mice from the Wines transgenic line were found at necropsy to have profound renal and genital abnormalities, it was thought that renal problems might be detected at an earlier stage in other mice. Renal function of seemingly healthy adult mice was investigated by analysis of urine (Figure 15). When urine samples were tested with urine analysis sticks, proteinuria was observed in $WT1^{+/-}$;P3:WT1-KTS animals (Figure 15 A). Coomassie staining of urine samples on protein gels confirmed proteinuria in $WT1^{+/-}$;P3:WT1-KTS animals by detecting the presence of a 67 kDa protein band (Figure 15 B). This band appeared in largest amounts from samples taken from $WT1^{+/-}$;P3:WT1-KTS mice although some $WT1^{+/-}$ littermates showed less, although detectable, protein. Protein was not seen in samples taken from wild type animals. Some $WT1^{+/-}$ mice seen to contain protein in the urine from the protein gel experiments failed to show proteinuria from urine stick analysis suggesting that the Coomassie urine detection method was

Figure 15. Detection of protein in urine samples as a means of assessing renal function in adult mice

The urine from adult mice was analysed with urine analysis sticks (A) and by PAGE (B). In this example urine from a 7 month WT1+/-; P3:WT1-KTS animal (sample 3) was compared with its wild type and WT1+/- littermates. The proteinuria indicator showed high levels of protein were present in sample 3 (A) and the same sample also showed the presence of a prominent 67K protein band on the coomassie stained protein gel (B).

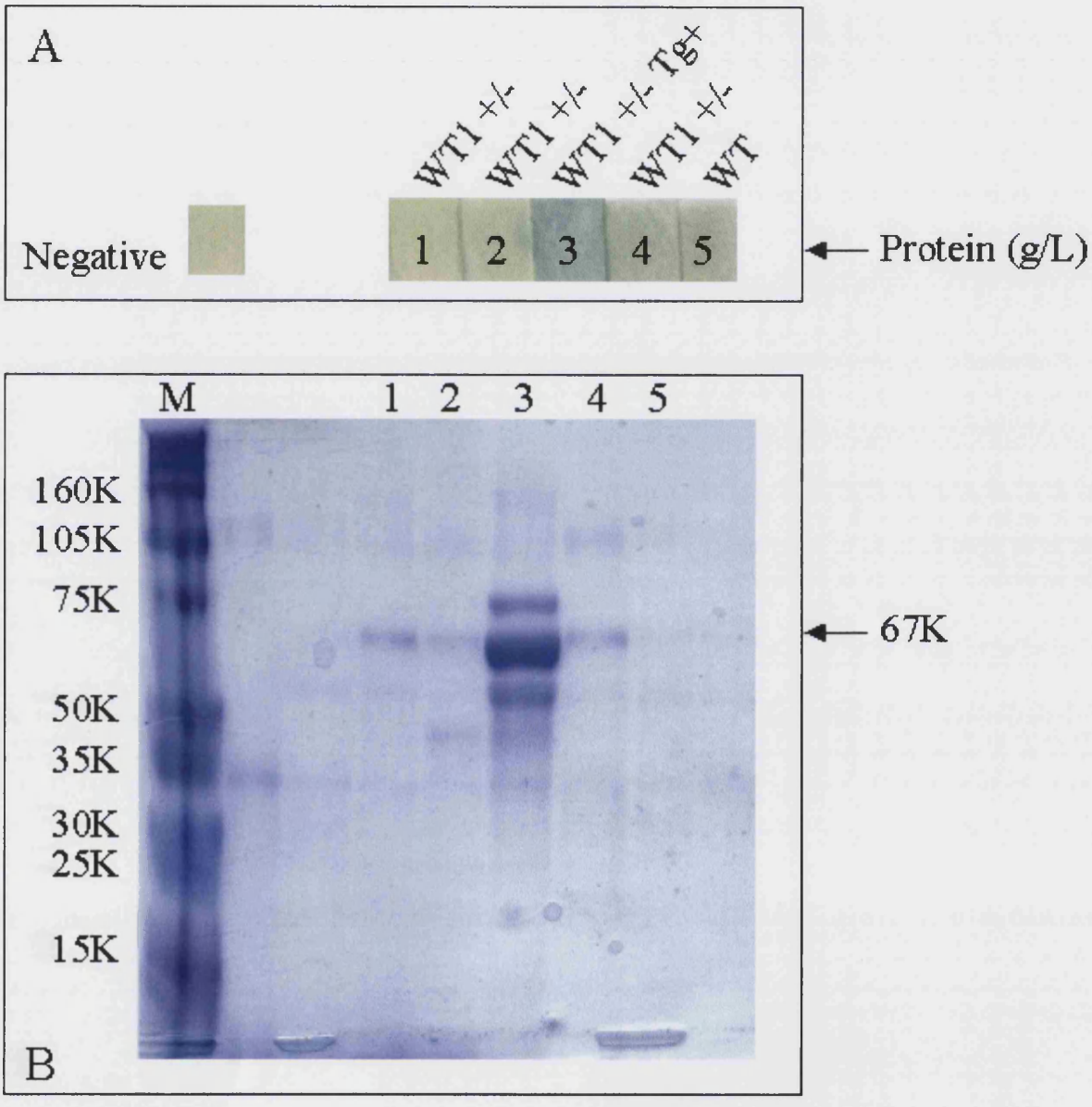
A
WT1 +/-
WT1 +/-
WT1 +/- Tg+
WT1 +/-
WT
Negative
1
2
3
4
5
Protein (g/L)
M
1
2
3
4
5
160K
105K
75K
50K
35K
30K
25K
15K
67K
B

more sensitive. Proteinuria and coomassie staining of urine samples only yielded positive results in animals over the age of 4 months. Proteinuria is a symptom of aberrant kidney function when the kidney fails to reabsorb and filter out proteins so they are present in the urine. These results show that in seemingly healthy transgenic animals there is a degree of renal failure that may progress to the state observed in the two Wines animals with enlarged, cystic kidneys. Measurements of proteinurea were made on the urine samples of 52 mice at ages ranging from 4-10 months (note that some mice were tested at two or more different ages)(Table 3). Out of these animals, 12 (1 $WT1^{+/+}$;P3:WT1-KTS animal and 11 $WT1^{+/-}$;P3:WT1-KTS animals) were shown to have greatly increased proteinuria in comparison to wild type littermates. Upon histological analysis it was confirmed that these animals had kidney defects and furthermore, in some cases, abnormalities of their testes and/or liver (Table 2).

Table 3. Number, age and sex of Wani animals, which showed over 20g/L protein using the urine stick analysis after raised protein levels in urine samples had been initially detected on a coomassie stained protein gel. A total of 52 animals were analysed (note, animals were tested first from the ages of 4-6 months and then again after 7 months).

Genotype	No of animals with proteinuria out of total number of animals for that genotype			
	Males 4-6 months old	Males 7-18 months old	Females 4-6 months old	Females 7-18 months old
WT1+/+	0/5	0/5	0/1	0/1
WT1+/+ ;P3:WT1-KTS	0/6	1/6	0/2	0/2
WT1+/-	0/9	0/9	0/10	0/10
WT1+/- ;P3:WT1-KTS	2/9	8/9	0/10	1/10

3.3.7 Comparison of morphology and protein expression between mouse mutants

The final group of experiments in this chapter, were an attempt to compare differences in genital development and protein expression patterns between wild type animals, WT1 mutants and another mouse model of sterility, the Ob mutant mouse. Morphology, immunostaining, apoptosis and proliferation analyses were carried out on the testis of adult Ob homozygous mice (Figure 16) and all adult testis and kidneys underwent immunohistological detection of WT1 and Basp1 proteins using the corresponding antibodies.

3.3.7.1 Ob mutants

Ob homozygotes had smaller testes than wild type animals, seminiferous tubules were decreased in size, with wider spaces between them and an increase in interstitial cells (Paisley, 2000). Within the seminiferous tubule there seemed to be less disorganization than in WT1+/-;P3:WT1-KTS mutant tubules (compare Figures 14 F and 16 B). Cell proliferation was decreased in Ob mutant testes (Figure 16 B) but still restricted to the periphery of the tubules as in wild type testis (Figure 16 A). Although apoptosis was mainly still restricted to the periphery of mutant tubules (Figure 16 D) the levels were increased in comparison with wild type tubules (Figure 16 C), there was however some apoptosis within the tubule suggesting that spermatogenic cells other than spermatagonia for example primary or secondary spermatocytes, were undergoing apoptosis. This pattern of apoptosis was not seen in testes of either wild type or $WT1^{+/-}$;P3:WT1-KTS (Figure 14 F) mutant mice. Finally, sertoli cells were still present at the periphery of Ob mutant seminiferous tubules, as shown by immunostaining with the WT1 antibody, a marker of sertoli cells (Figure 16 F). Notably, there were few gaps between the sertoli cells in Ob mutants (Figure 16 F) compared with wild type littermates (Figure 16 E), suggesting that the germ cells, that do not express detectable WT1, are missing in this mutant, which does not seem to be the case in the $WT1^{+/-}$;P3:WT1-KTS mutants (Figure 14 F).

3.3.7.2 Immunohistochemistry with the Basp1 antibody

An antibody raised against the putative WT1-interacting protein, Basp1, revealed that in the adult kidney Basp1 protein was expressed in similar if

Figure 16. Histological analysis mousecomparing Ob mutant and wild type testes

Proliferation (assayed using an anti-PCNA antibody; A and B), apoptosis (C and D), and WT1 expression (assayed using an anti-WT1 antibody; E and F) in the testis of wild type (A, C and E) and Ob mutant (B, D and F) adult mice (littermates at 7 months of age). The Ob mutant testis showed differences in proliferation (B) from the wild type (A) with cell proliferation in the mutant being decreased in many seminiferous tubules. Where there was proliferation, it was located at the periphery of tubules in a pattern similar to that of wild type tubules. The apoptosis in mutant testis tubules (D) was increased compared to that of wild type littermates (C) and was also located to the periphery of tubules. WT1 staining remains similar in mutant testes (F) as compared with wild type animal testes (E). In mutants, proliferation was confined to cells at the periphery of seminiferous tubules but appeared fainter than the staining in wild type samples.

Magnification (A), (B), x30, (C), (D) x100, (E), (F) x60. Scale bars A, B, E, F 200μm, C and D 100μm

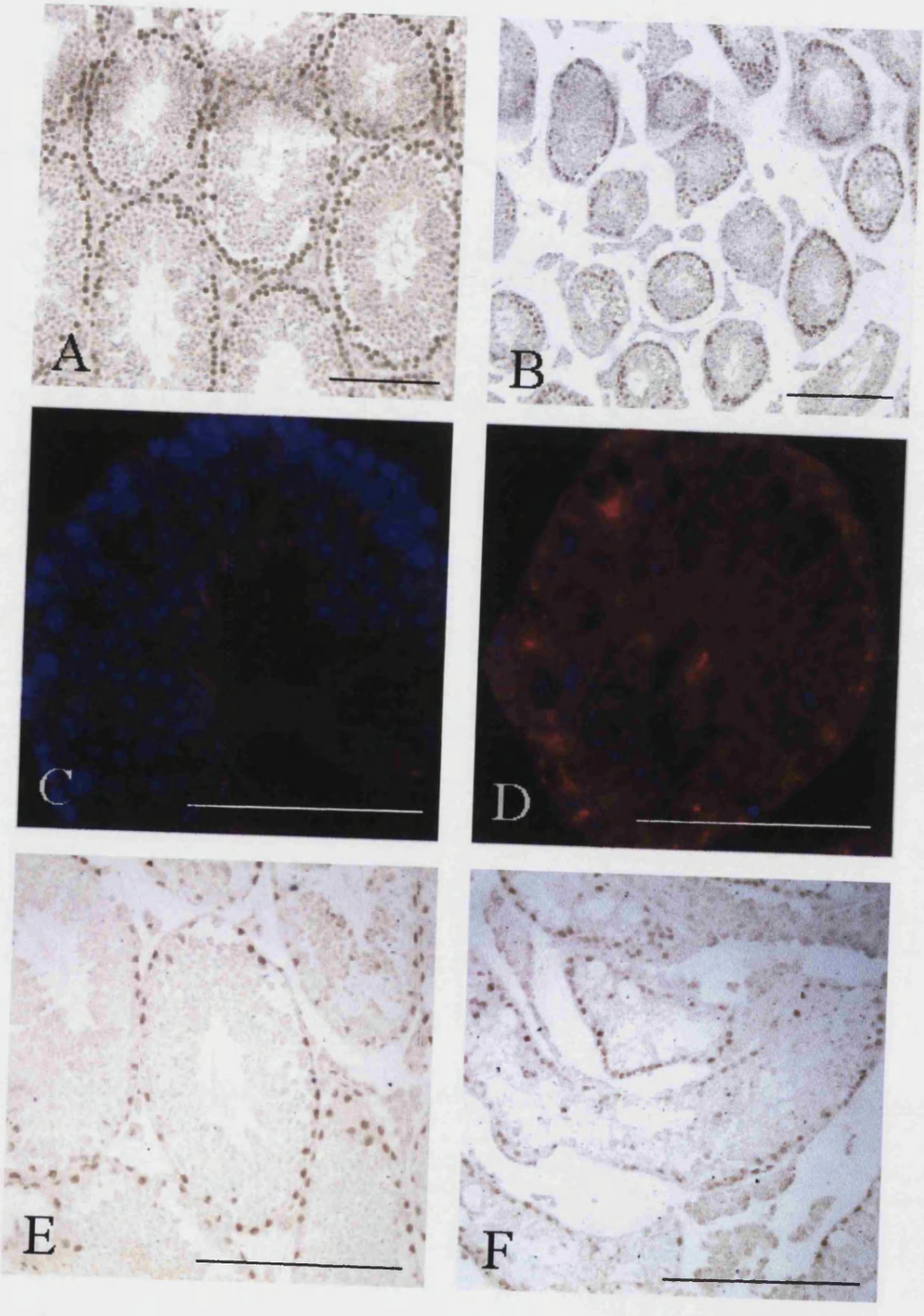
A
B
C
D
E
F

not identical locations to WT1 (Figure 17 A and B) , in what appear to be the podocyte cells of glomeruli. Some Basp1 was also detected in certain tubules in the kidney (Figure 17B), where WT1 was never seen in wild type animals.

In wild type testes Basp1 was located to the periphery of seminiferous tubules (Figure 17D), but was predominantly cytoplasmic, unlike the nuclear WT1. WT1 was also expressed at the periphery of the seminiferous tubules (Figure 17C), were it is known to mark Sertoli cells, but it was not possible to tell if the proteins were expressed in exactly the same cell types. However, the persistence of Basp1 staining in cells located away from peripheral cell layers suggests that Basp1 was localised in the germ cells. Basp1 expression patterns were unchanged in sections of kidney and testis from Wt1+/-;P3:WT1-KTS mutant mice (data not shown).

In cell culture, Basp1 and WT1 expression was seen in both Cos7 cells (Figure 17 E) and Hela cells (Figure 17F) although not in the same area due to the cytoplasmic localisation of the Basp1 protein, in contrast to the nuclear localisation of WT1 protein.

Figure 17. Basp1 expression in the kidneys and testes of adult wild type mice and in cultured cells.

Comparison of expression patterns of Basp1 and WT1 in kidneys (A and B), testes (C and D) and cell lines (E and F). The WT1 protein is expressed in glomerular podocytes (p) of the kidney (Panel A). Basp1 was expressed in similar regions within the glomerlus (g) and also in a number of tubules within the kidney (tu) (Panel B). In the testes, WT1 was expressed in sertoli cells (st) (Panel C) and Basp1 expression was also seen at the periphery of testicular tubules, probably including, though not necessarily restricted, to germ cells (tu) (Panel D). In Cos 7 cells (Panel E) and HeLa cells (Panel F) both the proteins are expressed within the same cells however, WT1 is expressed within the nucleus of cells (n) and Basp1 is seen in a cytplasmic pattern (c). In tissue sections endogenous proteins were detected using anti-WT1 (A and C) or anti-Basp1 (B and D) antibodies, using a secondary antibody conjugated to DAB (brown staining). In cultured cells (E and F) endogenous Basp1 was detected using an anti-Basp1 antibody conjugated to Texas Red and viewed under fluorescence (red channel). The cells had been transfected with constructs expressing WT1+KTS:GFP fusion protein (viewed in the green channel). Scale bars A-D 100μm, E and F 5μm

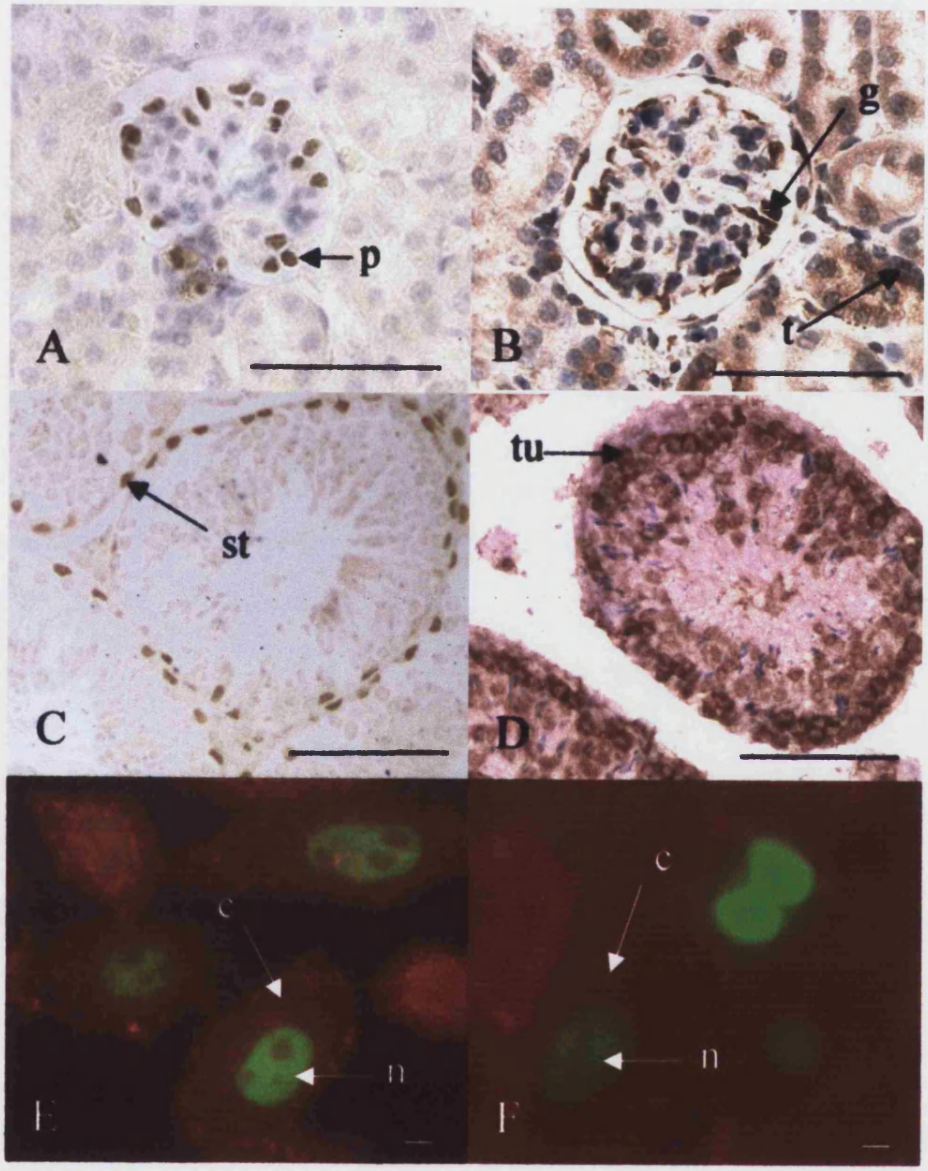
p
A
g
t
B
st
C
tu
D
c
n
E
c
n
F

3.4 Discussion

The experiments in this chapter investigated a number of aspects of WT1 expression. WT1 is essential for early genito-urinary development in mice (Kreidberg et al., 1993), however, its requirement in adults is less well characterised. A number of animal models exist where altered WT1 expression in mice result in abnormalities paralleling those of human disorders (Hammes et al., 2001; Kreidberg et al., 1993; Patek et al., 1999). It is thought that the WT1+KTS and WT1-KTS proteins are usually expressed in a ratio of 2:1 (Haber et al., 1990; Larsson et al., 1995; Little et al., 1992), this ratio is tightly conserved however some cell lines appear to have different ratios of these isoforms (Pritchard-Jones et al., 1990). It is thought that Frasier syndrome results from the reversal of the isoform ratio from 2:1 to 1:2, towards higher levels of WT1-KTS. This happens when WT1+KTS expression is lost from one allele, with a concomitant rise of WT1-KTS from the same allele as a result of mutations in intron 9 of the WT1 gene (Barbaux et al., 1997). Hence, Frasier syndrome not only highlights the essential requirement of WT1+KTS and WT1-KTS in the genito-urinary system, but the maintenance of their critical ratios. This chapter further investigates those critical ratios.

3.4.1 The P3:WT1-KTS transgene fails to rescue the phenotype of Wt1-/- knockout embryos

WT1 null embryos die prenatally at around E14.5 from cardiac defects. The kidneys and testes fail to form in these embryos (Kreidberg et al., 1993). A 280kb YAC spanning WT1 and its surrounding regulatory elements was able to partially rescue the null phenotype. The cardiac phenotype was rescued allowing progression to birth although the genito-urinary system was still affected in these animals resulting in postnatal death (Hammes et al., 2001). This data suggests that there are other *Wt1* regulatory elements outside this 280kb region,

however, in areas where there was correct expression of the transgene, it was possible to rescue the null phenotype. The expression of a 460kb YAC was able to more fully rescue the null phenotype but the resulting mice did go on to develop nephropathy, suggesting a requirement for further elements to provide normal expression (spatial patterns or levels) of WT1 (Guo et al., 2002).

Our experiments were aimed at investigating the involvement of a single isoform of *Wt1* in genito-urinary development. We utilized a transgenic approach with the creation of the P3:WT1-KTS transgene, in which a WT1-KTS cDNA sequence was placed under the control of the IGF2 P3 promoter and H19 enhancer elements. These same regulatory elements were previously shown to drive a LacZ reporter gene in the kidney, gonads, and liver in a manner that was temporally consistent with WT1 expression (Brenton et al., 1999). The aims of the experiments were first, to see if overexpressing WT1-KTS in a wild type or heterozygous knockout *Wt1* background ($WT1^{+/+}$;P3:WT1-KTS and $WT1^{+/-}$;P3:WT1-KTS transgenic mice) would result in any developmental disorders, either in embryos or in adult mice. WT1-KTS was chosen, rather than WT1+KTS specifically because the relative overexpression of WT1-KTS occurs in Frasier syndrome in humans. Second, we wanted to investigate whether it was possible for the single isoform to rescue any of the phenotypic features of the *Wt1* knockout (null) embryo (by generating $WT1^{-/-}$;P3:WT1-KTS embryos), and therefore understand better the level of redundancy between WT1 isoforms.

A total of 24 litters were analysed at embryonic stages from three transgenic lines (Section 3.3.2). Out of the 26 embryos that were $WT1^{+/+}$;P3:WT1-KTS, there was no difference in morphology of these embryos in comparison with wild type littermates or for that matter, the $WT1^{+/-}$;P3:WT1-KTS embryos, following histological analysis after sectioning and H & E staining of 10 embryos from each

genotype. The antibody detected the presence of the protein in wild type embryos but it was not possible to differentiate endogenous from exogenous protein in transgenic embryos. The $WT1^{-/-}$ embryos exhibited agenesis of the kidneys and testes as expected and it is possible to see evidence of pericardial effusion characterised by blood surrounding the heart in these embryos. The same pathologic features were also seen in the 12 $WT1^{-/-}$;P3:WT1-KTS embryos examined, indicating that the presence of the transgene was not able to rescue the null phenotype. We know the P3:WT1-KTS transgene is expressed from the results of RT-PCRs carried out previously (Duarte 1997) although levels of expression were not obtained. However, RT-PCR was carried out only on liver from 3 day old transgenic animals. Some further evidence of expression from the transgene was seen in hepatocytes of the adult liver in at least some transgenic samples. Since there is not usually any detectable WT1 expression in the liver of wild type animals it is possible that this expression was due to the transgene. Previous analyses of the *Igf2* P3 and *H19* enhancer have shown that these elements can direct expression in the embryonic liver, kidney, gonads and brain (Ward et al., 1997, Brenton et al., 1999). However, in these earlier studies the *Igf2* and *H19* regulatory elements were used to drive expression of reporter genes, the assays for which may be more sensitive than the anti-WT1 antibody used in this study. The P3:WT1-KTS transgene did not appear to cause any developmental disorders when present in $WT1^{+/+}$ or $WT1^{+/-}$ embryos and failed to rescue the null phenotype of $WT1^{-/-}$ embryos. This lack of an effect is likely due to low levels, or absence, of expression from the transgene during embryogenesis in the Wani, Wefi and Wines transgenic lines.

As to why the P3:WT1-KTS transgene failed to rescue the null phenotype in $WT1^{-/-}$P3:WT1-KTS embryos, there are a number of possibilities. The relatively low amounts of protein produced from our transgene may not have been

sufficient to compensate for intact WT1 function. This argument is supported by the fact that the antibody failed to detect transgenic protein in $WT1^{-/-}$;P3WT1-KTS embryos. Alternatively, although transgenic $WT1^{-/-}$;P3:WT1-KTS embryos may express WT1-KTS, they lack not only WT1+KTS but also the other isoforms of the protein, particularly those that include exon 5-encoded sequences. Transgenic experiments have shown that the splicing of the mammal specific exon 5 resulting the presence or absence of 17 amino acids within the protein, is not required for development or fertility (Natoli et al., 2002). However, these isoforms, along with the others must carry out some function and it is feasible that the action of the isoforms is carried not individually but in combination. It is possible that WT1-KTS cannot compensate for all WT1 isoforms sufficiently to rescue the null phenotype. This can be further illustrated by looking at data from experiments where WT1+KTS or WT1-KTS were specifically knocked out. The resulting animals showed better genito-urinary development than animals with the WT1 null allele. These animals would have had a mix of exon 5 isoforms whereas the WT1-/-;P3:WT1-KTS embryos do not. Finally, we cannot rule out the possibility that the P3:WT1-KTS transgene fails to rescue the Wt1 knockout phenotype because it does not sufficiently recapitulate the correct expression of WT1. Although RT-PCR has shown that animals express the transgene (at least in the liver at 5 days of age) the transgene has so far been undetectable in embryos using the available antibody possibly due to the fact that the WT1-KTS is expressed in amounts too low for the antibody to detect.

3.4.2 $WT1^{+/-}$;P3:WT1-KTS adult mice display pathological abnormalities

A number of mouse lines have been created with altered WT1 expression to try and unravel the enigma of WT1 function. I have mentioned the YAC rescue experiments (Moore et al., 1999; Moore et al., 1998) and the WT1 null (Kreidberg

et al., 1993) earlier in this chapter. Two other important experiments parallel the aims described in this chapter, that is the creation of mouse models of human disorders involving WT1 and the investigation of the roles of WT1+KTS and WT1-KTS function in murine development. Patek et al 1999 created a mouse line with truncations of Wt1 within the zinc finger region. Chimeric mice with cells carrying the heterozygous mutation showed urogenital abnormalities characteristic of DDS and illustrated that mice can develop urogenital abnormalities typical of human disease (Patek et al., 1999). Hammes et al (2001) developed transgenic animals where either the WT1+KTS or WT1-KTS isoforms were removed (Hammes et al., 2001). They reported that the complete removal of either isoform resulted in lethality with severe abnormalities in the kidneys of the pups. Heterozygous animals with reduced levels of WT1+KTS developed normally and were fertile however 70% of them went on to develop severe albuminuria and died due to renal insufficiency. Histological analysis of the kidneys demonstrated the presence of glomerusclerosis and nephropathy characteristic of FS as well as defects in the male sex determination process. In contrast, heterozygous animals with reduced levels of WT1–KTS had hypodysplastic kidneys and the presence of streak gonads showing that although both WT1 isoforms are require for correct urogenital development, they have differing functions.

Our transgenic approach was aimed at creating a similar imbalance of WT1-KTS:WT1+KTS ratios, but using an alternative strategy. The P3:WT1-KTS transgene allowed us to come up with a number of variables of isoform ratio in our mice when crossed with $WT1^{+/-}$ knockout (null) mice. The P3:WT1-KTS transgene was unable to exert a substantial effect in $WT1^{-/-}$;P3:WT1-KTS embryos as discussed earlier in this chapter. In these embryos any shift of isoform ratio caused by transgene expression was towards an excess of the

WT1-KTS isoform and the embryos died in mid-gestation with a similar pathology to both $WT1^{-/-}$ null mice (Kreidberg et al., 1993) and those animals with a homozygous reduction of WT1+KTS (Hammes et al., 2001). Previous analysis in our lab had revealed no pathological change in $WT1^{+/+}$;P3:WT1-KTS mice. This might be because the WT1 isoform ratio was not shifted far enough towards the WT1-KTS isoform, as is seen in FS and in the FS mouse model (Hammes et al., 2001). However, the previous study of $WT1^{+/+}$;P3:WT1-KTS mice was restricted to mice of up to 4 months of age and, although these were analysed histologically in reasonable numbers (16 wild type and 22 transgenic animals) (J.R. Dutton and A. Ward, personal communication) this may have been too early for the development of defects seen in this study.

3.4.2.1 Abnormalities in Wines animals

Two Wines $WT1^{+/-}$;P3:WT1-KTS transgenic males failed to produce any litters after a year of attempted breeding. These $WT1^{+/-}$;P3:WT1-KTS animals were culled and dissected. The necropsy revealed hugely enlarged kidneys and testis. Upon histological analysis it was demonstrated that both the kidneys and testes had been enlarged due to the presence of fluid filled cysts (Table 2 and Figure 7). The cystic testes were likely to have been the cause of the sterility of these males. The two animals were the only remaining Wines mice and we were therefore not able to analyse others from this line.

3.4.2.2 Abnormalities in Wani animals

Upon finding the cystic kidneys in the Wines mice, attention turned to the Wani P3:WT1-KTS transgenic animals. The breeding of this line was not obviously abnormal and these animals were seemingly healthy. The urogenital abnormalities of the Wines mice had not led to mortality, rather the mice were culled at 11 months to investigate the apparent sterility. Since these Wines

males both had grossly abnormal kidneys it seemed possible that the renal function of Wani mice could be impaired but perhaps to a lesser degree. 47 mice from the Wani line were tested regularly over the age of 4 months for renal function. Table 2 describes the findings. 12 mice developed severe proteinuria, of these the genotype of 1 mouse was $WT1^{+/+}$;P3:WT1-KTS,whereas all the remaining 11 mice were $WT1^{+/-}$;P3:WT1-KTS. 100% of $WT1^{+/-}$;P3:WT1-KTS from all the litters taken, at ages ranging from 6-11 months developed signs of proteinuria. Histological analysis revealed a range of disorders including hyperplastic and cystic kidneys, hypoplastic or hyperplastic and cystic testes, liver tumours and a cystic eye (Section 3.3.3). It would seem likely that, despite the difficulty in detecting WT1 protein expressed from the transgene, the shift in isoform ratio in these animals towards WT1-KTS, together with a reduction of endogenous WT1+KTS was critical in the observed pathogenesis.

Immunohistochemistry with an anti-WT1 antibody suggested that there was a range of situations with some animals showing increased or ectopic WT1 expression, whilst other had lost expression. Expression of WT1 protein in adults is normally restricted to podocytes of the kidney and sertoli cells of the testes. One affected animal had lost all sertoli and podocyte cell expression of WT1 whilst another gained expression within the tubules of the kidney. Expression of WT1 in the remaining 10 affected mice seemed higher than normal although maintained in the correct structures. WT1 is a key regulator of podocyte function with key podocyte-specific genes being down regulated in mice defective for WT1 expression (Guo et al., 2002). A defective podocyte phenotype has consistently been found in patients with Denys Drash syndrome and it has been shown that a common DDS mutation in the *WT1* gene can cause the development of glomerusclerosis when introduced into mice (Patek et al., 1999). The podocytes line the external surface of the blood vessels in the glomerulus

and play an important role in the maintenance of the basement membrane resulting from their foot processes which create rigid and definite structures lining the basement membrane of the glomerulus. In addition they support the capillary tuft and may influence the glomerular filtration rate. Impairment of these podocyte functions has been linked with the development of glomerular sclerosis (Guo et al., 2002). The podocyte abnormalities in DDS patients with mutations in *WT1*, highlight the requirement of the gene, not only in development but also throughout adult life. Our $WT1^{+/-}$;P3:WT1-KTS mice developed urogenital disorders later in life and they showed defects of WT1 expression in the podocytes with ectopic expression around the glomerulus. In the abnormal testes, ectopic WT1 expression was also observed. The sertoli cells have role in the testes in supporting the surrounding germ cells. They are the only testis cell type in which expression of WT1 is maintained throughout life. It could be that the function of WT1 in sertoli cells is similar to its role in podoctyes, in that WT1 could maintain the expression of downstream genes which are in turn responsible for the function of these key cell types with supportive roles within both the testes and kidneys. This would allow the podocytes to continue to maintain the glomerular filtration rate, essential for the normal function of a kidney, and the sertoli cells to maintain the germ cell population, essential for the normal function of the testes.

3.4.2.2.1 WT1 involvement in the liver

The ectopic expression of WT1 in certain hepatocytes could be due to the expression of the transgene in the liver (as argued above) since WT1 is not usually expressed in adult liver. A recent report has discussed the role of WT1 in the development of chronic hepatitis and cirrhosis and suggests the observation that WT1 is expressed in fetal liver but not in adult liver may be due to the role of WT1 in differentiation. In the same report, WT1 levels showed a marked

increase in livers with chronic hepatitis and cirrhosis. The increase of WT1 levels was seen in both man and rats. The authors also reported that the increase in WT1 levels was in proportion to a decrease in expression of the HNF4 transcription factor, which is thought to maintain liver function, metabolism and differentiation (Berasain et al., 2003). Therefore, WT1 is normally expressed in the immature, undifferentiated liver. The ectopic expression of WT1 in the abnormal livers of $WT1^{+/-}$;P3:WT1-KTS could result in a loss of differentiation and reversion to an immature, proliferating state. This would potentially explain the presence of liver tumours (provisionally diagnosed as hepatocarcinomas based on their morphology) in some of these mice. No other tumour was detected in these animals suggesting that the liver tumours were primary tumours. Only two types of primary liver tumour have been reported, the epithelial bile duct derived tumour and the hepatocyte derived hepatocarcinoma. Expression of WT1 in the hepatocytes would suggest the tumours to be hepatocarcinomas. The ectopic expression of WT1 in the liver was consistent with the idea that the transgene was expressed in tissues were the IGF2 P3 promoter and H19 enhancer elements have been shown to drive expression. However, although the liver tumours were associated with the presence of the transgene we cannot rule out that some or all of the WT1 expression observed in adult liver section was derived from reactivation of the single endogenous *Wt1* allele that remains in the affected mice which is normally expressed only during development but not in the adult liver.

3.4.2.2.2 WT1 involvement in the retina

WT1 involvement has been shown in the developing retina of the eye but the protein is not expressed in adult eyes (Pritchard-Jones et al., 1990). One of our $WT1^{+/-}$;P3:WT1-KTS animals presented with an enlarged eye and following dissection and histological analysis it was found that there was thickening of the

retina associated with strong WT1 expression. This concurs with the findings of Wagner et al 2002 that embryos with a targeted disruption of *Wt1* exhibit thinner retinas than age matched wild type littermates. They also reported that the WT1-KTS isoform could up-regulate the Pou4 transcription factor, which is critical for the survival of retinal ganglion cells (Wagner et al., 2002). In contrast, the retina of the cystic eye was thicker than its wild type. Maintenance or reactivation of WT1expression in the eye (either from the transgene or from the endogenous *Wt1* allele) after it has normally ceased might therefore have caused the enlarged and cystic phenotype.

3.4.2.3 WT1 involvement in the cell cycle

The role of WT1 in cardiac development, kidney development, and eye development as a switch of mesenchyme to epithelial states suggest that the protein is acing in the stimulation of cellular differentiation rather than proliferation. This is supported by the findings that WT1 levels are increased in Wilms' tumours and other neoplasias that involve mutations of the *WT1* gene (Hastie, 1993; Lee and Haber, 2001). This allows us to infer that mutations of *WT1* might result in an increase in cell proliferation. On the other hand, in the absence of WT1, the meetanephric mesenchyme undergoes extensive apoptosis (Kreidberg et al., 1993), again highlighting the role of WT1 in growth regulation.

The WT1-KTS isoform of WT1 has been shown to have stronger transcriptional role than WT1+KTS. WT1-KTS is able to bind with higher affinity to DNA while WT1+KTS has a higher affinity for RNA (Caricasole et al., 1996; Laity et al., 2000) (see further discussion in Chapter 4). WT1-KTS isoforms are generally more active in transcriptional regulation, binding regulatory regions of genes such as Steroidogenic factor SF1 (Cohen et al., 1997), P21(Englert et al., 1997),

amphiregulin (Lee, 1999) and IGF2 (Drummond et al., 1992; Duarte, 1997). WT1-KTS is linked to the induction of cell cycle arrest via the induction of the cyclin dependent kinase inhibitor p21 (Englert et al., 1997). Ectopic expression of WT1-KTS in some cell types leads to a G_1 cell cycle arrest. Following the stable transfection of WT1-KTS in rhaboid tumour cell lines, there is a marked increase in levels of the apoptotic factorBcl-2 (Del Rio-Tsonis et al., 1996). Dax-1 and MIS activation by WT1-KTS are essential for gonadal development (Parker et al., 1999). It is for these reasons that cell proliferation and apotosis in the $WT1^{+/-}$;P3:WT1-KTS were of interest.

There was a marked increase of cell proliferation in all of the abnormal organs. The pattern of cell proliferation was also disorganized in comparison to wild type animals, with proliferation no longer restricted to the usual areas (e.g. periphery of seminiferous tubules). Interestingly, there were also effects on the apoptosis levels in the same organs although these may not be as reliable a result as hoped for. The exposure differences in the images (Figure 13 C and E) with comparison to the other images (Figures A, B, D and E) suggest that the apparent dramatic increase seen if mutant sections may not be a true reflection of actual apoptotic events. Despite the favorable results provided by the negative controls (Figure G and H), it would be beneficial to use alternative independent methods to detect apoptosis to duplicate the results such as detailed microscopy to detect the presence of altered DNA structures. However, analysis of the given results shows that apoptosis was affected in all the abnormal organs with a general increase of apoptosis in comparison to wild type organs. Increased levels of apoptosis were seen throughout kidneys and livers whilst only the periphery of seminiferous tubules in the testes showed a marked apoptotic increase. In testes, apoptosis was restricted to areas where WT1 expression was seen, this was not the case in kidneys and livers where there

seemed to be no consistent pattern of apoptosis. This feature was not expected as there is an overall increase of WT1, not loss as seen in null animals where the mesenchyme undergoes complete apotosis. It is thought that the loss of WT1 causes this resulting apoptosis in the kidneys of null mice therefore it would not be expected that increased WT1 expression would also result in increased apoptosis. The apoptosis levels were not necessarily as high as the levels described for the metanephric mesenchyme of null animals however (Kreidberg et al., 1993). It may be that the upregulation of apoptosis was an indirect response to WT1 as a reaction to the increase in proliferation, or vice verse. This data suggests the WT1 dosage is critical for maintenance of the cell cycle and it may be that the reduction of WT1+KTS in conjunction with the increase of WT1-KTS is important in controlling the cell cycle process.

Overexpression of WT1-KTS in the $WT1^{+/-}$;P3:WT1-KTS transgenic mice may have resulted in the changes in cell proliferation and apoptosis seen in those mice with abnormal organs. In the cystic, tumourous or enlarged organs, WT1 expression was frequently abnormal. Although these changes in WT1 expression were not consistent among all animals assayed, this may be because affected organs from different animals were detected and assayed for WT1 expression at different pathologic stages. In the testis, ectopic WT1 expression may have resulted in increased activation of downstream targets outside of sertoli cells. This might result in the ectopic activation or repression of WT1 target genes in germ cells. The ectopic expression of the protein in the kidney, liver or adult eye could similarly result in the activation of downstream targets not normally activated in these organs.

3.4.3 Comparison between WT1$^{+/-}$;P3:WT1-KTS and Ob animals

WT1$^{+/-}$;P3:WT1-KTS animals with abnormal organs demonstrated changes in morphology, renal function, WT1 expression and cell turnover. It was of interest to see if this was specific for this animal model in comparison with other animals with genito-urinary abnormalities. The Ob mice provided us with an interesting comparison. As mentioned earlier in this chapter The Ob transgenic mice were identified from a screen for transgene insertional mutants in our laboratory (Paisley, 2000). Previous analysis of Ob testes has shown that the testes are reduced in mass in comparison to fertile hemizygous littermates. Testes of Ob animals also exhibit a significant difference in the relative abundance of various spermtatogenic cell-types. In comparison to WT1$^{+/-}$;P3:WT1-KTS animals, histological analysis revealed the Ob testes are smaller in size but the tubules are maintained in an organised structure that is similar to those of wild type testes. Cysts were never seen in Ob testes.

With regards to cell turnover, both proliferation and apoptosis was altered in Ob mutants as it was in abnormal organs from WT1$^{+/-}$;P3:WT1-KTS mice. Apoptosis was increased in both mutants, however the pattern of apoptosis was somewhat different with WT1$^{+/-}$;P3:WT1-KTS animals having apoptotic cells restricted solely to the periphery of the seminiferous tubules while Ob mutants had apoptosis of peripheral cells and also some apoptotic cells towards the lumen of tubules. Although it has not been proved, apoptosis in WT1$^{+/-}$;P3:WT1-KTS is most probably affecting only primary spermagonia and/or sertoli cells due to the location of the apoptotic cells. In the Ob mutants, the location of apoptotic cells within the tubules suggested that more mature germ cells are also being lost. This correlates with the general decrease in mass of Ob mutant testes. Proliferation in the WT1$^{+/-}$;P3:WT1-KTS was generally increased but the pattern of proliferation was also changed with a disorganized pattern of proliferating cells

throughout tubules. Ob mutants also had changes in proliferation, however levels were generally decreased in these mutants. Some tubules showed a relatively normal amount of proliferating cells at the periphery of tubules whereas other tubules were devoid of any proliferating cells. The increase of apoptosis together with a decrease of proliferation could account for the small but well-proportioned testes of the Ob mutants which are different from the enlarged and poorly organised structures in the testes of $WT1^{+/-}$;P3:WT1-KTS mice. However, given that the growth of adult testes has reached a steady state it is possible that the defects observed in both mutants could have arisen as a consequence of earlier events.

The cell turnover changes seen in $WT1^{+/-}$;P3:WT1-KTS mice related with changes in expression of WT1 in the affected organs. Ob mice however display normal patterns and levels of WT1 expression illustrating the morphological differences in Ob mutants are most likely to be unrelated to the WT1 pathway (in contrast to the $WT1^{+/-}$;P3:WT1-KTS mice). Interestingly, although the Basp1 protein was expressed in similar locations to WT1 within the kidney of embryos and adult mice, its expression was not affected in $WT1^{+/-}$;P3:WT1-KTS or Ob mutant mice, allowing us to conclude that while Basp1 may be a WT1 cosuppressor in at least some cell types, Basp1 expression may be regulated independently of WT1.

3.5 Conclusions

Taken together, the data from these experiments provides further evidence for the requirement of a critical ratio between the WT1+KTS and WT-KTS isoforms of WT1. By breeding animals carrying a P3:WT1-KTS transgene with $WT1^{+/-}$ animals we have been able to show that the transgene was not sufficient to

rescue the null phenotype in $WT1^{-/-}$;P3:WT1-KTS embryos. Alteration of the isoform balance in $WT1^{+/-}$;P3:WT1-KTS adult mice over the age of 6 months however, led to a range of interesting pathological features. Some of these features affected the genito-urinary system, mimicking aspects of human disorders in which WT1 is implicated. In most abnormal organs, there was an ectopic or increased WT1 expression detected using an anti-WT1 antibody. However, the absence of defects in $WT1^{+/+}$;P3:WT1-KTS mice suggests that the defects must be due to subtle changes in isoform ratios rather than ectopic expression of WT1. The liver tumours, however, most likely result from ectopic expression of the transgene as opposed to differences in isoform ratios as WT1 is not normally expressed in the liver. Considering this, we can assume that it is the excess expression of WT1-KTS in combination with the haploinsufficiency of WT1+KTS causing the pathological features and not solely a result of the haploinsufficiency of WT1+KTS as previously suggested (Hammes et al., 2001; Little et al., 1995). The changes in the genito-urinary system in the $WT1^{+/-}$;P3:WT1-KTS mice were distinct and specific to this subset of animals when compared with the Ob mice, an alternative model for genital abnormalities. This suggests, unsurprisingly, a WT1-specific path involved in the $WT1^{+/-}$;P3:WT1-KTS phenotype.

Chapter 4

INVESTIGATION OF THE SUBCELLULAR LOCALISATION OF WT1+KTS AND WT1-KTS

4.1 Summary

The previous chapter described the *in vivo* experiments investigating the role of WT1+KTS and WT1– KTS function in transgenic animals. In order to further characterise the mechanisms resulting in the functional differences of the two isoforms, a series of cell culture experiments were carried out in which the sub-cellular characteristics of the WT1+KTS and WT1–KTS were explored. Using a combination of transient transfections of GFP fusion constructs (of wild type and mutant KTS isoforms), and immunofluorescence, the experiments in this chapter describe their location within the cell, and their colocalisation with other sub cellular factors. As a result of this data, it has been possible to propose a model by which variations in structure within the zinc fingers, result in alternative localisation of the isoforms within cells, and finally affect the functions of these proteins. This chapter also describes experiments that investigate the function of a putative nucleolar localisation signal within WT1 and demonstrates that mutating specific regions of the WT1 isoforms results in the alteration of their localisation within the nucleus.

4.2 Introduction

4.2.1 Subcellular localisation of WT1+KTS and WT1-KTS isoforms

A detailed introduction to nuclear structure was presented in Chapter 1. WT1 encodes a zinc finger transcription factor expressed in multiple distinct isoforms (Haber et al., 1990). As mentioned in Section 1.2.3, of all WT1 isoforms, WT1+KTS and WT1-KTS are two of the most abundant. They also display differences in cellular localisation and interactions with different factors. Alteration of the critical ratio between WT1+KTS and WT1-KTS has been implicated in FS suggesting that these isoforms carry out essential roles in genito-urinary development. In generating inducible cell lines expressing wild type isoforms of WT1 as well as WT1 mutants, dramatic differences were observed in the subnuclear localisation of the induced proteins (Englert et al., 1995). Englert. *et. al.* (1995) were able to show that the WT1 isoform that binds with higher affinity to a defined DNA target, WT1-KTS, was diffusely localised throughout the nucleus. In contrast, expression of an alternative splicing variant with reduced DNA binding affinity, WT1+KTS, or WT1 mutants with a disrupted zinc finger domain resulted in a speckled pattern of expression within the nucleus. Though similar in appearance, the localisation of WT1 variants to sub nuclear clusters was clearly distinct from that of the essential splicing factor SC35, suggesting that WT1 is not directly involved in pre-mRNA splicing. Localisation to subnuclear clusters required the N terminus of WT1 and co-expression of a truncated WT1 mutant together with wild type WT1-KTS resulted in a physical association, the redistribution of WT1-KTS from a diffuse to speckled pattern, and the inhibition of its transcriptional transactivation activity (Englert et al., 1995). This suggested that different WT1 isoforms and WT1 mutants occupy distinct subnuclear compartments. As mentioned in Section 1.2.3 additional WT1 isoforms with distinct transcription-regulatory properties,

indicating further complexity of WT1 expression and activity have been described, making a total of 32 known WT1 protein isoforms arising from alternative splicing, as well as RNA editing (Scharnhorst et al., 1999). The sub nuclear localisation of WT1 has been shown to be dynamic. Actinomycin D treatment, known to inhibit cellular transcription, causing some splicing factors to relocate to large foci or surround the remnants of the nucleolus, results in the relocation of WT1 to areas surrounding the nucleoli. As described by Englert *et. al.* (1995), in Cos7 cells the sub cellular localisation pattern of the protein has been shown to be isoform dependent with WT1–KTS localising in a diffuse pattern with some domains of localisation but no nucleolar staining, whereas WT1+KTS displayed a greater association with nucleoli in speckled areas in a similar pattern to that of many splicing factors. In addition, following treatment of cells with actinomycin D, WT1–KTS isoforms no longer relocate to the nucleolus, whereas relocation of WT1+KTS to the periphery of the nucleolus occurs in a pattern resembling that of some splicing factors. In a separate study, staining of cells with antibodies specific for splicing and transcription factors identified WT1-KTS localisation in a transcription factor-like pattern (colocalisation was observed with the transcription factor Sp1), and in contrast to the Englert *et. al.* (1995) data, WT1+KTS colocalised with splicing factor speckles (Larsson et al., 1995). More recently, localisation of the protein to potential nuclear assembly sites has confirmed the suggested interaction of the WT1+KTS isoform with elements of the cell splicing machinery (Davies et al., 1998; Hastie, 2001), reinforcing the idea of distinct roles for the two WT1 isoforms, with WT1-KTS being involved in transcriptional activation and with WT1+KTS likely to be involved with the splicing machinery. As stated in Chapter 1, proteins containing the WTAR mutation, missing the entire zinc finger region, and WT1 mutant proteins containing deletions of amino acids 76-120, have displayed enhanced speckling. This suggests that the amino-terminal region of the protein is essential for the

speckling characteristics although this region of the protein is not involved in the association with splicing factors. As stated in Section 1.2.2, computer modeling has demonstrated the presence of a potential RNA recognition motif at the N-terminus similar to that in constitutive splicing factors (Kennedy et al., 1996). The speckling and splicing characteristics of the protein are therefore distinguishable. WT1–KTS has also been seen in speckled patterns however it is known that WT1–KTS shows less binding affinity with splicing factors. Overall, the patterns of WT1 sub-cellular distribution have been shown to be dynamic, with differences in the pattern of expression of isoforms that differ by the insertion or deletion of the three amino acids within the zinc finger region altering the location of the protein within the nuclei of cells. WT1–KTS has been shown to display a higher association with a number of transcription factors as shown by either colocalisation experiments in cells or promoter binding studies, for example induction of p21, Bcl-2, Dax-1, SF1, MIS and amphiregulin (Del Rio-Tsonis et al., 1996; Englert et al., 1995; Ladomery et al., 1999; Parker et al., 1999), while the WT1+KTS has been shown to have a stronger association to members of the splicing machinery (Bickmore et al., 1992; Davies et al., 1998; Hastie, 2001; Larsson et al., 1995), suggesting the isoforms carry out different functions within cells.

The ratio of WT1-KTS and WT1+KTS isoforms is essential for correct genito-urinary development since alteration of the ratio is the cause of Frasier syndrome (Barbaux et al., 1997; Klamt et al., 1998; Kohsaka et al., 1999). Also, the KTS alternative splice has been widely conserved during vertebrate evolution having been found in every species analysed, with the exception of FUGU, where the KTS insertion has been replaced with KPS (Miles et al., 1998), and even in this divergent instance the U2AF65 binding properties of the KPS sequence were shown to be the same as the KTS sequence (Davies et al., 2000). Given these

facts it seems important that the separate functions of WT1-KTS and WT1+KTS are understood and that one important aspect of this is to understand their differential localisation within cells.

4.2.2 Mutation of the KTS sequence

Mutation studies involving the three amino acids have shown that inserting extra amino acids, duplicating amino acids or deleting amino acids does not affect the binding of the WT1+KTS protein to interacting proteins. Following site directed mutagenesis, a number of constructs containing mutation of the KTS region were introduced into a yeast two-hybrid system. Mutation, or duplication of any or all three amino acids failed to remove the proteins ability to bind to splicing factor U2AF65 in this assay. Only upon removal of all three amino acids (ΔKTS), did the protein behave like the WT1–KTS protein (Davies et al., 2000). We can infer from this that the main function of inserting the three amino acids is the alteration of the structure of the protein at the zinc finger region resulting in the disruption of their normal function, and the specific amino acid sequence of the insertion is not necessarily important. It has however been illustrated that the spacing at KTS position, driven by the nucleotide sequence, is of fundamental importance in controlling the alternative splicing, and hence the generation of WT1+KTS and WT1-KTS ratios (Davies et al., 1998). It can therefore be hypotheised that the KTS has been widely conserved as a result of the importance of its coding nucleotides. Furthermore, mutations in the gene causing Denys Drash syndrome are clustered around the zinc finger encoding exons, particularly exons encoding ZF2 and ZF3 (Little et al., 1992).

4.2.3 Functional role of zinc finger region

By using WT1 fusion constructs containing different classes of DDS mutations it has been possible to show that the mutations do indeed disrupt DNA binding and

may either be acting in a dominant negative fashion, possibly through dimerisation between mutant and wild type WT1 isoforms and subsequent loss of DNA binding (Little et al., 1995). Either way, this data provides convincing evidence of the necessity of the correct conformation of the zinc finger regions in DNA binding and hence the function of the protein. Although the DNA binding of the zinc finger region is better characterised, it has also been observed that the zinc fingers are able to bind RNA, with zinc finger 1 playing a greater role in RNA binding than zinc fingers 2-4 which are structurally related and bind a similar consensus sequence to the three zinc fingers of the EGR1 transcription factor (Caricasole et al., 1996, Ladomery, 1999 #142). Frasier syndrome also highlights the requirement of the KTS region for correct development. The mutations in Frasier syndrome patients also affect the zinc finger region, however FS generally arises from mutations within the alternative splice donor signal that alters the ratio of WT1+KTS: WT1-KTS (Barbaux et al., 1997; Klamt et al., 1998; Kohsaka et al., 1999).

4.2.4 Investigation of the subcellular localisation of WT1 isoforms

The current data provides good evidence that much of the functional activity of WT1 resides in the zinc finger region. The DNA and RNA binding activity of the zinc finger region can result in the regulation of a number of target genes, and the mutations found in DDS that result in genito-urinary abnormalities, presumably as a consequence of altered DNA binding capacity, highlight the essential requirement of the zinc finger region. At the same time, the normal conservation of WT1+KTS and WT1-KTS isoforms is altered in FS, resulting in developmental abnormalities (Barbaux et al., 1997). As mentioned in section 4.2.1, the two isoforms are found in distinct regions of the cell with differing binding affinities or profiles of interaction for different groups of proteins. This suggests a distinct role for the isoforms in transcriptional and possibly

posttranscriptional pathways. The experiments described in this chapter were aimed at investigating further the sub cellular localisation of the two isoforms, as well as related mutants, using GFP fusion proteins and immunofluorescence. Following transient transfections of GFP fusion protein constructs, localisation of fluorescence was examined in a several cell types at 24 hour and 48 hour time points. These experiments were carried out in triplicate with at least 100 cells counted for each transfection. In some cases transfection was followed by treatment of the cells with actinomycin D and fluorescing cells were counted before and after treatment. The first set of experiments in this chapter look at the sub cellular localisation of wild type WT1–KTS and WT1+KTS isoforms in a number of cell lines, some of which express endogenous WT1 (HeLa, MCF7 and HEK293 cells), while others do not (Cos7). Cos7 cells were used for subsequent experiments as a matter of convenience.

4.2.5 Investigation of the nucleolar localisation of WT1

Another set of experiments describes the identification of a putative nucleolar localisation signal within zinc finger 2 of the protein. It is known that NoLS signals are often basic regions and many proteins that accumulate in the nucleolus contain basic elements which, when exposed, destroy nucleolar localisation in the protein. For example, the basic region of p80-coilin when exposed by the deletion of an acidic region resulted in the accumulation of coilin in the nucleolus (Tucker et al., 2000). Herpesvirus protein MEQ and PRRSV nucleocaspid protein, and two cellular proteins, rat spermatidal protein TP2 and human HICp40 have also been reported to contain NoLSs consisting of stretches of basic residues (Andersen et al., 2002). Further reports describe the characterisation of specific amino acid sequences that were able to direct fusion proteins to the nucleolus. For example, the nucleolar retention of U3 snRNA is mediated by a C'D box motif (Speckmann et al., 1999) and the NoLS of human

angiogenin (amino acids IMRRRGL) was sufficient to import GFP into the nucleolus (Lixin et al., 2001). The ING1 candidate tumour suppressor uses the RRQR amino acid sequence to direct GFP to the nucleolus. This sequence is also conserved in other nucleolar proteins including HIV-Tat and HIV-Ret and deletion of this sequence has been shown to ablate nucleolar localisation (Scott et al., 2001). Other groups have described proline-rich nucleolar retention motifs that require phosphorylation to regulate them (Catez et al., 2002). The presence of a bipartite NoLS has been reported, where both signals were required for nucleolar retention and the deletion of either signal was sufficient to impede localisation (Scott et al., 2001). Many of the sequences involved in nucleolar localisation involve Arginine repeats. The following experiments describe the identification/investigation of a putative NoLS within the zinc finger region of WT1.

4.2.6 Subcellular localisation of WT1 mutant constructs

A third set of experiments examined a number of mutant WT1GFP fusion constructs to determine how specific mutations might alter localisation in comparison with the relevant wild type WT1 isoforms. Site directed mutagenesis was used to create 6 mutants. DDS occurs as a result of mutations within the zinc finger region of WT1 (Little et al., 1992), highlighting the importance of the zinc fingers. A DDS truncation mutant was created that comprised WT1 protein missing part of zinc finger 3 and the entire zinc finger 4 region (WT1DDS), representing one of the most common WT1 mutant proteins found in patients with DDS. Examining the localisation of the WT1DDS mutation allowed us to identify possible mechanisms by which abnormalities within WT1 could affect normal development in DDS patients. Zinc finger-2 point mutations were also generated both within the full-length WT1+KTS (WT1+KTSZF2) and WT1-KTS (WT1-KTSZF2) proteins and also in the DDS truncated WT1 mutant

(WT1DDSZF2). It was thought that the mutation within zinc finger 2 might ablate the putative nucleolar localisation signal (mentioned above), hence altering the nucleolar localisation of the mutant proteins. The final set of mutants created comprised only the zinc finger region from either WT1+KTS (ZF+KTS) or WT1–KTS (ZF-KTS), fused to GFP. This addressed the function of the zinc fingers in isolation, within the cell. Truncated WT1 protein containing the zinc-finger domains was previously shown to be sufficient to confer nuclear localisation (Davies et al., 2000), but our experiments assess the influence of both WT1-KTS and WT1+KTS zinc finger regions on sub-nuclear distribution.

4.2.7 Colocalisation studies of WT1 isoforms

The final set of experiments in this chapter considers the co-localisation of WT1 isoforms with other nuclear factors known to associate with the nucleolus. Findings from recent research have shown that the nucleus is a highly dynamic organelle containing distinct sub-compartments (Dundr and Misteli, 2001). These structures are characterised by the absence of delineating membranes but are still considered compartments for several reasons. Firstly, they contain specific resident proteins and can be morphologically identified by light and electron microscopy. More recently, a number of these proteins have been visualised in living cells by the use of green fluorescent protein (GFP) technology. Finally, some of these compartments have been isolated biochemically (Lamond and Earnshaw, 1998). As described in Section 4.2.1, WT1-KTS co-localises with transcription factors and WT1+KTS shows co-localisation with splicing factors generally found to be restricted to specific areas of the nucleus (Dundr and Misteli, 2002). Using two antibodies, one recognising nucleolar protein B23, which is expressed within the dense granular regions of the nucleolus, and the other recognising PSP1 protein, which is associated with a new group of peri-nucleolar organelles termed paraspeckles (Fox et al., 2002),

we have examined WT1–KTS localisation to speckles and investigated the sub-nucleolar localisation of both wild type WT1+KTS and mutant fusion proteins.

4.3 Results

4.3.1 Subcellular localisation of WT1+KTS and WT1-KTS

The subcellular localisation of a number of GFP fusion proteins and mutants were investigated (Figure 18) in Cos7 cells both before and after actinomycin D treatment. Examination of expression patterns of GFP WT1+KTS and WT1–KTS isoforms allowed the two protein isoforms to be distinguished (Figure 19). At 24 hours following transfection of a GFP: WT1+KTS expression construct into Cos7 cells, the majority of cells presented a diffuse pattern of fluorescence within the nuclei combined with accumulation in the nucleolus (Figure 19 A and B). Examining the cells under DIC confirms the nucleolar expression. The pattern of accumulation within the nucleoli was patchy, with fluorescence occurring in an uneven configuration (Figure 19 A). After treatment of the cells with actinomycin D, virtually all the cells showed GFP accumulation in and around the nucleolus with a diffuse pattern within the rest of the nucleus (Figure 19 B). WT1–KTS on the other hand showed a completely different pattern of localisation, with the protein being expressed in punctate configurations with patchy expression throughout the nucleus. Fewer cells showed accumulation of the GFP: WT1-KTS fusion protein in the nucleolus than in the GFP: WT1+KTS transfections (Figure 19 C). Treatment with actinomycin D also yielded results that differed from those of WT1+KTS with actinomycin D treatment. Upon actinomycin D treatment WT1-KTS did not accumulate in the nucleolus and the transient punctate pattern, seen prior to treatment, was lost (Figure 19 D).

Figure 18. Diagrammatic representation of WT1 constructs investigated

All proteins were expressed as GFP fusion proteins, with GFP fused at the N-terminus and therefore distant from the zinc finger region in most constructs. The native isoforms WT1+KTS and WT1-KTS were full length WT1 (A and B). WT1DDS construct was truncated at zinc finger three representing a mutant protein found in DDS patients (C). The WT1DDSZF2 mutant was truncated at zinc finger 3 and also carried a mutation in the putative NoLS within zinc finger 2 (D). WT1+KTSZF2 and WT1-KTSZF2 were full-length isoforms carrying the same mutation in the putative NoLS in zinc finger 2 (E and F). ZFWT1+KTS and ZFWT1-KTS were the isolated zinc finger regions from WT1+KTS and WT1-KTS respectively (G and H). The presence of the mutation within the putative NoLS is indicated by a star.

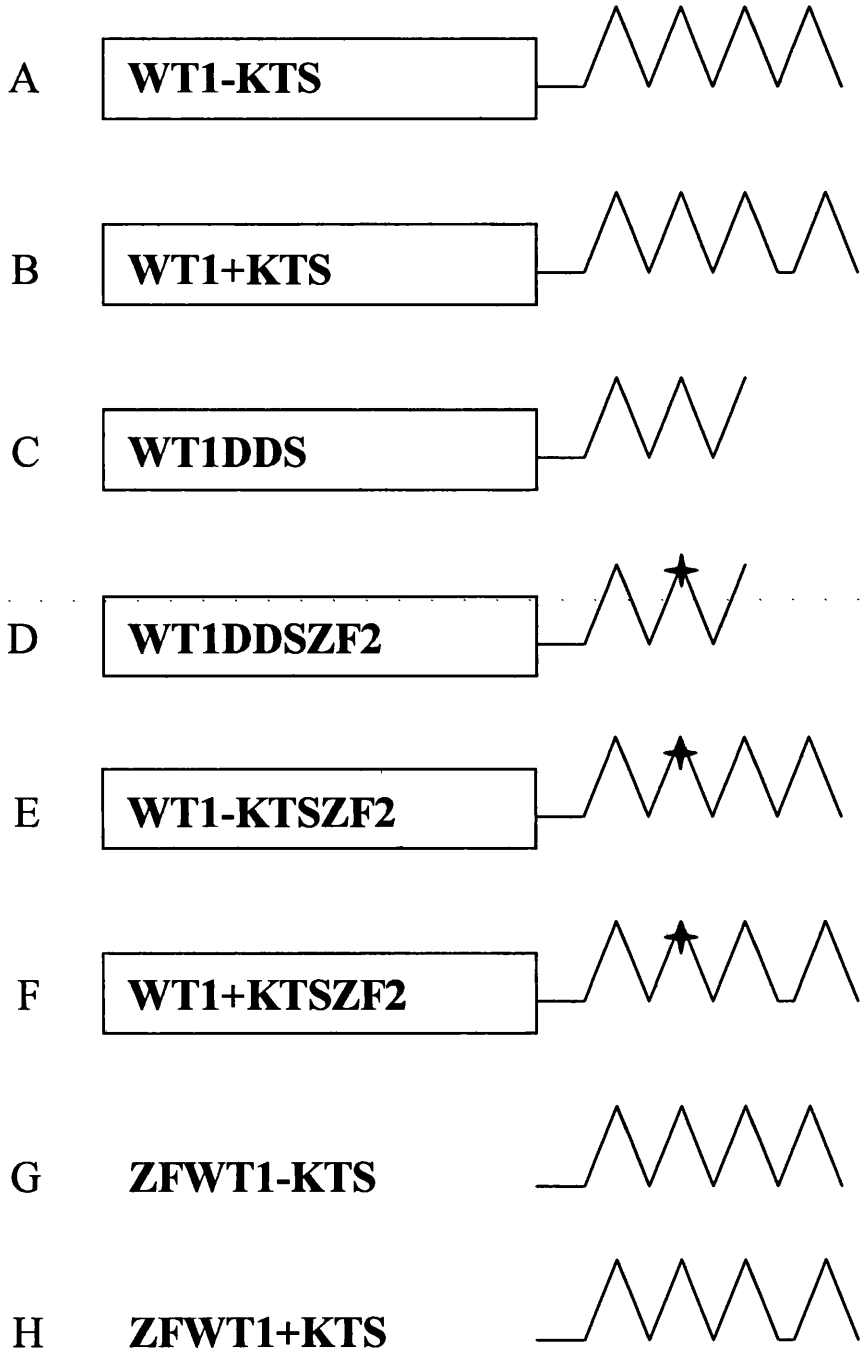
A
WT1-KTS
B
WT1+KTS
C
WT1DDS
D
WT1DDSZF2
E
WT1-KTSZF2
F
WT1+KTSZF2
G
ZFWT1-KTS
H
ZFWT1+KTS

Figure 19. Nuclear distribution patterns typical of WT1-KTS and WT1+KTS GFP fusion protieins

Expression of WT1+KTS (A and B) and WT1-KTS (C and D) fusion proteins in Cos7 cells 24 hours post transfection both before (A and C) and after actinomycin D treatment (B and D). WT1+KTS typically shows diffuse nuclear expression and accumulation within nucleoli of Cos7 cells (A) and after actinomycin D treatment nucleolar expression was restricted to areas at the periphery of nucleoli (Figure B). In WT1–KTS transfected cells, GFP expression was seen in speckles and discreet domains throughout the nucleus (C) and this pattern remained after treatment with actinomycin D (D). Scale bars 5μm

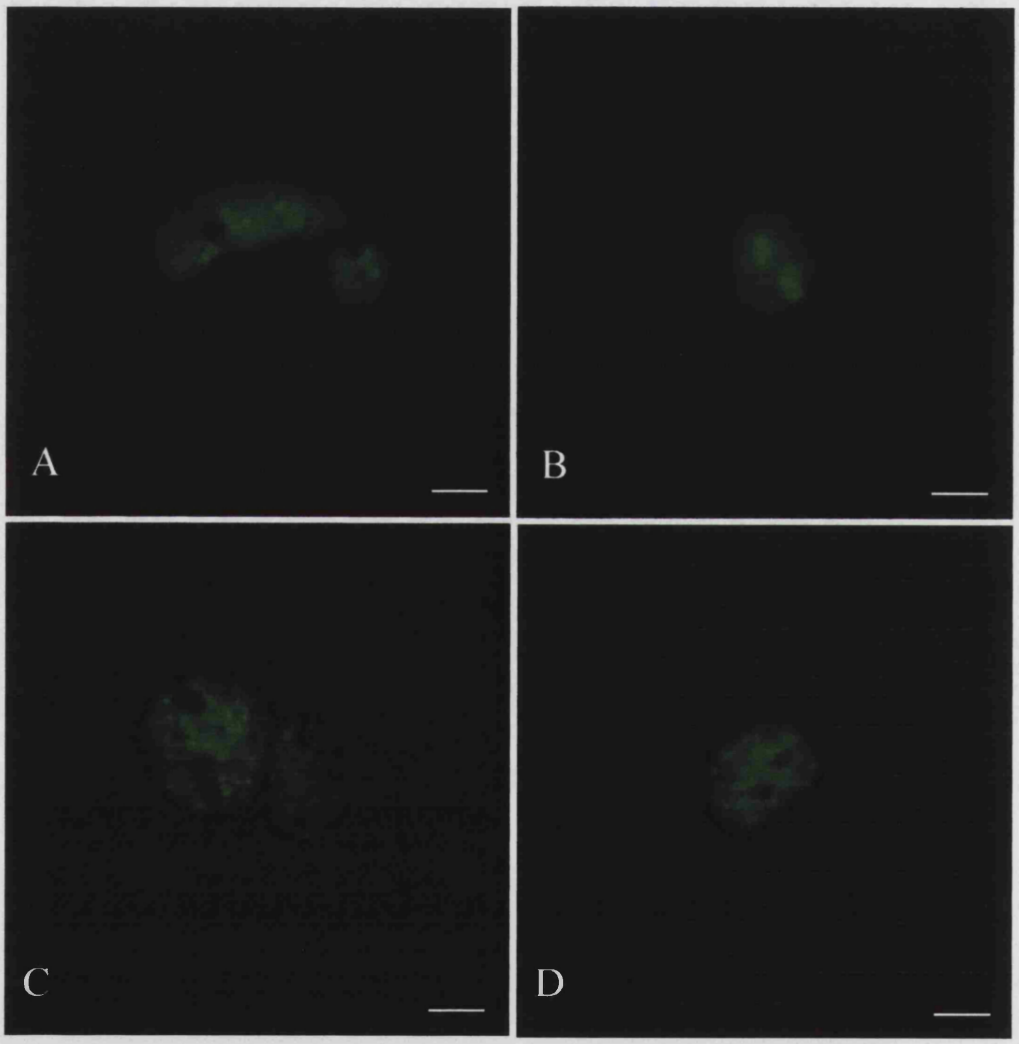
A
B
C
D

The isoform-specific nature of the expression patterns was quantified by counting, in duplicate and in a blind fashion, at least 100 cells transfected with each construct to determine the numbers of cells expressing GFP in the different patterns (Figure 20). Before treatment with actinomycin D, 68% of the cells transfected with WT1+KTS displayed a strong nucleolar pattern on a diffuse background; 12% of cells showed a diffuse pattern of expression throughout the cell; 18% of cells showed a diffuse GFP expression in the nucleus without expression in the nucleolus. Cells expressing GFP diffusely throughout, with patchy nuclear expression and accumulation in the nucleolus was the smallest subsets of cells seen with only 2% of cells showing this pattern. These numbers changed dramatically upon treatment of transfected cells with actinomycin D, with almost all the cells (95%) showing accumulation of GFP within the nucleolus against a background of diffuse nuclear expression. The remainder of transfected cells either had a diffuse (2%) or patchy (3%) nuclear expression with diffuse nucleolar accumulation. For cells expressing WT1-KTS the patterns were significantly different (Table A). Patchy non-nucleolar patterns predominated and counted for 28% of patterns seen. Another group of patterns seen in cells transfected with WT1-KTS, the punctate, speckled patterns, were never seen in cells transfected with WT1+KTS. The large amount of cells expressing nucleolar staining in WT+KTS compared to the nucleolar staining of WT1-KTS and the presence of speckles in WT1-KTS transfection compared to the lack of speckles in WT1+KTS transfections were both significant observations. The speckled patterns for WT1–KTS accounted for 29% of cells but were transient and had disappeared at 48 hours after transfection. The speckled patterns also disappeared following actinomycin D treatment, and although an increase in nucleolar expression was seen in actinomycin D treated cells transfected with WT1-KTS (from 16% before treatment to 38% after treatment), this was not significant (Table A) whereas the change seen before

Figure 20. Cell counts of subcellular localisation patterns following transfections of Cos7 cells with expression vectors encoding WT1+KTS and WT1-KTS GFP fusion proteins

Cells were scored at 24 hours post transfection, before (left panels) and after actinomycin D (A D) treatment.

Patterns of interest between WT1+KTS and WT1-KTS constructs were analysed using the Mann Whitney U Statistocal tests to identify significant differences ($p>0.05$) in the subcellular localisation patterns between constructs. (Table A)

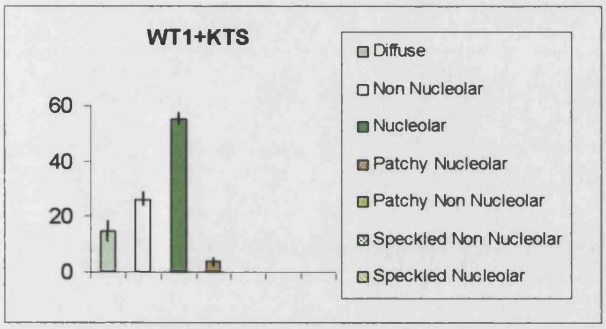

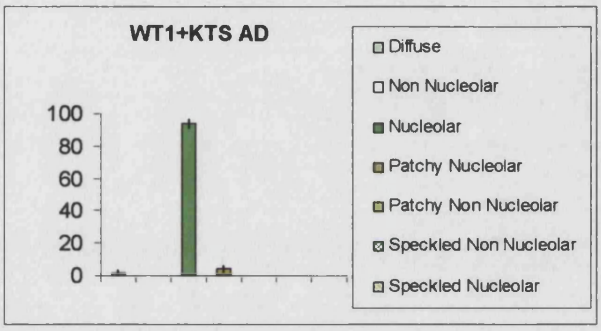

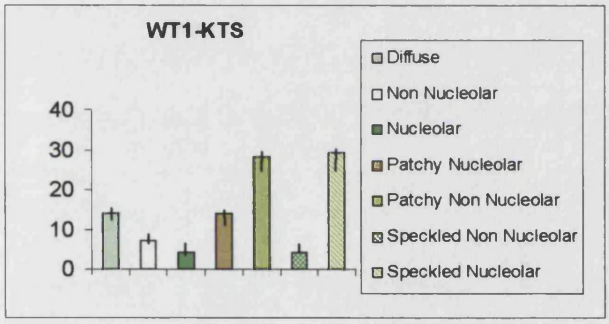

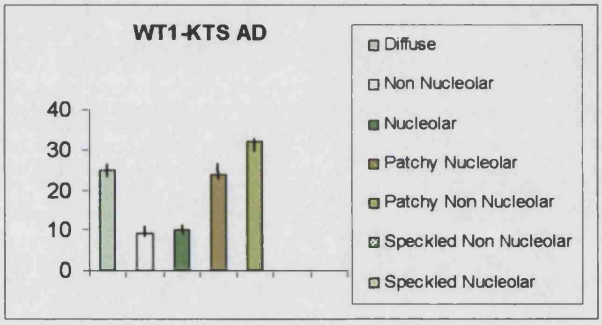

Constructs		Pattern	Significant difference (p)
WT1+KTS	WT1-KTS	Nucleolar	0.0002
WT1+KTS	WT1-KTS	Speckled	0.0004
WT1+KTS	WT1+KTS AD	Nucleolar	0.004
WT1-KTS	WT1-KTS AD	Speckled	0.0008
WT1-KTS AD	WT1-KTS AD	Nucleolar	0.064

and after actinomycin D treatment of WT1+KTS transfected cells was highly significant (Table A).

4.3.2 Subcellular localisation of the DDS mutant protein

A common mutation seen in DDS patients, involves an insertion of an arginine at nucleotide 1156 of exon 9, resulting in a frame-shift at amino acid 386 and the truncation of WT1 in zinc finger 3. This creates a mutant protein lacking part of zinc finger 3 and all of zinc finger 4. Upon transfection of cells with a mutant WT1: GFP fusion protein that mimics this DDS truncation mutant (WT1DDS), the observed patterns of expression in some cells showed similarities to either the native WT1+KTS or WT1–KTS isoforms (Figure 21; described below). However, another subset of cells displayed patterns seen neither in WT1+KTS or WT1–KTS transfected cells with void nucleoli, lacking any GFP expression (Figure 21 A). These void nucleoli were only seen in cells transfected with the WT1DDS mutant. A minority of cells displayed punctate expression (Figure 21 B) as seen in WT1–KTS transfected cells. Following actinomycin D treatment, the expression pattern was similar to that of WT1+KTS with accumulation of GFP into the nucleolus of the majority of cells (Figure 21 C).

Scoring of at least 200 cells at 24 hours after transfection (Figure 22 and Table B) revealed that 51% had the void pattern, this was a statistically significant difference between the WT1DDS mutant and wild type WT1+KTS, while 29% had a pattern of nucleolar accumulation, making this the second most abundant group (not a statistically significant difference in this pattern between the wild type and WT1DDS mutant). The remaining 20% of cells expressed diffuse patterns (11%), patchy nucleolar (5%) and patchy non-nucleolar patterns (5%). After actinomycin D treatment there was a dramatic increase in the number of

Figure 21. Expression of GFP WT1 truncation mutants (WT1DDS) in Cos7 cells 24 hours post transfection

Mutant WT1 protein truncated within zinc finger 3 (WT1DDS mutant) was expressed in a variety of patterns. Many of the transfected cells displayed void patterns with no expression in the nucleolus (A). Other cells showed similar patterns to WT1–KTS with speckles throughout the nucleus and also discreet domains of fluorescence (B). After actinomycin D treatment, the majority of cells showed the same pattern as the WT1+KTS isoform, with accumulation of GFP in the nucleolus (C). Scale bars 5μm

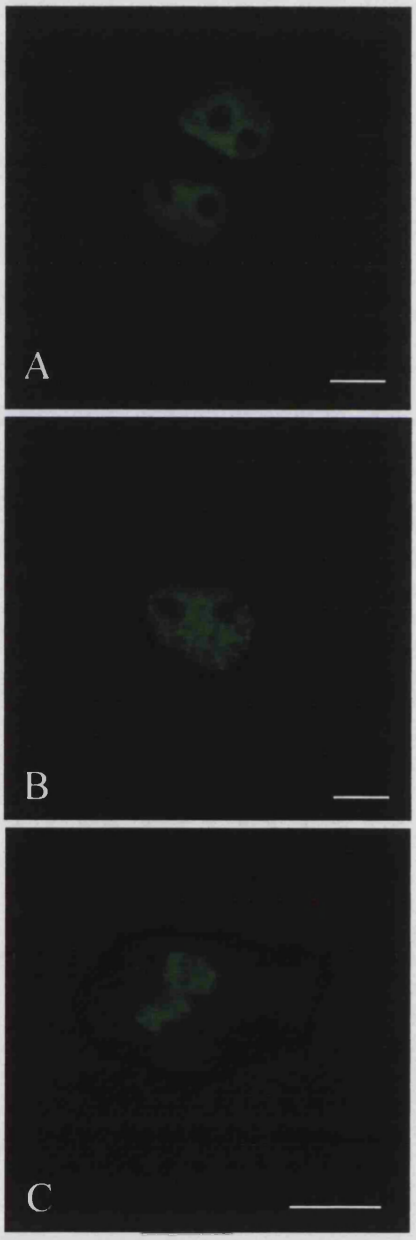
A
B
C

Figure 22. Cell counts of subcellular localisation following transfection of Cos7 cells with an expression vector encoding WT1DDS mutant protein as a GFP fusion

Cells were scored at 24 hour post transfection, both before (upper panel) and after actinomycin D (A D) treatment.

Patterns of interest between WT1DDS mutants and wild type WT1+KTS constructs with and without AD treatment were analysed using the Mann Whitney U Statistocal tests to identify significant differences ($p>0.05$) in the subcellular localisation patterns between constructs (Table B).

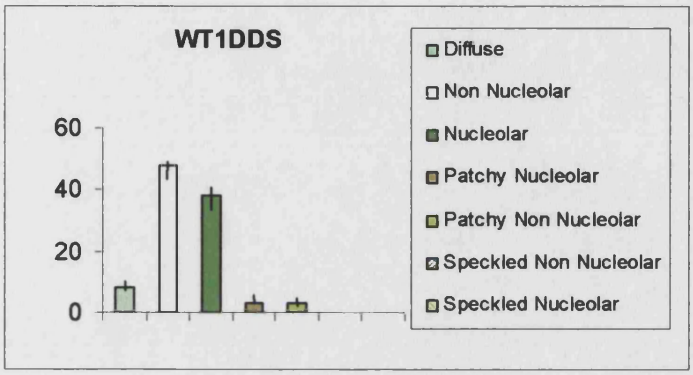

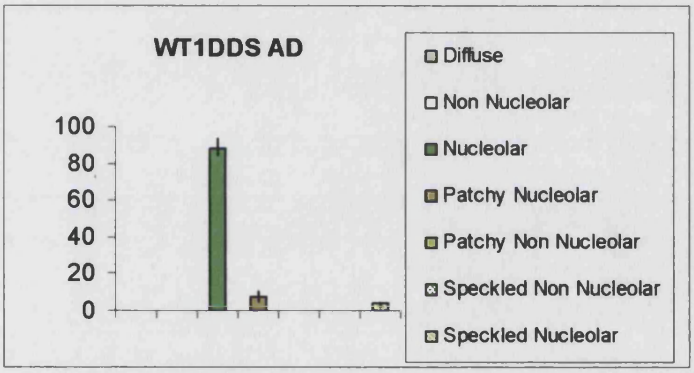

Constructs compared		Pattern	Significant difference (p)
WT1+KTS	WT1DDS	Nucleolar	0.058
WT1+KTS	WT1DDS	Non Nucleolar	0.001
WT1DDS	WT1DDS AD	Nucleolar	0.004
WT1DDS	WT1DDS AD	Non Nucleolar	0.0001
WT1+KTS AD	WT1DDS AD	Nucleolar	0.076

Figure 23. Alignment of WT1 putative NoLS amino acid sequence with characterised NoLSs

Letters highlighted in red identify amino acids with greater homology/conservation, e.g. (present in at least half of the aligned sequences). Black box surrounding two arginine residues within the WT1 sequence identifies the amino acids that were mutated by site-directed mutatgenesis in WT1ZF2 mutants.

Protein	NoLS
WT1+/-KTS	-KRHQRRHT-
hING1	-KRSRRQRR-
HTLV-1REX	-RPRRSQRK-
Coilin	-KKLKKRNK-
MDM2	-KKNKRKNK-
Fibrillarin	-KKMQQENM-
Nop5	-KKKKKRGK-
Lactoferrin	-RRRG-

Figure 24. Typical expression patterns of zinc finger 2 mutant (WT1ZF2) GFP fusion proteins in Cos7 cells 24 hours post transfection

Mutation of the putative nucleolar localisation signal does not alter distribution patterns of WT1 isoforms. WT1+KTSZF2 expression was maintained in the nucleolus with a diffuse pattern throughout the nucleus, the pattern typical for WT1+KTS(A). WT1-KTSZF2 was located to discreet domains throughout the nucleus, as was WT1-KTS (B). The WT1DDSZF2 mutant was expressed in a similar pattern to the WT1DDS mutant. Scale bars 5μm

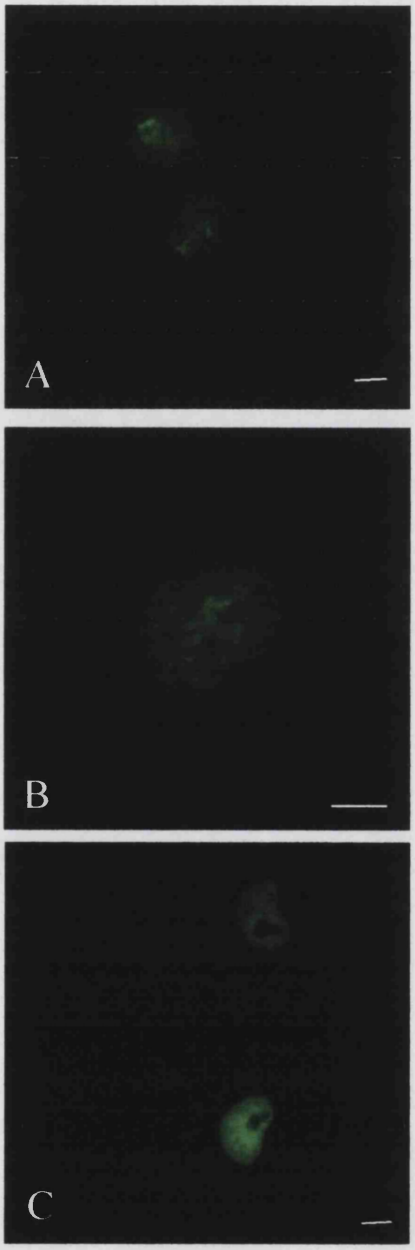
A
B
C

cells displaying nucleolar accumulation with 91% of cells presenting this expression pattern. This difference in nucleolar staining before and after AD treatment for the WT1DDS mutant was significant and similar to the change in nucleolar staining seen in pre and post AD treatment of WT+KTS. There was also a significant decrease in the number of cells displaying the void non-nucleolar pattern of expression. Most of the remaining cells had a pattern of nucleolar accumulation with patchy nuclear expression (6%), while a small subset had a speckled pattern (as in cells transfected with WT1–KTS) combined with nucleolar localisation (4%). It can be said that the DDS truncation mutant, therefore behaved in a fashion that includes features reminiscent of both native protein isoforms.

4.3.3 Investigation of a putative nucleolar localisation signal

The following experiments investigate properties of a putative nucleolar localisation signal identified in the WT1 zinc finger region. Carrying out a Blast search of the zinc finger region of the WT1 protein with the NCBI database resulted in the identification of a sequence of 8 amino acids in WT1 zinc finger 2. This region showed some homology to the nucleolar localisation signal of six proteins, and most closely resembled the NoLS motifs of hING1 and HTLV-1REX (Figure 23). Two arginines within the WT1 putative NoLS were particularly well conserved, with at least one being present in almost all of the aligned NoLS sequences. Site directed mutagenesis was used to mutate these arginines to a serine and a glycine in GFP fusions of both native WT1 isoforms (WT1-KTSZF2 and WT1+KTSZF2) and also in the DDS truncation mutant (WT1DDSZF2). The majority of COS7 cells transfected with WT1+KTSZF2 (Figure 24 A), WT1-KTSZF2 (Figure 24 B) and WT1DDSZF2 (Figure 24 C), showed patterns that were indistinguishable from those seen with the respective original protein isoforms.

Scoring of at least 200 cells from duplicate experiments showed the WT1ZF2 mutants localised within the cell in a similar fashion to their wild type isoform counterparts and the only significant change seen was the lack of speckles seen in the WT1ZF2-KTS while speckles are present in wild type WT1-KTS (Figure 25 and Table C). 69% of WT1+KTSZF2 showed a diffuse nucleolar localisation and this number increased to 92% following actinomycin D treatment. These numbers were similar to the figures for wild type WT1+KTS of 68% and 95%, respectively (Figure 19). The WT1-KTSZF2 data showed a fairly equal distribution of cells expressing in diffuse (20%), diffuse non-nucleolar (20%), diffuse nucleolar (19%), patchy non-nucleolar (19%) and patchy nucleolar patterns (18%). After treatment with actinomycin D, numbers remained fairly similar. This is similar to the numbers seen for transfections with wild type WT1-KTS (Section 4.3.1).

While the majority of WT1DDSZF2 cells displayed diffuse nucleolar patterns (48% before actinomycin D and 94% following treatment), the second most abundant group were those cells with void nucleoli (22% of transfected cells) and there were a further 18% of cells displaying speckled patterns. Following actinomycin D treatment these patterns were almost entirely replaced, with 96% of cells exhibiting nucleolar accumulation of WT1DDSZF2. Again, these results show that the WT1DDSZF2 mutant was behaving in a similar fashion to transfections of cells with the WT1DDS (Section 4.3.2). Data from these experiments showed that the mutation of the putative nucleolar localisation signal within WT1 zinc finger 2 was not sufficient to alter localisation of the different protein isoforms following their transfection into Cos7 cells.

Figure 25. Cell counts of subcellular localisation patterns following transfections of Cos 7 cells with expression vectors encoding WT1+KTSZF2, WT1-KTSZF2 and WT1DDSZF2 mutants as GFP fusions. Cells were scored at 24 hours post transfection, both before (left panels) and after actinomycin D (AD) treatment.

Patterns of interest between WT1ZF2 mutants and wild type WT1 constructs with and without AD treatment were analysed using the Mann Whitney U Statistocal tests to identify significant differences ($p>0.05$) in the subcellular localisation patterns between constructs (Table C).

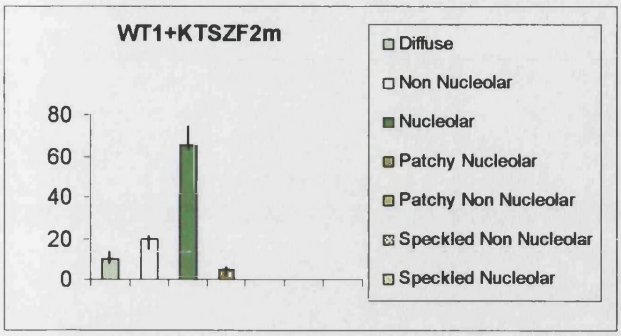

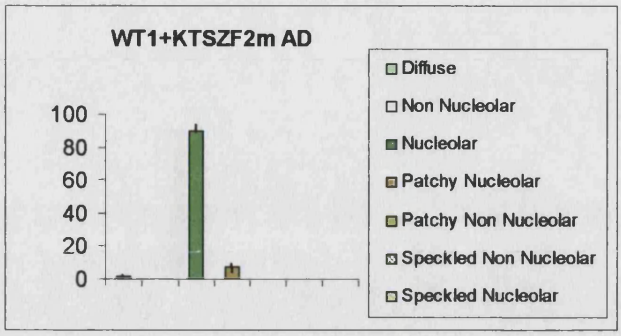

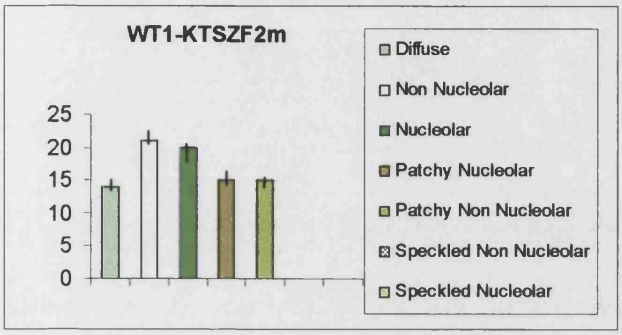

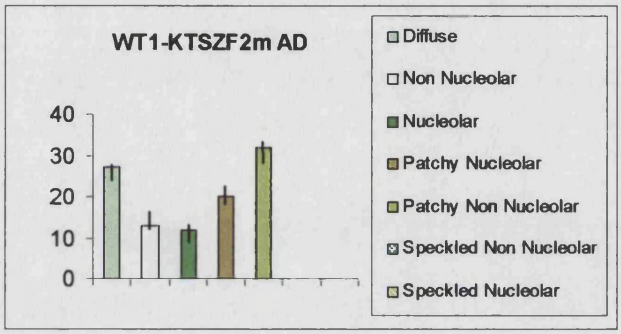

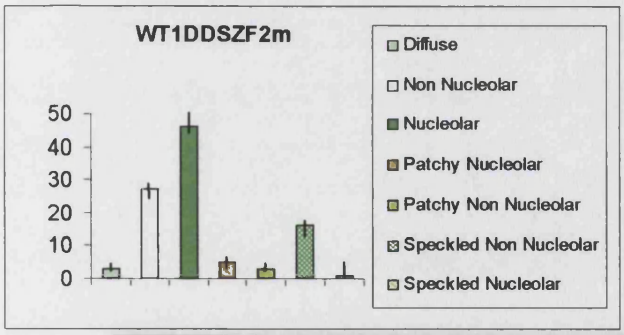

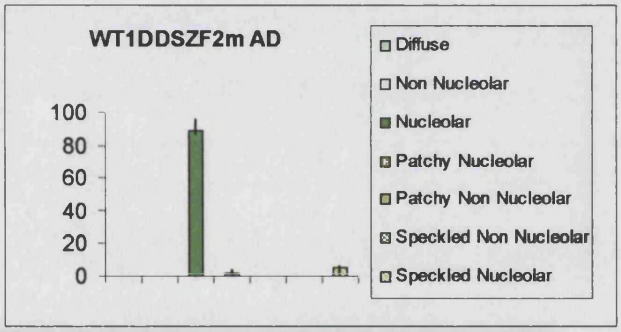

Constructs compared		Pattern	Significant difference (p)
WT1+KTS	WT1+KTSZF2m	Nucleolar	0.086
WT1-KTS	WT1-KTSZF2m	Speckled	0.0004
WT1DDS	WT1DDSZF2m	Nucleolar	0.065
WT1+KTS AD	WT1+KTSZF2m AD	Nucleolar	0.078
WT1+DDSZF2m	WT1DDSZF2m AD	Nucleolar	0.008

4.3.4 Localisation of the zinc finger regions of WT1

The next set of experiments in this chapter investigated the function of the zinc finger region of the protein. The zinc finger region GFP fusion mutants, ZFWT1+KTS and ZFWT1-KTS were created by N-terminal truncation of the native protein fusions, resulting in removal of all of the WT1 sequence except for the zinc finger region. These mutants were transfected into Cos7 cells and the resulting expression scored at 24 hours post transfection both with and without actinomycin D treatment. The results show interesting isoform-specific differences, with the ZFWT1+KTS fusion protein localising to nucleoli at all times and the ZFWT1–KTS fusion protein localizing in a similar fashion to the wild type (full length) WT1–KTS isoform. The behaviour of the ZFWT1+KTS mutant was very different to wild type WT1+KTS, with 97% of ZFWT1+KTS cells displaying nucleolar localisation, significantly higher to that of WT1+KTS (Figures 26 and 27 and Table D). This increased to over 99% after treatment with actinomycin D and at 72 hours post transfection, GFP expression remained strong in the nucleolus. These results were markedly different from those of wild type WT1+KTS (Section 4.3.1) where only 68% of cells transfected showed nucleolar accumulation whilst the others showed a variety of patterns. Only after actinomycin D treatment did 95% of the cells show nucleolar accumulation a similar figure to that of ZFWT1+KTS. The ZFWT1-KTS showed expression patterns similar to wild type WT1-KTS (Section 4.3.1). These results demonstrate the different sub-cellular localisation properties of the native WT1 protein isoforms may result primarily from the zinc finger region and although the zinc finger region of WT1+KTS is sufficient for nucleolar localisation, there may be a region elsewhere in the protein responsible for directing the protein out of the nucleolus.

Figure 26. Expression of the zinc finger region of WT1+KTS (ZFWT1+KTS) in Cos 7 cells 24 hours after transfection

Expression of the zinc finger region of WT1+KTS in Cos7 cells 24 hours after transfection both before (upper panel) and after actinomycin D treatment. Almost all transfected cells showed accumulation of the ZFWT1+KTS mutant within the nucleolus. Scale bars 5μm

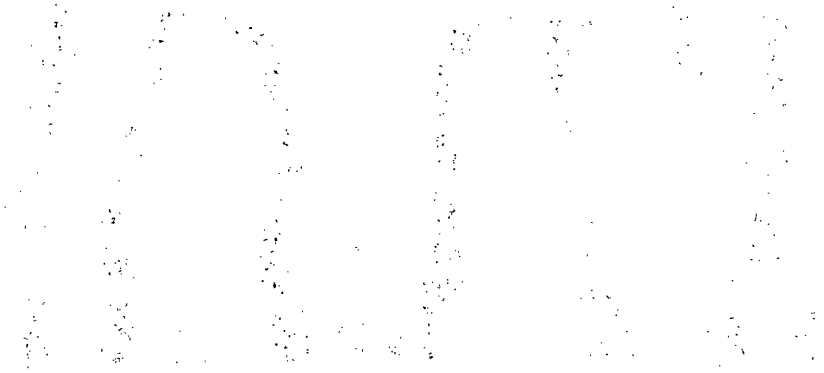

Figure 27. Cell counts of subcellular localization patterns following transfections of Cos 7 cells with an expression vector encoding the zinc finger regions of WT1+KTS (ZFWT1+KTS) fused with GFP

Cells were scored at 24 hours post transfection, both before (upper panel) and after actinomycin D treatment.

Patterns of interest between ZFWT1 mutants and wild type WT1+KTS constructs with and without AD treatment were analysed using the Mann Whitney U Statistocal tests to identify significant differences ($p>0.05$) in the subcellular localisation patterns between constructs (Table D).

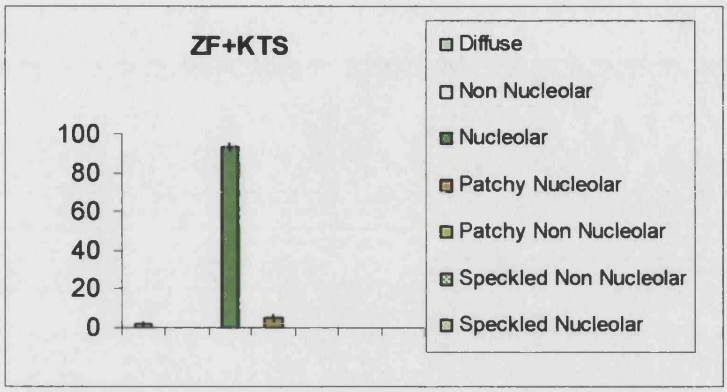

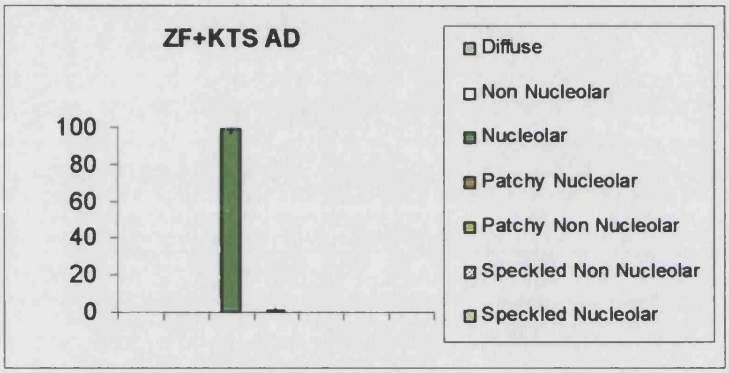

Constructs compared		Pattern	Significant difference (p)
WT1+KTS	ZF+KTS	Nucleolar	0.0002
ZF+KTS	ZF+KTS AD	Nucleolar	0.09
WT1+KTS AD	ZF+KTS AD	Nucleolar	0.087

4.3.5 Comparing the distribution of WT1 isoforms with other nuclear factors

4.3.5.1 Distribution of WT1 isoforms compared with nucleolar factor B23

The final sets of experiments investigated further the differential localisation of WT1 isoforms. The WT1: GFP fusion constructs were transfected into cells and localisation was compared with two nucleolar markers by immunofluorescence. The first colocalisation experiments investigated the distribution of green fluorescence associated with the WT1: GFP fusion proteins, together with an antibody recognizing the nucleolar protein B23 and detected using a red fluorescent secondary antibody (Figure 28). The B23 protein is known to localise to the dense granular compartment (DGR) of nucleoli and the anti-B23 antibody stains the nucleolus of Cos7 cells in a characteristic manner (Okuwaki, 2001) (Figure 28 A, D and G). Cells were transiently transfected with WT1: GFP constructs, WT1-KTS (Figure 28 B), WT1+KTS (Figure 28 E) and ZFWT1+KTS (Figure 28 H) and co-localisation was examined (merged images, Figures 28 C, F and I). B23 and WT1–KTS do not co-localise, as expected since WT1-KTS distribution is largely non-nucleolar (Figures 28 A, B and C). It was expected that B23 and WT1+KTS might co-localise as both are expressed in the nucleolus. However, this was not the case (Figures 28 D, E and F). B23 is known to colocalise to the DGR (Figure 28 A, D and G) of the nucleolus, whereas WT1+KTS was localised at the surface of the nucleolus (28 Figure E and F), either in peri-nucleolar regions or to the interchromatin regions of the nucleolus where B23 is not found (28 Figure F). However, transfection of the ZFWT1+KTS mutant resulted in a different pattern of expression within the nucleolus (Figures 28 G, H and I), with the isolated zinc fingers co-localising with B23 in the dense granular regions. This suggests that the zinc fingers are required for the nucleolar localisation of WT1, with the zinc finger region of WT1+KTS being sufficient for nucleolar localisation, but with signals elsewhere in the protein being involved in its localisation to specific areas of the nucleolus.

Figure 28. Colocalisation of WT1 isoforms with nucleolar factor B23 in Cos7 cells

Nucleolar localisation of B23 (A, D and G), WT1 GFP fusion proteins expressed in the same Cos7 cells (B, E and H), merged images of the same (C, F and I). WT1-KTS (B) did not show any colocalisation with B23 (C). WT1+KTS (E) was localized to different regions of the nucleolus to B23 (F). ZFWT1+KTS (H) colocalised with B23 in the nucleolus (Figure I). Scale bars 5μm

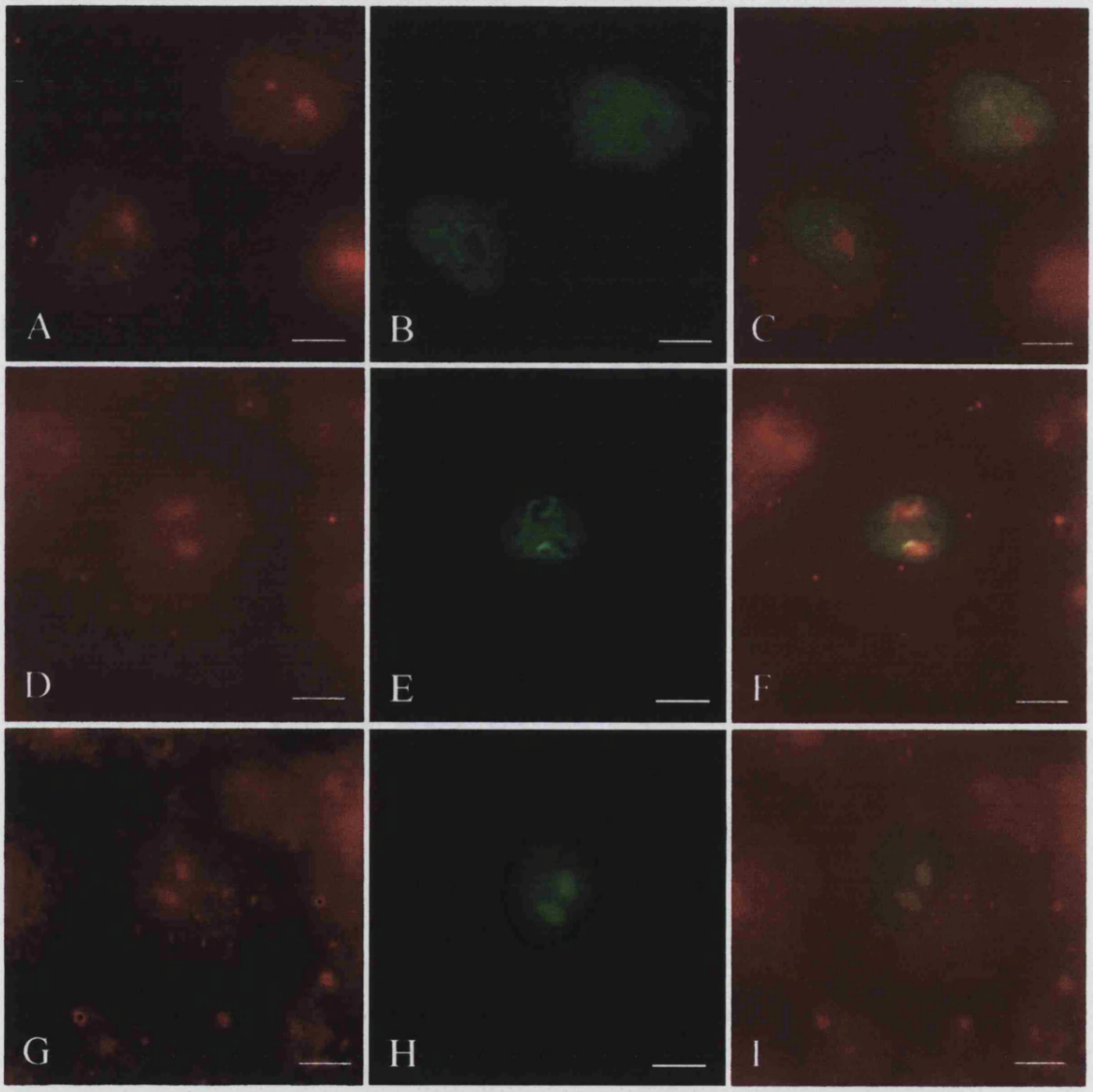
A
B
C
D
E
F
G
H
I

4.3.5.2 Distribution of WT1 isoforms compared with the paraspeckle protein PSP1

The following set of experiments investigated the colocalisation of WT1 with the paraspeckle protein, PSP1 (Figure 29). PSP1 has been found to localise to paraspeckles within the nucleus (Fox et al., 2002) and exhibits similar patterns to the speckles seen in WT1-KTS. The function of these paraspeckles is as yet unknown but anti-PSP1 was used in experiments with WT1+KTS and WT1–KTS in an attempt to identify areas to which WT1–KTS could be localising. Interestingly, it was found that 2 patterns of PSP1 expression occurred in Cos7 cells. PSP1 was expressed in nuclear speckles (Figure 29 A and L) similar to those previously reported (Fox et al., 2002). However, PSP1 was also observed in nucleolar patterns (Figure 29 I) similar to those seen in WT1+KTS transfected cells (Figure 29 J), a pattern not previously reported for PSP1. Although WT1–KTS localises to speckles within the nucleus (Figure 29 B and E), they are distinct from the PSP1-positive speckles (Figures 29 A, and C) suggesting that the organelles or regions to which WT1–KTS localise have a separate function. As expected, cells in which PSP1 expression is seen in the nucleolus (Figure 29 D) show no colocalisation with WT1–KTS (Figures 28 E and F). Nucleolar PSP1 however (Figure 29 I and K), colocalises in precisely the same pattern as nucleolar WT1+KTS (Figure 29 J and K), indicating that both proteins localise to the same regions of the nucleolus. These experiments illustrate the diverse compartmentalisation of the nucleus with different proteins being restricted to specific regions.

The similarities between the expression of PSP1 in the nucleoli of Cos7 cells with patterns seen for nucleolar WT1+KTS prompted the final set of experiments in this chapter. Expression of PSP1 was examined in the nucleus before and

Figure 29. Comparison of distribution of Paraspeckle protein Psp1 with WT1 isoforms in Cos7 cells

Detection of the presence of paraspeckles with the anti psp1 paraspeckle protein within Cos7 cells (A, D, G and J), compared with WT1GFP fusion protein expression within the same cells after transient transfection with WT1–KTS (B and E) or WT1+KTS (H and K), and merged images of the same (C, F, I and L). Localisation of psp1 within paraspeckles (A). WT1-KTS expression seen in a speckled pattern (B). WT1-KTS did not colocalise with psp1 in paraspeckles (C). Psp1 was also found in a nucleolar pattern in some cells (D). WT1-KTS was expressed in discreet domains within the nucleus (E). The nucleolar psp1 expression did not colocalise with WT1–KTS domains (F). The nucleolar pattern of paraspeckles (G) did colocalise with the nuclear pattern of WT1+KTS (I). In a separate subset of cells, the paraspeckle pattern of psp1 (J) did not colocalise with WT1+KTS (L). Scale bars 5μm

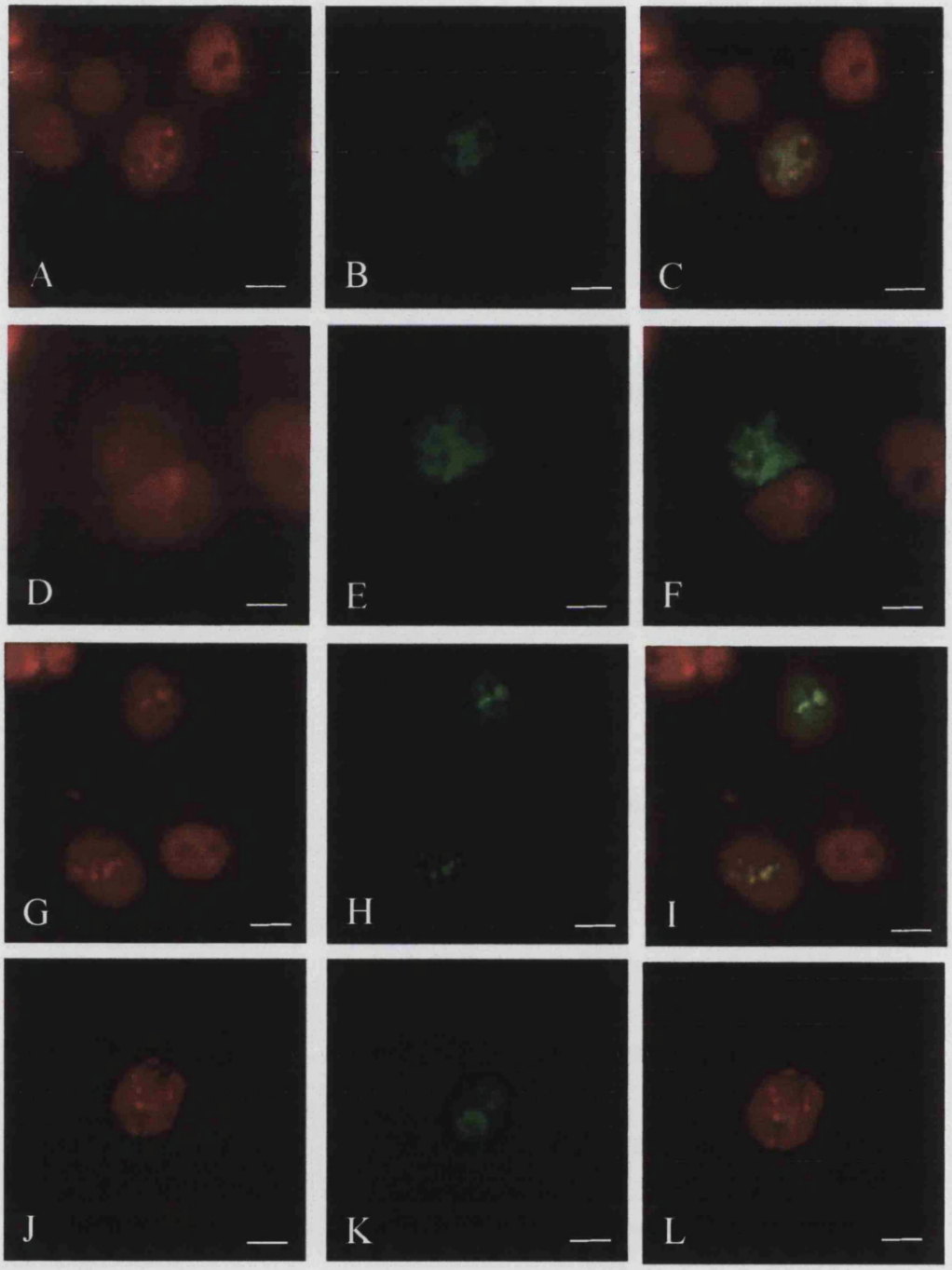
A
B
C
D
E
F
G
H
I
J
K
L

after actinomycin D treatment. PSP1 has been reported to be associated with paraspeckles in the nucleus (Fox et al., 2002) (Figure 30 A). While there were cells showing this characteristic speckled pattern of expression, a subset of cells showed a nucleolar pattern similar to that seen in WT1+KTS cells (Figure 30 B). Upon treatment of WT1+KTS transfected cells with actinomycin D some WT1+KTS localised to peri-nucleolar regions of the nucleus (Figure 30 C). Immunofluorescence of actinomycin D treated Cos7 cells with anti-PSP1 showed a similar pattern of expression to that of WT1+KTS (Figure 30 D).

4.4 Discussion

4.4.1 Distinct transient sub nuclear patterns of nuclear WT1 distribution

The differential GFPWT1+KTS and GFPWT1-KTS localisation patterns in live Cos7 cells (Section 4.3.1, Figure 19 and 20) recapitulate the characteristic nuclear patterns previously reported using WT1 antibodies in fixed cells (Englert et al., 1995; Larsson et al., 1995) GFPWT1-KTS was located mostly in a patchy, non-nucleolar and speckled patterns. Whereas WT1+KTS was seen in diffuse patterns throughout the nucleus with nucleolar localisation of the isoform seen in 68% of cells. Furthermore, no cells transfected with WT1+KTS displayed the speckled pattern seen in WT1-KTS transfected cells. These patterns showed that the nuclear distribution may be determined by isoform type, consistent with the hypothesis that the WT1+KTS and WT1-KTS isoforms might each control a separate aspect of gene expression (Bickmore et al., 1992; Englert, 1998). It should be noted that the presence of the variety of different patterns seen in each transfection suggests that within each transfection, there are cells at varying stages of the cell cycle. The differing patterns arise because WT1 expression may differ throughout the cell cycle. Using cell cycle specific

Figure 30. Comparison of Psp Paraspeckles and WT1+KTS GFP fusion protein localisation in Cos7 cells 24 hours post transfection

Psp1 stains paraspeckle structures within the nucleus of Cos7 cells (A). In another subset of cells psp1 includes expression in a nucleolar pattern (B). Upon treatment with actinomycin D, WT1+KTS expression was seen associate with the periphery of the nucleolus (C). After actinomycin D treatment Psp1 showed expression at the periphery of the nucleolus in a pattern similar to that of WT1+KTS in treated cells (D). Scale bars 5μm

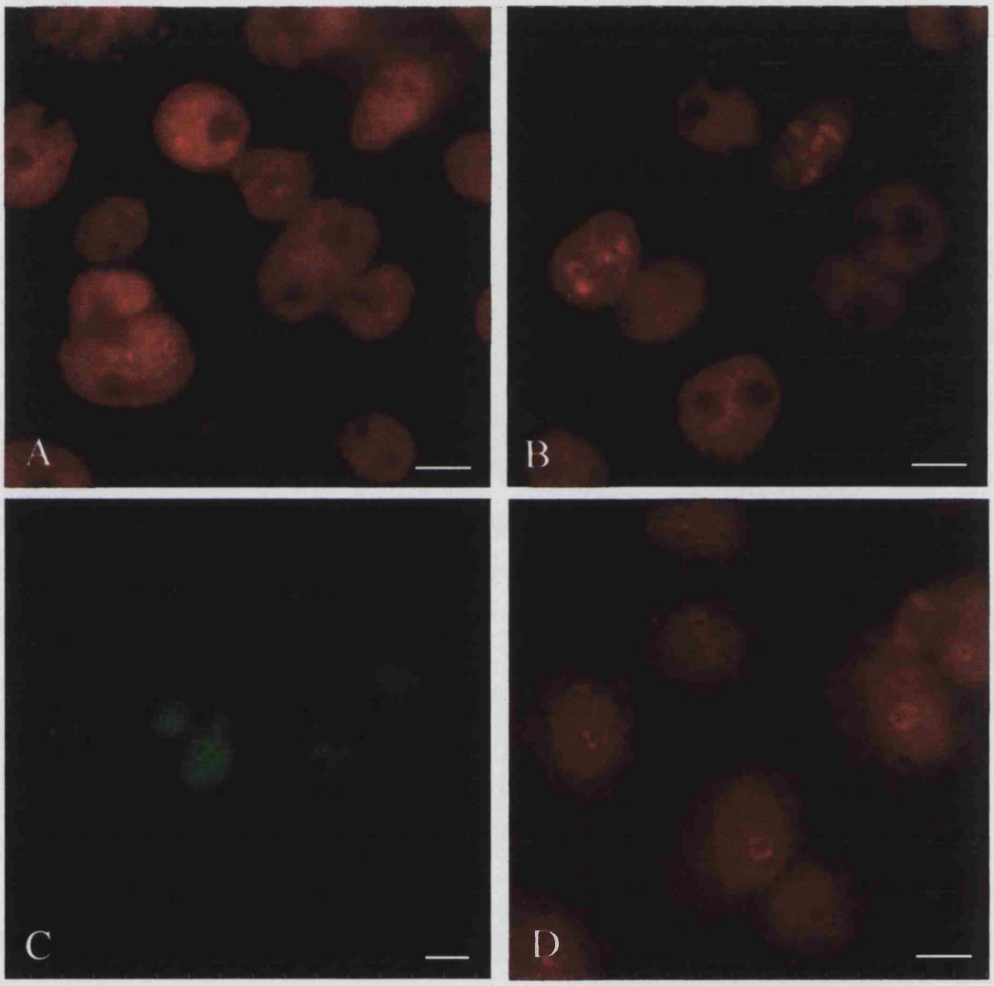
A
B
C
D

markers, it would be possible to identify stages of the cell cycle. The alternate location of the two isoforms within nuclei suggests that the isoforms may be interacting with different subsets of proteins associated with different functions and subnuclear locations. Particularly, the intimate interaction between WT1+KTS and the nucleolus may enable this isoform to become incorporated into the splicing machinery. Results in this chapter are from experiments in which Cos7 cells lacking endogenous WT1 were transiently transfected with GFP fusion proteins of the two WT1 isoforms. The characteristic expression patterns of the two WT1 isoforms were also seen in cells expressing endogenous WT1 (Dutton, 2003), but only transiently. Thus, in HeLa, MCF7 and HEK cells, the pattern of expression of WT1+KTS and WT1-KTS seven hours after transfection showed the distinct patterns of distribution described here for Cos7 cells but expression patterns becoming indistinguishable at 24 hours post transfection (the time at which most of the results were collected from Cos7 cells). It should also be noted that it became difficult, if not impossible to distinguish between the isoforms in Cos7 cells at 48 hours post transfection. Taken together, our observations of WT1: GFP fusion proteins in several cell types suggest that WT1-KTS and WT1+KTS are initially localised in an isoform-specific manner before being expressed in a complex, overlapping pattern within the cell. Progression to the indistinguishable patterns of distribution appears to be more rapid in some cell types than in others and may correlate with the presence of endogenous WT1 in the host cell type. The presence of cells within the population of transfected Cos7 cells that displayed more complicated patterns of nuclear staining (Figure 20) (cells with both diffuse and patchy areas and nucleolar staining) can be described as transient patterns of expression as these patterns disappear over time or actinomycin D treatment, reflecting the dynamic nature of the nucleus with proteins moving rapidly between structures and accumulating transiently (Misteli, 2001b).

4.4.2 Subnuclear patterns of WT1 isoform distribution also differ in transcriptionally quiescent cells

Actinomycin D treatment causes cells to become transctriptionally quiescent resulting in a rearrangement of the nuclear architecture and a relocation of proteins to different areas within the cell. Following actinomycin D treatment of Cos7 cells transfected with GFPWT1+KTS and GFPWT1-KTS characteristic isoform-specific distribution patterns were again observed (Section 4.3.2, Figure 18), further suggestive of different nuclear functions. 98% of WT1+KTS cells displayed nucleolar accumulation. WT1-KTS speckles disappeared suggesting that these speckles may have been due to transient accumulation or lost as a direct consequence of transcriptional quiescence. The majority of WT1-KTS transfected cells instead exhibited a patchy pattern, typical of transcription factors locating to sites of transcription in the nucleus suggesting that within one experiment, the cells within each transfection may be at different stages of transcriptional activity. Some would therefore be transcriptionally active and express one pattern of WT1-KTS and others would be transcriptionally quiescent and express alternative patterns. Treatment of cells with Actinomycin D allows a distinction of the isoform dependent patterns seen in Cos7 cells at 24 hours post-transfection and in the HeLa, MCF7 and HEK cells at 48 hours post-transfection. Given that Acinomycin D treatment causes the inhibition of transcription, this suggests that the distinct patterns of expression can only be completely identified in transcriptionally quiescent cells.

4.4.3 Alternative subnuclear localisation of WT1DDS

The subnuclear localisation of a GFP fused WT1 truncation mutant found in some Denys Drash patients (WT1DDS) showed that this mutant protein could locate to areas in the cell reminiscent of either WT1+KTS or WT1-KTS protein

(Section 4.3.2, Figure 21 and 22). At 24 hours after transfection most cells (51%) had a pattern unlike the typical patterns of either native isoform, with diffuse nucleoplasmic fluorescence and dark nucleoli devoid of any GFP. There was also a subset of cells with a speckled pattern such as that seen in WT1-KTS transfected cells. However following actinomycin D treatment, the expression pattern of WT1DDS was more like the pattern typical of WT1+KTS, with the majority of cells accumulating the protein in the nucleolus. The mutant protein lacks part of the third zinc finger and the entire fourth WT1 zinc finger. The KTS motif is therefore absent in the WT1DDS mutant, yet it was able to locate to the nucleolus in a similar fashion to WT1+KTS. Substitution of KTS with other sequences between the third and fourth zinc finger, resulted in proteins with WT1+KTS-like properties, suggesting that the KTS amino acid sequence is not critical for the differences between WT1+KTS and WT1-KTS (Davies et al., 2000; Hastie, 2001). Removal of the fourth zinc finger in the WT1DDS mutant construct may have had a similar structural affect on the protein as insertion of KTS, for instance, if the essential role of the KTS insertion is to alter the conformation of the fourth zinc finger with respect to other parts of the folded protein. This could possibly allow the protein to associate with an alternative interacting protein, or proteins, allowing trafficking of the WT1+KTS isoform to the nucleolus. It has been hypotheised that mutations in WT1 of DDS patients result in proteins that act in a dominant fashion by dimerizing with wild type protein. It has alternatively been suggested that haploinsufficiency may be a cause with a reduction of wild-type protein being sufficient to result in a disease phenotype (Little et al., 1993). The mutant protein described in this chapter behaved more like the WT1+KTS and production of this protein from a mutated allele could therefore cause a perturbation of the isoform ratio with increased WT1+KTS activity. The presence of speckles in cells transfected with WT1DDS was suggestive of WT1-KTS and these speckles also disappeared after time or

actinomycin D treatment suggesting they were transient patterns as in WT1-KTS transfections.

4.4.4 Significance of the putative NoLs within WT1 zinc finger 2

Zinc finger 2 of the WT1 protein includes a region with some homology with the NoLs of a number of nucleolar factors, suggesting that WT1 zinc finger 2 might contain all or part of the signal directing WT1+KTS to the nucleolus. The potential NoLS identified for WT1 aligns with a number of characterised nucleolar proteins such as hING1 and HIV-1REX nucleolar proteins. Consistent with the observation that WT1+KTS is intimately associated with the nucleolus, the discovery of a putative NoLS within the protein suggested a mechanism by which WT1+KTS could enter the nucleolus. Mutation of the two central arginine residues in the signal (which are the most highly conserved amino acids across other NoLS sequences) to a serine and a glycine resulted in the production of the ZF2 mutants, WT1+KTSZF2, WT1-KTSZF2 and WT1DDSZF2 (Section 4.3.4, Figures 24 and 25). These mutants allowed a functional investigation of the NoLs function in the subcellular localisation of WT1in live Cos7 cells. The subcellular localisation of the mutants was not changed from wild type patterns of distribution and failed to ablate nucleolar localisation. This can be interpretated in a number of ways. Firstly, the amino acid sequence in WT1 may not be a functional NoLS. Alternatively, it is possible that the mutation does not sufficiently alter the structure of the signal. Here, it should be noted that when the central residues were mutated in p80 Coilin, this was sufficient to cause aberrant localisation of the mutated protein, preventing its entry into the nucleolus. Equivalent amino acids were not mutated in both proteins. Although the central arginine was affected in both proteins, the p80 Coilin mutants also had a mutated serine whereas a second arginine was affected in the WT1 mutants. In the alignment of the NoLSs of different proteins (Figure 23) from the

NCBI database, the signals contain serines or arginines as their central residues. It may be that there is a certain degree of redundancy between these amino acids in the activity if a NoLS and it was for this reason that both arginines were mutated in the WT1 mutants. Another possibility is that a second NoLS, located elsewhere in the protein, may be involved in the nucleolar localisation of WT1 and that, at least under some circumstances, this second signal may be sufficient for this purpose. Another group has reported the presence of bipartite signals for nucleolar localisation. For instance, in the ING1 protein, two signals were required for nucleolar retention and mutation of one site was not sufficient to affect nucleolar localisation, however upon mutation of both sites together, nucleolar localisation was prevented (Scott et al., 2001). This suggests the possibility that WT1 might also have a second NoLS elsewhere in the protein. Clearly, further experiments would be needed to test this idea and unfortunately examination of other nucleolar proteins does not allow us to assemble a strong consensus sequence for the second part of a bipartite NoLS.

Interestingly, the putative signal was present on zinc finger 2 in both WT1+KTS and WT1-KTS, yet WT1-KTS does not locate to regions of the nucleolus. This scenario is consistent with the earlier suggestion that the role of the KTS insertion could be to alter zinc finger conformation and that this is the mechanism by which differences in isoform function are carried out. Insertion of KTS could change the conformation of WT1, preventing the fourth zinc finger from blocking the NoLs. Removal of this fourth zinc finger would then allow the NoLs to relocate the protein to the nucleolus via trafficking proteins or by association with proteins residing within the nucleolus. Inversely, the fourth zinc finger might block the NoLs on zinc finger 2 in WT1-KTS preventing the association with trafficking or nucleolar proteins, and hence, preventing nucleolar localisation of WT1-KTS. The failure for the database to identify further regions of homology to

nucleolar factors may have been due to the nature of NoLs sequences. As yet, only a few sequences have been identified. The signals are often encoded by small stretches of amino acids falling into broad, undistinguished groups. These range from basic stretches of amino acids (Speckmann et al., 1999; Tucker et al., 2000), to small stretches of amino acids with no homology to other signals (Lixin et al., 2001; Scott et al., 2001), and proline-rich sequence requiring phosphorylation to become active (Catez et al., 2002). It is therefore possible that the putative NoLs is part of a bipartite signal allowing the relocation of WT1+KTS to the nucleolus. Mutation of both signals may be required to abolish nucleolar localisation, however mutation of the identified NoLs was not sufficient for this purpose.

4.4.5 Requirement of the zinc fingers for nucleolar localisation

Transfection of the zinc finger fusion protein mutant constructs (ZFWT1+KTS and ZFWT1-KTS) in live Cos 7 cells (Section 4.3.5, Figures 26 and 27) allowed further characterisation of the zinc finger region and differences within this region with relation to the WT1+KTS and WT1-KTS isoforms. A putative NoLs was identified within the zinc finger region (Section 4.4.4) suggesting the involvement of this region in nucleolar localisation. The KTS insert within the zinc finger region of the protein has also been implicated in altering the DNA and RNA binding properties of the protein (Davies et al., 1998; Haber et al., 1990; Larsson et al., 1995; Renshaw et al., 1997). Major functional differences between WT1+KTS and WT1-KTS may therefore be located within the zinc finger region, highlighting the importance of this region of the protein. The differences in subcellular localisation of the isoforms were discussed earlier (Section 4.4.1) suggesting functional differences exist between WT1-KTS and WT1+KTS. The observation that the zinc finger regions of the two isoforms behave differently

from one another when isolated from the rest of the protein helps to reinforce this.

ZFWT1-KTS behaved in a similar fashion to full-length WT1–KTS, suggesting that the zinc fingers continued to interact with at least some of the appropriate proteins complexes. A dramatic change was seen when comparing the full-length WT1+KTS fusion protein and ZFWT1+KTS, with all of the mutant protein entering and remaining in the nucleolus. It is possible to draw several conclusions from these observations. Differences in isoform function do result from differences in the zinc finger region, with the two isolated zinc finger regions regulating distinct localisation patterns. The presence of a putative NoLS within the zinc finger-2 region is consistent with the nucleolar localisation of the isolated ZFWT1+KTS. In the context of the entire protein, this sequence might work in parallel with a second sequence to confer nucleolar localisation to the protein (as discussed in the previous section). In the absence of the rest of the protein, however, the signal might be sufficient to direct the protein into the nucleolus. Interestingly, ZFWT1–KTS failed to enter the nucleolus, suggesting structural differences between the zinc finger regions of the two isoforms results in suppression of a NoLS specifically in WT1–KTS. Accumulation of ZFWT1+KTS protein in the nucleolus suggests there may be signals located outside of the zinc finger region that are required for transport of the protein out of the nucleolus which are as yet uncharacterised.

4.4.6 Colocalisation of WT1 isoforms with nuclear factors

A further insight into the subcellular localisation of the two isoforms came from the colocalisation studies using antibodies recognizing the paraspeckle protein PSP1 and nucleolar factor B23 (Section 4.3.6, Figures 28 and 29). Paraspeckles have been reported to be a distinct set of speckles within the

nucleus, characterised by the PSP1 marker (Fox et al., 2002). PSP1 has been found to localise to paraspeckles within the nucleus and exhibits similar patterns to the speckles seen in WT1-KTS. The function of these paraspeckles is as yet unknown but given that WT1-KTS localises to a subset of speckles within the nucleus anti-PSP1 was used in experiments with WT1+KTS and WT1–KTS in an attempt to identify areas to which WT1 could be localising. The failure of WT1–KTS to colocalise with paraspeckles suggests that WT1–KTS compartmentalises within distinct domains that differ from PSP1. Interestingly, a novel PSP1 pattern of distribution was seen in the nucleolus, following actinomycin D treatment, strongly resembled patterns seen for WT1+KTS also after actinomycin D treatment (Figure 30). Both proteins preferentially relocated to the nucleolus with a perinucleolar pattern in transcriptionally quiescent cells. Many splicing factors have been shown to be located in a characteristic speckled pattern within the nucleus, that some have termed "splicing speckles". The nucleolus is the centre of rDNA transcription and ribosome biogenesis (Olson et al., 2000). More recently additional functions have been attributed to the nucleolus. For example, it may also be a site for the biogenesis and maturation of other ribonucleoprotein machinery including the signal recognition particle (Politz, 2000), the spliceosomal small nuclear RNPs (Lange, 2000), and telomerase (Mitchell, 1999). The nucleolus may also participate in processing or export of some mRNAs and tRNAs (Bertrand, 1998; Schneiter, 1995) and can control the activities of P53 by a sequestration mechanism (Visitin and Amon, 2000). Moreover, association between the nucleolus and other nuclear bodies, such as the perinucleolar compartment (Huang, 2000) and the cajal body also raise the possibility that nucleoli have additional functions (Gall, 2000). A recent study identified 271 nucleolar proteins and a subset of these factors were shown to accumulate in nucleoli specifically when transcription is inhibited (Andersen et al., 2002). These proteins included P80 Coilin, and various RNA binding

proteins. The feature of proteins associating and dissociating with the nucleolus through the cell cycle may be involved in regulating the localisation of nuclear factors and thereby controlling their access to interaction partners. Photobleaching experiments for PSP1 have revealed that PSP1 constantly traffics through the nucleolus yet has a steady state accumulation within paraspeckles. However when transcription is inhibited, PSP1 rapidly relocalises to the nucleolar periphery (Fox et al., 2002). Interestingly, it has been reported that many of the proteins that associate with the nucleoli after actinomycin D treatment contain RNA and DNA binding motifs (Andersen et al., 2002). This suggests a possible novel role for the nucleolus in the cell cycle and. It is possible to hypothesise that WT1+KTS cycles throughout the nucleus but relocates to the nucleolus following transcriptional inhibition to interact with other proteins, for example proteins involved in the splicing machinery.

The B23 protein is known to localise to the dense granular compartment (DGR) of nucleoli and the anti-B23 antibody stains the nucleolus of Cos7 cells in a characteristic manner (Okuwaki, 2001). Interestingly, WT1+KTS failed to colocalise with the B23 protein, illustrating the presence of different subnucleolar compartments. It is evident from these experiments that WT1+KTS is not expressed within the DGR of the nucleolus. The patterns of localisation for WT1+KTS in the nucleolus were similar to that of the paraspeckle protein after actinomycin D treatment. It has been reported that PSP1 locates to the perinucleolar caps following actinomycin D treatment (Fox et al., 2002) so it is fair to assume that WT1+KTS may also be located at the perinucleolar caps. It may be at these locations that the protein interacts with components of the splicing machinery that also associate with the perinucleolar caps. Surprisingly, the zinc finger region of WT1+KTS (ZFWT1+KTS) which accumulated in the nucleolus showed a striking difference in nucleolar localisation to full length

WT1+KTS. Whereas WT1+KTS fails to colocalise with B23 and displays a pattern similar to the perinucleolar staining of PSP1, ZFWT1+KTS showed complete colocalisation with B23 in the DGR of the nucleolus. One can assume from this that although the WT1 zinc fingers may be sufficient for nucleolar localisation of the protein, the amino-terminal region of the protein is essential for the protein to localise correctly within the nucleolus. It may be that the amino terminus interacts with WT1-associated proteins or alters WT1+KTS conformation hence allowing the zinc finger region to interact with factors necessary for its correct sub-nucleolar distribution.

4.5 Conclusions

The experiments in this chapter have allowed a detailed investigation of the subcellular localisation of WT1. Transfection of WT1 GFP fusion proteins of WT1+KTS, WT1-KTS and mutant isoforms into live Cos7 cells has enabled the identification of a number of characteristic distribution patterns for these proteins. WT1-KTS is distributed in a patchy pattern throughout the nuclei of cells in patterns reminiscent of transcription factors (Larsson et al., 1995), whilst WT1+KTS is expressed more evenly throughout nuclei and tends to accumulate in the nucleolus. This intimate association of WT1+KTS with nucleoli is increased following actinomycin D treatment suggesting a metabolic control of nucleolar association, which may allow WT1+KTS to come into contact and interact with other proteins involved in the splicing machinery. WT1+KTS is not present in the DGR of the nucleolus, as it failed to colocalise with the DGR expressed B23 protein, but it does exhibit some overlap in pattern with PSP1, particularly at the perinucleolar caps.

The presence of a putative NoLs suggested a mechanism by which WT1+KTS preferentially could be entering the nucleolus. Experiments aimed at proving the function of the putative NoLS within zinc finger two were inconclusive. Mutation of the putative NoLS did not prevent nucleolar targeting of WT1+KTS, however, this signal could be part of a bipartite signal as has been seen in some other nucleolar proteins. The signal is also present in WT1-KTS isoforms but the structural differences caused by the insertion of KTS could prevent the signal from functioning in WT1-KTS. Alternatively, a NoLS sequence may reside elsewhere within the WT1 zinc finger region. Investigation of the isolated zinc finger regions of both isoforms illustrated the requirement of the zinc fingers for

the nucleolar localisation of WT1+KTS since ZFWT1+KTS, and not ZFWT1-KTS was found to accumulate in the nucleolus. The structural differences arising from the KTS insertion may again be the explanation for ZFWT1-KTS not accumulating in the nucleoli. Colocalisation experiments using antibodies for the nucleolar protein B23 showed that the ZFWT1+KTS mutant shows a changed localisation from wild type WT1+KTS suggesting that while the zinc fingers may be necessary for nucleolar localisation, the amino terminus is also required for the correct function. Finally, analysis of the WT1DDS construct showed that this mutation found in patients with DDS results in a protein that behaves in a similar fashion to wild type WT1+KTS and could cause a perturbation of the isoform ratio if expressed from the mutant allele in DDS patients. In conclusion the differences in subcellular distribution between the WT1+KTS and WT1-KTS isoforms parallel functional differences between them. Differences between their locations in the cell could result in association with diverse groups of proteins resulting in functional differences, with WT1+KTS involved predominantly in posttranscriptional processes such as splicing, and WT1-KTS involved in transcriptional processes. The KTS insertion is essential for these differences in function, maybe due to conformation changes between the third and fourth zinc fingers. Finally, the mutant constructs highlight the role of the zinc finger region in the subcellular localisation and more specifically, the nucleolar localisation of the protein as illustrated by accumulation of ZFWT1+KTS to nucleoli of Cos7 cells.

Chapter 5

GENERAL CONCLUSIONS

The studies carried out in this report were aimed at investigating the functions of WT1-KTS and WT1+KTS isoforms in the development of the murine genito-urinary system, as well as the mechanisms by which the isoforms exert these functions at a cellular level. That WT1 is essential for the correct development of the genito-urinary system has been extensively discussed earlier in this thesis (Kreidberg et al., 1993). It has also been argued that the WT1-KTS and WT1+KTS isoforms have distinct and diverse functions, as indicated in both animal models and cell lines. It was therefore necessary to examine further the relationship between these WT1 isoforms and this was done using a two-pronged approach:

5.1 Transgenic experiments

The first experimental strategy utilised transgenic mice in order to explore the effects on developmental processes when WT1 isoform ratios were altered. By breeding animals with a P3: WT1-KTS transgene with animals heterozygous for the *WT1* null allele, it was possible to obtain litters of animals with various WT1+KTS : WT1-KTS ratios. Analysis of the gross morphology of both embryos and adult mouse organs revealed that $WT1^{+/-}$;P3 :WT1-KTS animals over the age of 6 months displayed a number of pathological features, some of which affected the genito-urinary system. These mice had reduced amounts of endogenous WT1 and expression of the P3: WT1-KTS transgene, would therefore tend to alter the normal WT1+KTS : WT1-KTS ratios towards higher

levels of WT1-KTS. The pathological features of the $WT1^{+/-}$;P3 :WT1-KTS mice mimic certain aspects of the human disorder, Frasier syndrome, where a similar change in WT1 isoform ratios is implicated.

The failure for the $WT1^{+/+}$;P3: WT1-KTS mice to develop pathological abnormalities, suggests that the observed effects are not simply due to ectopic transgene expression. Instead, a critical ratio exists between WT1+KTS and WT-KTS and the effect of the transgene was insufficient to alter this when both endogenous Wt1 alleles were intact, but was sufficient when one endogenous allele was disrupted, in $WT1^{+/-}$;P3 :WT1-KTS mice.

The expression pattern of WT1 was changed in the affected $WT1^{+/-}$;P3 :WT1-KTS organs with ectopic foci of expression seen in the kidneys. The testis, showed a general disorganisation of structure that was associated with ectopic WT1 expression. Given that WT1 expression is normally restricted to the podocytes of the kidneys and the sertoli cells of the testes in adult life, the presence of ectopic foci within the kidneys and testes could suggest the presence of ectopic podocytes and sertoli cells in affected organs. WT1 expression within podocytes and sertoli cells may have similar functions, to maintain the expression of key downstream genes, which in turn maintain the critical equilibrium between cell proliferation and division within the testes and kidneys. Ectopic expression of WT1 was also seen in abnormal livers where WT1 is not normally expressed. This abnormal expression in the liver could have been due to the expression of the transgene in the liver driven by the IGF2 P3 promoter and H19 enhancer but could also have arisen from endogenous Wt1 as an indirect consequence of transgene expression. Ectopic expression was not always seen in affected organs however.

The changes in proliferation and apoptosis observed in affected kidney and testis samples suggested that a critical dose of WT1 levels is essential for maintenance of the cell cycle and it may be that the reduction of WT1+KTS, in conjunction with the increase of WT1-KTS, is critical in the cell cycle process.

The P3: WT1-KTS transgene failed to rescue the null phenotype in $WT1^{-/-}$;P3 :WT1-KTS embryos. This may have been due to the fact that WT1-KTS was not alone sufficient to compensate for intact *WT1* function and cannot be substituted for the other isoforms lost in the knockout embryos.
The changes in the genito-urinary system in the $WT1^{+/-}$;P3:WT1-KTS mice were distinct and specific to this subset of animals when compared with Ob mutant mice, an alternative model for genital abnormalities. This further suggests that a WT1-specific path is responsible for the $WT1^{+/-}$;P3:WT1-KTS phenotype.

In conclusion, the transgenic data illustrates the requirement for maintenance of a critical ratio of WT1KTS isoforms in adult murine development. Alteration of this ratio can result in the development of pathological abnormalities, some of which mimic those seen in human disorders where WT1 is implicated. Abnormalities within the genito-urinary system of affected animals resulting from altered isoform ratios suggest that while these isoforms may have overlapping roles, they may also carry out separate functions within developmental processes.

3.6 Future Directions

Most importantly, it would be of value to detect the presence of the P3:WT1-KTS in affected organs and in embryos. As illustrated by the embryo data, the anti-WT1 antibody was not sufficiently sensitive to detect protein expressed from the transgene. Ectopic expression of the transgene was however detectable in

affected livers using the same antibody. This detection could be carried out with RT-PCR of organs from embryos in the future. Although we have not analysed the hearts of the $WT1^{+/-}$;P3:WT1-KTS animals, these might be another interesting organ to analyse. No obvious abnormalities of the heart were observed in our animals upon dissection but histological analysis may have revealed cardiac abnormalities given that WT1 null animals die from cardiac defects and the protein is known to be expressed in the developing heart and is implicated in cardiac development. It would be interesting to identify other factors, possibly downstream targets of WT1 in tissue samples derived from $WT1^{+/-}$;P3:WT1-KTS animals, and investigate possible abnormal expression of these targets as a means of understanding of the role of WT1 in genito-urinary development and its interaction with other molecules essential in these processes.

5.2 Cell culture experiments

The transgenic models allowed the examination of the effects of changing WT1 isoform ratios *in vivo*. An alternative experimental approach was to identify the possible mechanisms by which the two isoforms exert their different functions at the cellular level. The second approach utilised cell biology techniques to elucidate the way in which the WT1-KTS and WT1+KTS isoforms function at the cellular level. The aim of the cell biology experiments was to identify differences between the isoforms with regards to their cellular localisation and interactions within cells, as a means of understanding how the KTS insertion might affect WT1 function. This was achieved by using a combination of transient transfections of GFP fusion constructs (made with both wild type and mutant WT1 isoforms), and immunofluorescence.

Upon examination of the subcellular localisation of GFP fusion constructs of the two isoforms it has been possible to reiterate previous findings that the two isoforms can be found in distinct regions of the cell with WT1+KTS associating with the nucleolus [Englert, 1995 #81]. This intimate association of WT1+KTS with nucleoli is increased following actinomycin D treatment, suggesting a metabolic control of nucleolar association that may allow WT1+KTS to interact with a specific pool of proteins, including those involved in mRNA splicing.

The identification of a putative NoLS within zinc finger-2 illustrated a possible mechanism by which WT1+KTS could enter the nucleolus. Although this motif was also present in WT1-KTS the structural differences in the zinc finger region between the two isoforms, caused by the KTS insertion, could render the NoLS inactive in WT1-KTS. Mutation of this motif failed to prevent the nucleolar accumulation of the protein however the presence of a bipartite NoLS has been reported in at least one other protein [Scott, 2001 #253]. Further analysis of the zinc finger region demonstrated that the zinc finger region of WT1+KTS was required for the nucleolar localisation of WT1+KTS, with mutant GFP constructs consisting solely of the zinc finger region of WT1 retaining the capacity to localise to the nucleolus. Again, structural differences within the zinc finger region arising from the insertion could explain the failure of the isolated zinc finger region of WT1-KTS to enter the nucleolus.

The differential co-localisation of the WT1-KTS and WT1+KTS isoforms to other subcellular proteins suggests that they have differing binding affinities or profiles of interaction for different groups of proteins. This highlights the possibility of distinct roles for the isoforms in transcriptional and possibly posttranscriptional pathways. Again, the KTS insertion may be essential for these differences in

function, possibly due to conformational changes involving the third and fourth zinc fingers.

Frasier syndrome also highlights the requirement of the WT1 KTS region for correct genito-urinary development, with mutations in Frasier syndrome patients also affect the zinc finger region. Examination of the subcellular localisation of a mutant WT1 protein, carrying a mutation found in another human disease, DDS, showed that the mutation resulted in a protein that behaves in a similar fashion to wild type WT1+KTS. This was despite the absence of the KTS amino acids in the DDS mutant protein, which was prematurely truncated within the third zinc finger. The result suggested that this type of mutation could act by causing what is effectively a perturbation of the WT1-KTS and WT1+KTS isoform ratio when expressed from the mutant allele in DDS patients.

In conclusion, these observations draw a parallel with the reports that the two WT1 isoforms have different functions within cells. Differences between the localization of WT1-KTS and WT1+KTS in the cell could result in their association with diverse groups of proteins, resulting in functional differences. Conformational differences between the third and fourth zinc finger arising from the KTS insertion could be essential for distinguishing the protein isoforms in at least two possible ways: first, being involved in locating the isoforms to different regions within the cell; second, by changing the capacity of the two isoforms to associate with interacting proteins. The result of the insertion would therefore enable WT1+KTS to be involved predominantly in posttranscriptional processes such as splicing, and WT1-KTS in transcriptional processes. Taken together, the differences in WT1 isoform function might also help explain the abnormalities seen in $WT1^{+/-}$;P3: WT1-KTS transgenic models with differences in isoform ratio.

4.6 Future Directions

A number of experiments would be required to fully understand the mechanisms by which WT1+KTS and WT1-KTS function in cells. In order to fully characterise the effects that structure would have on the subcellular localisation of the proteins, a number of mutant constructs would be helpful. Firstly, the subcellular localisation of a zinc finger region construct containing the DDS truncation could help to characterise the critical region required for nucleolar localisation. If this continued to accumulate within the nucleolus one could presume that the nucleolar localisation region was in zinc fingers one or two. The next step would be to create mutations within the putative NoLS signal in GFP zinc finger fusion proteins to ask whether these were still capable of nucleolar localisation. Should this indicate that the identified sequence does not act as a NoLS, deletion mutation analysis of the zinc fingers could be used to determine the zinc finger sequences required for nucleolar localisation empirically. Conversely, if zinc finger 2 in isolation were still able to accumulate in the nucleolus this would provide further evidence in favour of the zinc finger-2 localisation signal. In parallel, further truncation mutants could help detect the presence of a second signal within the amino terminus of the protein. Although the mechanisms by which nucleolar localisation signals function is still unknown, it seems likely that trafficking proteins are involved in this process.

Another area of interest would be the identification of putative trafficking proteins involved in the direction of WT1+KTS to areas of splicing and perhaps other, WT-KTS interacting proteins that could allow WT1-KTS to move to areas of transcriptional activity. It is possible that the movement of the isoforms occurs by diffusion, however, identification of associating proteins would still be helpful in identifying the mechanisms by which the isoforms function. Finally, it would be interesting to see what effect the inhibition of WT1+KTS translocation to the

nucleolus might have on the cell cycle, on cell death, proliferation or differentiation. In parallel, the forced accumulation of WT1-KTS within the nucleolus could be attempted, by fusing the protein with a characterised NoLS, and might also have effects on live cells that could aid our understanding of isoform-specific functions of WT1.

BIBLIOGRAPHY

Andersen, J., Lyon, C. E., Fox, A. H., Leung, A. K., Lam, Y. W., Steen, H., Mann, M. and Lamond, A. I. (2002). Directed Proteomic analysis of the human nucleolus. *Current Biology* **12**, 1-11.

Armstrong, J. F., Pritchard-Jones, K., Bickmore, W. A., Hastie, N. D. and Bard, J. B. (1993). The expression of the Wilms' tumour gene, WT1, in the developing mammalian embryo. *Mech Dev* **40**, 85-97.

Barbaux, S., Niaudet, P., Gubler, M. C., Grunfeld, J. P., Jaubert, F., Kuttenn, F., Fekete, C. N., Souleyreau-Therville, N., Thibaud, E., Fellous, M. et al. (1997). Donor splice-site mutations in WT1 are responsible for Frasier syndrome. *Nat Genet* **17**, 467-70.

Bard, J. B. L. (2002). Growth and death in the developing mammalian kidney: signals, receptors and conversations. *BioEssays* **24**, 72-82.

Bardeesy, N., Zabel, B., Schmitt, K. and Pelletier, J. (1994). WT1 mutations associated with incomplete Denys-Drash syndrome define a domain predicted to behave in a dominant-negative fashion. *Genomics* **21**, 663-4.

Beau, C., Vivian, N., Munsterberg, A., Dresser, D. W., Lovell-Badge, R. and Guerrier, D. (2001). In vivo analysis of the regulation of the anti-Mullerian hormone, as a marker of Sertoli cell differentiation during testicular development, reveals a multi-step process. *Mol Reprod Dev* **59**, 256-64.

Berasain, C., Herrero, J.I., Garcia-Trevijano, E.R., Avila, M.A., Esteban, J.I., Mato, J.M., Prieto. J. (2003). Expression of Wilms' tumor suppressor in the liver with cirrhosis: relation to hepatocyte nuclear factor 4 and hepatocellular function. *Hepatology* **38**, 148-157.

Bertrand, E., Houser-Scott, F., Kendall, A., Singer, R.H. and Engelke, D.R. (1998). Nucleolar localization of early tRNA processing. *Genes and Development* **12**, 2463-2468.

Bickmore, W. and Sutherland, H. G. E. (2002). Addressing protein localisation within the nucleus. *The EMBO Journal* **21**, 1248-1254.

Bickmore, W. A., Oghene, K., Little, M. H., Seawright, A., van Heyningen, V. and Hastie, N. D. (1992). Modulation of DNA binding specificity by alternative splicing of the Wilms tumor wt1 gene transcript. *Science* **257**, 235-7.

Bitgood, M. J., Shen, L. and McMahon, A. P. (1996). Sertoli cell signaling by Desert hedgehog regulates the male germline. *Curr Biol* **6**, 298-304.

Brenton, J. D., Drewell, R. A., Viville, S., Hilton, K. J., Barton, J. F.-X, Surani, M. A. (1999). A silencer element identified in Drosophila is required for imprinting of H19 reporter transgenes in mice. *Proc Natl Acad Sci U S A* **96**, 9242-9247.

Caricasole, A., Duarte, A., Larsson, S. H., Hastie, N. D., Little, M., Holmes, G., Todorov, I. and Ward, A. (1996). RNA binding by the Wilms tumor suppressor zinc finger proteins. *Proc Natl Acad Sci U S A* **93**, 7562-6.

Carpenter, B., Hill, K. J., Charalambous, M., James, D. I., Lahiri, D., Anderson, J. S., Schumacher, V., Royer-Pokora, B., Mann, M., Ward, A. et al. (2002). BASP1 is a transcriptional cosuppressor for the Wilms' tumour suppressor protein WT1. *In press.*

Catez, F., Erard, M., Schaerer-Uthuttalt, N., Kindbeiter, K., Madjar, J. J. and J., D. J. (2002). Unique motif for nucleolar retention and nuclear export regulated by phosphorylation. *Molecular and Cellular Biology* **22**, 1126-1130.

Charlieu, J. P., Larsson, S., Miyagawa, K., van Heyningen, V. and Hastie, N. D. (1995). Does the Wilms' tumour suppressor gene, WT1, play roles in both splicing and transcription? *J Cell Sci Suppl* **19**, 95-9.

Cohen, H. T., Bossone, A., Zhu, G., McDonald, G. A. and Sukhatme, V. P. (1997). Sp1 is a critical regulator of the Wilms' tumour-1 gene. *The Journal of Biological Chmeistry* **272**, 2901-2913.

Coppes, M. J., Huff, V. and Pelletier, J. (1993). Denys-Drash syndrome: relating a clinical disorder to genetic alterations in the tumor suppressor gene WT1. *J Pediatr* **123**, 673-8.

Davies, J. A. and Bard, J. B. L. (1998). Development of the metanephric kidney. *Current Topics in Developmental Biology* **39**, 245-302.

Davies, J. A. and Davey, M. G. (1999). Collecting duct morphogenesis. *Pediatric Nephrology* **13**, 535-541.

Davies, R. C., Bratt, E. and Hastie, N. D. (2000). Did nucleotides or amino acids drive evolutionary conservation of the WT1 +/-KTS alternative splice? *Hum Mol Genet* **9**, 1177-83.

Davies, R. C., Calvio, C., Bratt, E., Larsson, S. H., Lamond, A. I. and Hastie, N. D. (1998). WT1 interacts with the splicing factor U2AF65 in an isoform-dependent manner and can be incorporated into spliceosomes. *Genes Dev* **12**, 3217-25.

Del Rio-Tsonis, K., Covarrubias, L., Kent, J., Hastie, N. D. and Tsonis, P. A. (1996). Regulation of the Wilms' tumor gene during spermatogenesis. *Dev Dyn* **207**, 372-81.

Dressler, G. R., Deutsch, U., Chowdhury, K., Nornes, H. O. and Gruss, P. (1990). Pax-2, a new murine paired-box containing gene and its expression in the developing excretory system. *Develoment* **109**, 787-795.

Dressler, G. R. and Douglass, E. C. (1992). Pax-2 is a DNA-binding protein expressed in embryonic kidney and Wolms' tumour. *Proceedings of the National Academy of Science (USA)* **89**, 1179-1183.

Drummond, I. A., Madden, S. L., Rohwer-Nutter, P., Bell, G. I., Sukhatme, V. P. and Rauscher, F. J. d. (1992). Repression of the insulin-like growth factor II gene by the Wilms tumor suppressor WT1. *Science* **257**, 674-8.

Duarte, A. (1997). Regulation of gene expression by the Wilms' tumour suppressor, WT1. In *Wolfson College*, (ed., pp. 240. Oxford: Oxford University.

Dudley, A. T., Lyons, K. M. and Robertson, E. J. (1995). A requirement for Bone morphogenic protein-7 of the mammalian kidney and eye. *Genes and Development* **9**, 2795-2807.

Dundr, M. and Misteli, T. (2001). Functional architecture in the cell nucleus. *Biochemical Journal* **356**, 297-310.

Dundr, M. and Misteli, T. (2002). Nucleolomics: an inventory of the nucleolus. *Mol Cell* **9**, 5-7.

Englert, C. (1998). WT1- more than a transcription factor? *Trends in Biochemistry* **23**, 383-393.

Englert, C., Maheswaran, S., Garvin, A. J., Kreidberg, J. and Haber, D. A. (1997). Induction of p21 by the Wilms' tumor suppressor gene WT1. *Cancer Res* **57**, 1429-34.

Englert, C., Vidal, M., Maheswaran, S., Ge, Y., Ezzell, R. M., Isselbacher, K. J. and Haber, D. A. (1995). Truncated WT1 mutants alter the subnulear localisation of the wild-type protein. *Proceedings of the National Academy of Science USA* **92**, 11960-11964.

Fox, A. H., Lam, Y. W., Leung, A. K., Lyon, C. E., Andersen, J., Mann, M. and Lamond, A. I. (2002). Paraspeckles: a novel nuclear domain. *Curr Biol* **12**, 13-25.

Franke, U., Holmes, L. B., Atkins, L. and Riccardi, V. M. (1979). Aniridia-Wilms' tumour association: evidence for specific deletion of 11p13. *Cytogenetic cell genetics* **24**, 185-192.

Frasier, S. D., Bashore, R. A. and Mosier, H. D. (1964). Gonadoblastoma associated with pure gonadal dysgenesis in monozygotic twins. *Journal of Pediatrics* **64**, 740-745.

Gall, J. G. (2000). Cajal bodies: the first 100 years. *Annu Rev Cell Developmental Biology* **16**, 273-300.

Gashler, A. L., Bonthron, D.T., Madden, S.L., Rauscher, F.J., Collins, T., Sukhatme, V.P. (1992). Human platelet-derived growth factor A chain is transcriptionally repressed by the Wilms' tumour suppressor WT1. *Proc Natl Acad Sci U S A* **89**.

Ginsburg, M., Snow, M. and McLaren, A. (1990). Ptimordial germ cells in the mouse embryo during gastrulation. *Development* **110**, 521-528.

Godin, R. E., Takaesu, N. T., Robertson, E. J. and Dudley, A. T. (1998). Regulation of BMP7 expression during kidney development. *Development* **125**, 3473-3482.

Grobstein, C. (1955). Inductive Interaction in the development of the mouse metanephros. *Journal of Experimental zoology* **130**, 319-340.

Guo, J. K., Hammes, A., Chaboissier, M. C., Vidal, V., Xing, Y., Wong, F. and Schedl, A. (2002a). Early gonadal development: exploring Wt1 and Sox9 function. *Novartis Found Symp* **244**, 23-31; discussion 31-42, 253-7.

Guo, J. K., Menke, A. L., Gubler, M. C., Clarke, A. R., Harrison, D., Hammes, A., Hastie, N. D. and Schedl, A. (2002b). WT1 is a key regulator of podocyte function: reduced expression levels cause crescentic glomerulonephritis and mesangial sclerosis. *Hum Mol Genet* **11**, 651-9.

Haber, D. A., Buckler, A. J., Call, K. M., Pelletier, J., Sohn, R. L. and Housman, D. E. (1990). Altternative splicing and genomic structure of the Wilms' umour gene WT1. *Proceedings of the National Academy of Science USA* **88**, 9618-9622.

Hamilton, T. B., Borel, F. and Romaniuk, P. J. (1998). Comparison of the DNA binding characteristics of the related zinc finger proteins WT1 and EGR1. *Biochemistry* **37**, 2051-8.

Hammes, A., Guo, J. K., Lutsch, G., Leheste, J. R., Landrock, D., Ziegler, U., Gubler, M. C. and Schedl, A. (2001). Two splice variants of the Wilms' tumor 1 gene have distinct functions during sex determination and nephron formation. *Cell* **106**, 319-29.

Hastie, N. D. (1993). Wilms' tumour gene and function. *Curr Opin Genet Dev* **3**, 408-13.

Hastie, N. D. (2001). Life, sex, and WT1 isoforms--three amino acids can make all the difference. *Cell* **106**, 391-4.

Hebert, M. D., Szymczyk, P. W., Shpargel, K. B. and Matera, A. G. (2001). Coilin forms the bridge between Cajal bodies and SMN, the spinal muscular atrophy protein. *Genes Dev* **15**, 2720-9.

Hellmich, H. L., Kos, L., Cho, E. S., Mahon, K. A. and Zimmer, A. (1996). Embryonic expression of glial cell-line derived neurotrophic factor (GDNF) suggests multiple developmental roles in neural differentiation and epithelial-mesenchymal interactions. *Mechanisms of Development* **54**, 95-106.

Hoyle, C., Narvaez, V., Alldus, G., Lovell-Badge, R. and Swain, A. (2002). Dax1 expression is dependent on steroidogenic factor 1 in the developing gonad. *Mol Endocrinol* **16**, 747-56.

Huang, S. (2000). Review: perinuclear structures. *Journal of Structural Biology* **129**, 233-240.

Ingraham, H. A., Lala, D. S., Ikeda, Y., Luo, X., Shen, W. H., Nachtigal, M. W., Abbud, R., Nilson, J. H. and Parker, K. L. (1994). The nuclear receptor steroidogenic factor 1 acts at multiple levels of the reproductive axis. *Genes and Development* **8**, 2302-2312.

Jeffs, B., Meeks, J. J., Ito, M., Martinson, F. A., Matzuk, M. M., Jameson, J. L. and Russell, L. D. (2001). Blockage of the rete testis and efferent ductules by ectopic Sertoli and Leydig cells causes infertility in Dax1-deficient male mice. *Endocrinology* **142**, 4486-95.

Jin, D. K., Kang, S. J., Kim, S. J., Bang, E. H., Hwang, H. Z., Todokoro, K., Yamada, M. and Koshaka, T. (1999). Transcriptional regulation of PDGF-A and TGF-beta by +KTS WT1 deletion mutants and a mutant mimicking Denys-Drash syndrome. *Renal Faillure* **21**, 685-94.

Kappel, A., Ronicke, V., Damert, A., Flamme, I., Risau, W. and Breier, G. (1999). Identification of Vascular Endolthelian Growth Factor (VEGF)

Receptor-2 (Flk-1) promoter/enhancer sequencces sufficient for angioblast and endothelial cell-specific transcription in transgenic mice. *Blood* **93**, 4284-4292.

Kennedy, D., Ramsdale, T., Mattick, J. and Little, M. (1996). An RNA recognition motif in Wilms' tumour protein (WT1) revealed by structural modelling. *Nat Genet* **12**, 329-31.

Kingsley, D. M. (1995). The TGF beta superfamily: new members, new receptor and new genetic tests of fuction in different organisms. *Genes and Development* **8**, 133-146.

Klamt, B., Koziell, A. B. and Poulat, F. (1998). Frasier syndrome is caused by defective alternative splicing leading to an altered ratio of WT1 +/- KTS splice isoforms. *Human Molecular Genetics* **74**, 709-714.

Knudson, A. G. and Strong, L. C. (1972). Mutation and cancer: a model for Wilms' tumour of the kidney. *Journal of the Nation cancer institute* **48**, 313-324.

Kohsaka, T., Tagawa, M., Takekoshi, Y., Yanagisawa, H., Tadokoro, K. and Yamada, M. (1999). Exon 9 mutations in the WT1 gene, without influencing KTS splice isoforms, are also responsible for Frasier syndrome. *Hum Mutat* **14**, 466-70.

Koopman, P., Gubbay, J., Vivian, N., Goodfellow, P. and Lovell-Badge, R. (1991). Male development of chromosomally female mice transgenic for SRY. *Nature* **35**, 117-125.

Koziell, A., Charmandari, E., Hindmarsh, P. C., Rees, L., Scambler, P. and Brook, C. D. G. (2000). Frasier syndrome, part of the Denys Drash coninuum or simply a WT1 gene associated disorder or intersex and nephropathy. *Clinical Endicrinology* **52**, 519-524.

Koziell, A. and Grundy, R. (1999). Frasier and Denys-Drash syndromes: different disorders or part of a spectrum? *Arch Dis Child* **81**, 365-9.

Kreidberg, J., Sariola, H., Loring, J. M., Maeda, M., Pelletier, J., Housman, D. and Jaenisch, R. (1993). WT-1 is required for early kidney development. *Cell* **74**, 679-691.

Ladomery, M. R., Slight, J., Mc Ghee, S. and Hastie, N. D. (1999). Presence of WT1, the Wilm's tumor suppressor gene product, in nuclear poly(A)(+) ribonucleoprotein. *J Biol Chem* **274**, 36520-6.

Laity, J. H., Chung, J., Dyson, J. H. and Wright, P. (2000). Alternative splicing of Wilms' tumour suppressor protein modulates DNA binding activity through isoform-specific DNA induced conformational changes. *Biochemistry* **39**, 5341-5348.

Lamond, A. I. and Earnshaw, W. C. (1998). Structure and function in the nucleus. *Science* **280**, 547-53.

Lamond, A. I. and Gasser, S. M. (2002). Nucleus and gene expression. *Curr Opin Cell Biol* **14**, 259-61.

Lange, T. S., Gerbi, S.A. (2000). Transient nucleolar localisation of U6 small nuclear RNA in Xenopus Laevis oocytes. *Mol Biol Cell* **11**, 2419-2428.

Larsson, S. H., Charlieu, J.-P., Miyagawa, K., Engelkamp, D., Rassoulzadegan, M., Ross, A., Cuzin, F., van Heyningen, V. and Hastie, N. D. (1995). Subnuclear loacalisation of WT1 in splicing or transcription factor domains is regulated by alternative splicing. *Cell* **81**, 391-401.

Lechner, M. and Dressler, G. (1997). The molecular basis of embryonic kidney development. *Mechanisms of development* **62**, 105-120.

Lee, S. B. and Haber, D. A. (2001). Wilms' tumour and the WT1 gene. *Experimental Cell Research* **264**, 74-99.

Lee, S. B., Huang, K., Palmer, R., Truong, V.B., Herzlinger, D., Kolquist, K.A., Wong, J., Paulding, C., Yoon, S.K., Gerald, W., Oliner, J.D., Haber, D.A. (1999). The Wilms' suppressor WT1 encodes a transcriptional activator of amphiregulin. *Cell* **98**, 663-673.

Lin, L.-F. H., Doherty, D. H., Lile, J. D., Bektesh, S. and Collins, F. (1993). GDNF: a glial cell-line derived neurotrophic for midbrain and dopiminergic neurons. *Science* **260**, 1130-1132.

Little, M., Holmes, G., Bickmore, W., van Heyningen, V., Hastie, N. and Wainwright, B. (1995). DNA binding capacity of the WT1 protein is abolished by Denys-Drash syndrome WT1 point mutations. *Hum Mol Genet* **4**, 351-8.

Little, M. H., Dunn, R., Byrne, J. A., Seawright, A., Smith, P. J., Pritchard-Jones, K., van Heyningen, V. and Hastie, N. D. (1992a). Equivalent expression of paternally and maternally inherited WT1 alleles in normal fetal tissue and Wilms' tumours. *Oncogene* **7**, 635-41.

Little, M. H., Prosser, J., Condie, A., Smith, P. J., Van Heyningen, V. and Hastie, N. D. (1992b). Zinc finger point mutations within the WT1 gene in Wilms tumor patients. *Proc Natl Acad Sci U S A* **89**, 4791-5.

Little, M. H., Williamson, K. A., Mannens, M., Kelsey, A., Gosden, C., Hastie, N. D. and van Heyningen, V. (1993). Evidence that WT1 mutations in Denys-Drash syndrome patients may act in a dominant-negative fashion. *Hum Mol Genet* **2**, 259-64.

Little, N. A., Hastie, N. D. and Davies, R. C. (2000). Identification of WTAP, a novel Wilms' tumour 1-associating protein. *Hum Mol Genet* **9**, 2231-9.

Lixin, R., Efthymiadis, A., Henderson, B. and Jans, A. (2001). Novel Properties of the nucleolar targeting signal of human angiogenin. *Biochemical and Biophysical Research Communications* **284**, 185-193.

Lohrum, M. A., Ashcroft, M., Kubbutat, M.H., Vousden, K.H. (2000). Identification of a cryptic nucleolar-localisation signal in MDM2. *Nature Cell Biology* **2**, 179-181.

Lyon, C. E. and Lamond, A. I. (2000). The nucleolus. *Curr Biol* **10**, R323.

Mah, S. P., Saueressig, H., Goulding, M., Kitntner, C. and Dressier, G. R. (2000). Kidney development in Cadherin-6 mutants: delayed mesenchyme-to-epithelial conversion and loss nephrons. *Developmental Biology* **223**, 38-53.

Matera, A. G. (1998). Of coiled bodies, gems, and salmon. *J Cell Biochem* **70**, 181-92.

Matera, A. G. (1999). Nuclear bodies: multifaceted subdomains of the interchromatin space. *Trends Cell Biol* **9**, 302-9.

McTaggart, S. J., Algar, E., Chow, C. W., Powell, H. R. and Jones, C. L. (2001). Clinical spectrum of Denys-Drash and Frasier syndrome. *Pediatr Nephrol* **16**, 335-9.

Miles, C., Elgar, G., Coles, E., Kleinjan, D. J., van Heyningen, V. and Hastie, N. (1998). Complete sequencing of the Fugu WAGR region from WT1 to PAX6: dramatic compaction and conservation of synteny with human chromosome 11p13. *Proc Natl Acad Sci U S A* **95**, 13068-72.

Miles, C. G., Slight, J., Spraggon, L., O'Sullivan, M., Patek, C., Hastie, N.D. (2003). Mice lacking the 68-amino-acid, mammal-specific N-terminal extension of WT1 develop normally and are fertile. *Mol Cell Biol* **23**, 2608-13.

Miquerol, L., Gertenstein, M., Harpal, K., Rossant, J. and Nagy, A. (1999). Multiple developmental roles of VEGF suggested by a LacZ-tagged allele. *Developmental Biology* **212**, 307-322.

Misteli, T. (2001a). Protein dynamics: implications for nuclear architecture and gene expression. *Science* **291**, 843-7.

Misteli, T. (2001b). Where the nucleus comes from. *Trends Cell Biol* **11**, 149.

Mitchell, J. R., Wood, E., Collins, K. (1999). A telomerase component is defective in the human disease dyskeritosis congenita. *Nature* **402**, 551-555.

Miyamoto, N., Yoshida, M., Kuratani, S., Matsuo, I. and Aizawa, S. (1997). Defects of urogenital development in mice lacking Emx2. *Development* **124**, 1653-1664.

Moore, A. W., McInnes, L., Kreidberg, J., Hastie, N. D. and Schedl, A. (1999). YAC complementation shows a requirement for Wt1 in the development of epicardium, adrenal gland and throughout nephrogenesis. *Development* **126**, 1845-57.

Moore, A. W., Schedl, A., McInnes, L., Doyle, M., Hecksher-Sorensen, J. and Hastie, N. D. (1998). YAC transgenic analysis reveals Wilms' tumour 1 gene activity in the proliferating coelomic epithelium, developing diaphragm and limb. *Mech Dev* **79**, 169-84.

Moore, M. W., Klein, R. D., Farinas, I., Sauer, H., Armanini, M., Phillips, H., Reichardt, L. F., Ryan, A. M., Carver-Moore, K. and Rosenthal, A. (1996). Renal and neuronal abnormalities in mice lacking GDNF. *Nature* **382**, 76-79.

Mrowka, C. and Schedl, A. (2000). Wilms' tumor suppressor gene WT1: from structure to renal pathophysiologic features. *J Am Soc Nephrol* **11 Suppl 16**, S106-15.

Munsterberg, A. and Lovell-Badge, R. (1991). Expression of the mouse anti-mullerian hormone gene suggests a role in both male and female sexual differentiation. *Development* **113**, 613-24.

Natoli, T. A., Liu, J., Eremina, V., Hodgens, K., Li, C., Hamano, Y., Mundel, P., Kalluri, R., Miner, J. H., Quaggin, S. E. et al. (2002a). A Mutant Form of the Wilms' Tumor Suppressor Gene WT1 Observed in Denys-Drash Syndrome Interferes with Glomerular Capillary Development. *J Am Soc Nephrol* **13**, 2058-67.

Natoli, T. A., McDonald, A., Alberta, J. A., Taglienti, M. E., Housman, D. E. and Kreidberg, J. A. (2002b). A mammal-specific exon of WT1 is not required for development or fertility. *Mol Cell Biol* **22**, 4433-8.

Okuwaki, K., Matsumoto, K., Tsujimoto, M., Nagata, K. (2001). Function of nucleophosmin/B23, a nucleolar acidic protein asa a histone chaperone. *FEBS Letters* **506**, 272-276.

Olson, M. O. J., Dundr, M. and Szebeni, A. (2000). The nucleolus: an old factory with unexpected capabilities. *Trends in Cell Biology* **10**, 189-196.

Paisley, D. J. (2000). Characterisation of two mouse mutant lines generated by transgenic insertional mutagenesis. In *Biology and Biochemistry*, (ed., pp. 298. Bath: University of Bath.

Palmer, R. E., Kotsianti, A., Cadman, B., Boyd, T., Gerald, W. and Haber, D. A. (2001). WT1 regulates the expression of the major glomerular podocyte membrane protein Podocalyxin. *Curr Biol* **11**, 1805-9.

Paraskeva, G. C., Jackson, F. R. (1984). Cell culture. *Oxford Press*

Parker, K. L., Schedl, A. and Schimmer, B. P. (1999). Gene interactions in gonadal development. *Annu Rev Physiol* **61**, 417-33.

Patek, C. E., Little, M. H., Fleming, S., Miles, C., Charlieu, J.-P., Clarke, A. R., Miyagawa, K., Christie, S., Doig, J., Harrison, D. J. et al. (1999). A zinc finger truncation of murine WT1 results in the characteristic urogenital abnormalities of Denys-Drash syndrome. *Proceedings of the National Academy of Science* **96**, 2931-2936.

Pelletier, J., Bruening, W., Kashtan, C. E., Mauer, S. M., Manivel, J. C., Striegel, J. E., Houghton, D. C., Junien, C., Habib, R., Fouser, L. et al. (1991). Germline mutations in the Wilms' tumor suppressor gene are associated with abnormal urogenital development in Denys-Drash syndrome. *Cell* **67**, 437-47.

Pichel, J. G., Shen, L., Sheng, H. Z., Granholm, A. C., Drago, J., Grinberg, A., Lee, E. J., Huang, S. P., Saarma, M., Hoffer, B. J. et al. (1996). Defects in enteric intervention and kidney development in mice lacking GDNF. *Nature* **382**, 73-76.

Politz, J. C., Yarovol, S., Kilroy, S.M., Gowda, K., Zwieb, C., Penderson, T. (2000). Signal recognition particle components in the nucleolus. *Proc Natl Acad Sci U S A* **97**, 55-60.

Pritchard-Jones, K., Fleming, S., Davidson, D., Bickmore, W., Porteous, D., Gosden, C., Bard, J., Buckler, A., Pelletier, J., Housman, D. et al. (1990). The candidate Wilm's Tumour gene is involved in genitourinary development. *Nature* **346**, 194-197.

Quaggin, S. E., Schwartz, L., Cui, S., Igarashi, P., Deimling, J., Post, M. and Rossant, J. (1999). The basic-helix-loop-helix protein pod1 is critically important for kidney and lung organogenesis. *Development* **126**, 5771-83.

Renshaw, J., King-Underwood, L. and Pritchard-Jones, K. (1997). Differential splicing of exon 5 of the Wilms tumour (WT1) gene. *Genes Chromosomes and Cancer* **19**, 256-266.

Ryan, G., Steele-Perkins, V., Morris, J. F., Rauscher III, F. G. and Dressler, G. R. (1995). Repression of Pax-2 by WT1 during normal kidney development. *Development* **121**, 867-875.

Sanchez, M. P., Silos-Santiago, I., Frisen, J., He, B., Lira, S. A. and Barbacid, M. (1996). Renal agenisis and the absence of enteric neurons in mice lacking GDNF. *Nature* **382**, 70-73.

Saxen, L. (1987). Organogenesis of the kidney. Cambridge: Cambridge University Press.

Scharnhorst, V., Dekker, p., van der Eb, A. J. and Jochemsen, A. G. (1999). Internal translation initiation generates novel WT1 protein isoforms with distinct biological properties. *Journal of Biological Chemistry* **274**, 23456-23462.

Schedl, A. and Hastie, N. D. (2000). Cross-talk in kidney development. *Curr Opin Genet Dev* **10**, 543-9.

Scheer, U. and Hock, R. (1999). Structure and function of the nucleolus. *Current Opinion in Cell Biology* **11**, 385-390.

Schneiter, R., Kadowaki, T., Tartakoff, A.M. (1995). mRNA transport in yeast: Time to reinvestigate functions of the nucleolus. *Mol Biol Cell* **6**, 357-370.

Schuchardt, A., D'Agati, V., Larsson-Blomberg, L., Constantini, F. and Pachnis, V. (1994). Defects in kidney and enteric nervous system of mice lacking the tyrosine kinase receptor Ret. *Nature* **367**, 380-383.

Schuchardt, A., D'Agati, V., Pacnis, V. and Constantini, F. (1996). Renal agenesis and hypodyplasia in ret-k- mutatnt mice result from defects in ureteric bud development. *Development* **122**, 1919-1929.

Scott, M., Boisvert, F. M., Vieyra, D., Johnston, R. N., Bazett-Jones, D. P. and Riabowol, K. (2001). UV induces nucleolar translocation of ING1

through two distinct nucleolar targeting sequences. *Nucleic Acids Research* **29**, 2052-2058.

Shawlot, W. and Behringer, R. R. (1995). Requirement for Lim1 in head-organizer function. *Nature* **374**, 425-30.

Slack, JMW. (2001). Essential Developmental Biology: Blackwell Science.

Speckmann, W., Narayanan, A., Terns, R. and Terns, M. (1999). Nuclear Retention elements of U3 small Nucleolar RNA. *Molecular and Cellular Biology* **19**, 8412-8421.

Srinivas, S., Goldberg, M. R., Watanabe, T., D'Agati, V., Al-Aqwati, Q. and Constantini, F. (1999a). Expression of green fluorescent protein in the ureteric bud of transgenic mice: A new tool for the analysis of ureteric bud morphogenesis. *Developmental Genetics* **24**, 241-251.

Srinivas, S., Wu, Z., Chen, C.-M., D'Agati, V. and Constantini, F. (1999b). Dominant effects of RET receptor misexpression and ligand dependent RET signalling of the ureteric bud. *Development* **126**, 1375-1386.

Staal, F. J., Meeldijk, J., Moerer, P., Jay, P., van de Weerdt, B. C., Vainio, S., Nolan, G. P. and Clevers, H. (2001). Wnt signaling is required for thymocyte development and activates Tcf-1 mediated transcription. *Eur J Immunol* **31**, 285-93.

Swain, A. and Lovell-Badge, R. (1999). Mammalian sex determination: a molecular drama. *Genes and Development* **13**, 755-767.

Swain, A., Zanaria, E., Hacker, A., Lovell-Badge, R. and Camerino, G. (1997). Dax1 expression is consistent with a role in sex determination as well as in adrenal and hypothalmus function. *Nature Genetics* **12**, 404-409.

Tucker, K. E., Berciano, M. T., Jacobs, E. Y., LePage, D. F., Shpargel, K. B., Rossire, J. J., Chan, E. K., Lafarga, M., Conlon, R. A. and Matera, A. G. (2001). Residual Cajal bodies in coilin knockout mice fail to recruit Sm snRNPs and SMN, the spinal muscular atrophy gene product. *J Cell Biol* **154**, 293-307.

Tucker, K. E., Massello, L. K., Gao, L., Barber, T. J., Hebert, M. D., Chan, E. K. and Matera, A. G. (2000). Structure and characterization of the murine p80 coilin gene, Coil. *J Struct Biol* **129**, 269-77.

Vidal, V. P., Chaboissier, M. C., de Rooij, D. G. and Schedl, A. (2001). Sox9 induces testis development in XX transgenic mice. *Nat Genet* **28**, 216-7.

Visitin, R., Amon, A. (2000). The nucleolus: the magician's hat for cell cycle tricks. *Current Opinion in Cell Biology* **12**, 752.

Wagner, K. D., Wagner, N., Vidal, V. P., Schley, G., Wilhelm, D., Schedl, A., Englert, C. and Scholz, H. (2002). The Wilms' tumor gene Wt1 is required for normal development of the retina. *Embo J* **21**, 1398-405.

Wagner, K. D., Wagner, N., Schedl, A. (2003). The complex life of WT1. *J Cell Sci* **116**, 1653-1658.

Ward, A., Fisher, R., Richardson, L., Pooler, J.A, Squire, S., Bates, P., Shaposhnikov, R., Hayward, N., Thurston, M., Graham, C. F. (1997). Genomic regions regulating imprinting and insulin-like growth factor-II promoter 3 activity in transgenics: novel enhancer and silencer elements. *Genes and Function* **1**, 36.

Ward, A., Pooler, J. A., Miyagawa, K., Duarte, A., Hastie, N. D. and Caricasole, A. (1995). Repression of promoters for the mouse insulin-like growth factor II-encoding gene (Igf-2) by products of the Wilms' tumour suppressor gene wt1. *Gene* **167**, 239-43.

Wolpert, L., Beddington, R., Brockes, J., Jessell, T., Lawrence, P. and Meyerowitz, E. (1998). Principles of Development. Oxford: Oxford University Press.

Yang, Y., Jeanpierre, C., Dressler, G. R., Lacoste, M., Niaudet, P. and Gubler, M. C. (1999). WT1 and PAX-2 podocyte expression in Denys-Drash syndrome and isolated diffuse mesangial sclerosis. *Am J Pathol* **154**, 181-92.